

DECLASSIFIED UNCLASSIFIED

This material contains information affecting the national defense of the United States within the meaning of the Espionage Laws, Title 18, U. S. C., sections 793 and 794. The transmission or the revelation of its contents in any manner to an unauthorized person is prohibited by law.

NOTICE: THIS MATERIAL MAY BE PROTECTED BY COPYRIGHT LAW (TITLE 17 US CODE)

CORRELATION DETECTION USING STORED SIGNALS

by

Classification Changed

TO: UNCLASSIFIED

By Authority of:

PAUL ELIOT GREEN, JR.

DD 254 For AF 19(122)500
P. E. Green Jr. 11 Oct 63
AF Liaison Lab Date
Liaison office 25 Jan 63

A.B., University of North Carolina
(1944)

M.S., North Carolina State College
(1948)

For SRO
Date 12 Jul 66
SRO Log No. 772 40

SUBMITTED IN PARTIAL FULFILLMENT OF THE REQUIREMENTS FOR THE DEGREE OF DOCTOR OF SCIENCE

at the

MASSACHUSETTS INSTITUTE OF TECHNOLOGY

September, 1953

Signature of Author Paul E. Green Jr.
Department of Electrical Engineering, August 24, 1953

Certified by William B. Davenport, Jr.
Thesis Supervisor

Accepted by _____
Chairman, Departmental Committee on Graduate Students

Archives
MASS. INST. TECH.
June-11-1956
LIBRARIES

DECLASSIFIED

UNCLASSIFIED

CORRELATION DETECTION USING STORED SIGNALS

by

Paul Eliot Green, Jr.

ABSTRACT

The problem of sending a message, consisting of a sequence of symbols, through additive white gaussian noise is discussed with reference to military communication requirements. The NOMAC system, a type of communication system employing noise-like signals and crosscorrelation detection, is described as a meaningful answer to this problem. In order for desired operating characteristics to be achieved, synchronized reference copies of the signalling waveforms must be available independently at both transmitter and receiver. In the past, operating NOMAC systems have used the expedient of transmitting these waveforms to the receiver by an auxiliary communication channel, thus circumventing storage and synchronization problems, but at the expense of a reduction in system performance.

Preparatory to investigating ways of storing the reference signals, a study is made of the degree of synchronization required and the amount of distortion which can be tolerated. It is found that these problems are not of an insuperable order of magnitude and so attention proceeds to possible storage methods. The nature of the correlation operation suggests storage either as the impulse response of a matched filter or simply as a function of time. Of these two, it is concluded that in spite of rather more difficult synchronization problems, the process of storage of a function of time is more immediately practical. Accordingly, an experimental system has been devised, deriving its stable time base from a crystal oscillator and producing signals of required characteristics. A description of this system and its performance is followed by an outline of the problems of providing synchronization in actual operating use, together with suggested procedure for accomplishing this.

The original assumption that the channel was disturbed only by additive white gaussian noise is sometimes an incomplete picture of operating conditions. Of the factors which have been neglected, perhaps the most important is the multipath condition. In an effort to judge the usefulness of NOMAC systems in a more meaningful frame of reference, the effect of quasistationary multipath conditions is analyzed. From this study the superior performance with multipath of either storage type system is demonstrated as is the advantage of using wide band signals (originally postulated on the basis of military considerations alone).

It is concluded that signal storage systems of the type developed experimentally are practical and that further implementation should proceed not only along these lines but also toward the development of a practical matched filter system. The results of the multipath study confirm the importance of these two techniques.

Thesis Supervisor: Dr. Wilbur B. Davenport, Jr.

Title: Group Leader, Lincoln Laboratory, M.I.T.

ACKNOWLEDGEMENT

In conducting the research described here, the author has benefited from the help and interest of a number of people. He would especially like to express his deepest appreciation to Dr. W. B. Davenport, Jr., who in supervising the research in his careful and searching fashion has been a constant source of inspiration and encouragement. He is lastingly indebted to Mr. Robert Price, who through his keen interest and understanding has contributed greatly in the course of many discussions. In the formative phases of this research, the writer benefited greatly from discussions with his friend Dr. B. L. Basore, and Professor R. M. Fano. The work has enjoyed the closest possible support from the directors of the Research Laboratory of Electronics and Lincoln Laboratory, to whom the author would like to express his thanks. Miss Ann Field and Mrs. Virginia Johnson have performed numerous calculations, and Miss Roberta Gagnon has exercised considerable skill and clairvoyance in typing the present manuscript.

CONTENTS

TITLE PAGE	i
ABSTRACT	ii
ACKNOWLEDGEMENT	iv
TABLE OF CONTENTS	v
LIST OF FIGURES	vii
CHAPTER I. CORRELATION DETECTION OF NOISE-LIKE SIGNALS	
1.1 A Communication System Model	1
1.2 The Case of Additive White Gaussian Noise	3
1.3 Crosscorrelation Detection	5
1.4 NOMAC Systems	10
1.5 The Storage Problem	13
CHAPTER II. OUTPUT SIGNAL-TO-NOISE RATIO	
2.1 Significance and Definition of Output Signal-to-Noise Ratio	15
2.2 Low-Pass Fixed Detection	17
2.3 Matched Filter Detection	21
2.4 Continuous operation of the Low-Pass Detector	21
2.5 Continuous Operation of the Band-Pass Detector	27
2.6 Interpretation and Remarks	31
CHAPTER III. PROBLEMS OF STORAGE	
3.1 Introduction	40
3.2 Desynchronization	42
A. Low-Pass Detection of Fixed Low-Pass Signals	45
B. Low-Pass Detection of Fixed Band-Pass Signals	51
C. Matched Filter Detection	56
D. Low-Pass Continuous Detection	57
E. Band-Pass Continuous Detection	59
3.3 Amplitude Distortion.	60
A. Low-Pass and Matched Filter Detection	61
B. Band-Pass Detection.	64
3.4 Frequency Distortion	67
3.5 Conclusions	68

CONTENTS (cont'd)

CHAPTER IV. AN EXPERIMENTAL STORED-SIGNAL SYSTEM

4.1 Introduction 72

4.2 Requirements on the Storage Medium 72

4.3 Description of the Experimental System 77

4.4 Experimental Results 86

4.5 The Synchronization Problem 89

CHAPTER V. MULTIPATH EFFECTS

5.1 Introduction 95

5.2 Stored-Signal System (Continuous Signals) 98

 A. Band-Pass Detection 98

 B. Low-Pass Detection 103

5.3 Transmitted-Reference System (Continuous Signals). 105

5.4 Matched Filter System and Stored Signal System Using
Fixed Signals. 109

5.5 A Comparison of System Performance 110

CHAPTER VI. CONCLUSIONS 120

REFERENCES 125

APPENDIX. SCHEMATIC DIAGRAMS OF EXPERIMENTAL STORED-SIGNAL SYSTEM . 129

BIOGRAPHICAL NOTE 135

LIST OF FIGURES

FIGURE	PAGE	TITLE
1.1	2	A Communication System Model
1.2	2	The Mean-Square Difference Receiver
1.3	6	Correlation Detectors
2.1	18	Correlation Detectors of Figure 1.3 Modified for $(S/N)_0$ Calculation
2.2	18	Spectra Involved in Low-Pass Continuous $(S/N)_0$ Calculation
2.3	18	Vector Diagrams Representing Output Signal and Noise
3.1	48	Effect of Desynchronization on Fixed Low-Pass Signals
3.2	48	Effect of Desynchronization on Fixed Band-Pass Signals
3.3	52	Effect of Rate Desynchronization on Output Signal-to-Noise Ratio for Low-Pass or Matched Filter Detection of Low-Pass Rectangular-Band Signals
3.4	52	Relative Correlator Output Signal-to-Noise Ratio for Symmetrical Peak-Clipping
4.1	79	Block Diagram of Digital Signal Generator
4.2	80	Experimental Stored-Signal System
4.3	84	1500- μ sec Section of Output Noise-Like Signal Waveform
4.4	79	Block Diagram of Experimental System Using Stored Signal Generator of Figure 4.1
4.5	87	Stored-Signal Normalized Power Density Spectra for Three Different Stagger-Tuning Configurations
4.6	87	Output Voltage Versus Time Desynchronization for Experimental System
5.1	101	Transmission Path Impulse Response and Related Functions
5.2	112	Signal Output Power and Signal-to-Self-Noise Ratio for Stored-Signal System Using Band-Pass Continuous Detection
5.3	113	Signal Output Power and Signal-to-Self-Noise Ratio for Stored-Signal System using Low-Pass Continuous Detection
5.4	114	Signal Output Power and Output Signal-to-Self-Noise Ratio for Transmitted Reference System
A.1	130	Driver Unit Schematic Diagram
A.2	131	Commutator Schematic Diagram
A.3	132	Resonator Unit Schematic Diagram
A.4	133	5-mc Oscillator Schematic Diagram
A.5	133	Sideband Generator Schematic Diagram
A.6	134	Channel Noise Source Schematic Diagram
A.7	134	Correlator Unit Schematic Diagram

CHAPTER I

CORRELATION DETECTION OF NOISE-LIKE SIGNALS

1.1 A Communication System Model

The basic purpose of any communication system is the transmission from one point to another of data in the form of certain messages chosen out of a set of possible messages. Such a system is the one schematized in Figure 1.1. The message emanating from the source and intended for the destination is assumed to be a sequence of independent symbols. Certain signals x_i are used to represent the various symbols and these are sent by the transmitter to the receiver through an intervening medium denoted as the channel. The action of the channel is such that it causes the received signals y_j to be in general different from the x_i . In fact, since the channel acts on the x_i in a random way, it is possible that a given y_j may result from a particular x_i one time and another the next. Inasmuch as the sequence of symbols will not be known in advance at the receiver there will be for the receiver an ambiguity or uncertainty, even after receiving a y_j as to which symbol was intended. Upon reception of a y_j , the receiver must therefore deal with a situation described not by a certainty as to which signal x_i was sent, but only by the various probabilities that different signals x_i were sent.

In some communication environments¹ these probabilities are actually available at the receiver, in principle, since it may be assumed to have knowledge of the a priori symbol probabilities $p(x_i)$ and of the channel transition probabilities $p(y_j/x_i)$ (the probability that if x_i is sent,

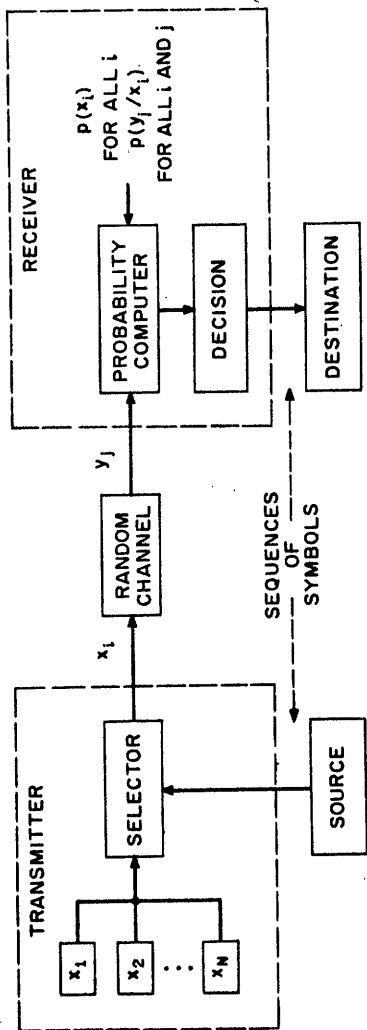


Fig.1.1. A communication system model.

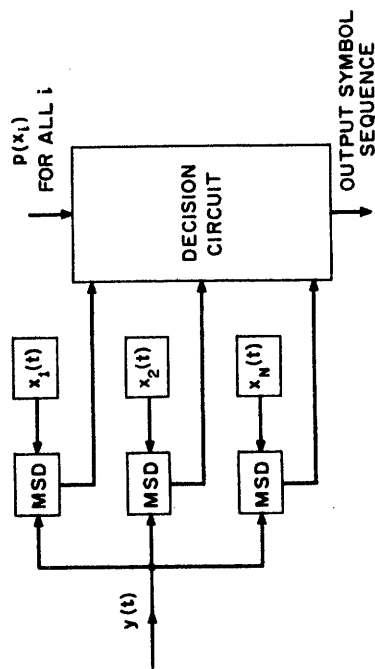


Fig.1.2. The mean-square difference receiver.

y_j is received). That these data are sufficient to determine the desired a posteriori probabilities $p(x_i/y_j)$ can be seen by writing

$$p(y_j/x_i)p(x_i) = p(x_i/y_j)p(y_j), \quad (1.1)$$

from which

$$p(x_i/y_j) = \frac{p(x_i)p(y_j/x_i)}{p(y_j)}. \quad (1.2)$$

In the communication systems of interest in the present study the destination requires as its input the original sequence of symbols with as few errors as possible. The complete function of the receiver is therefore not fulfilled merely by determining the various probabilities $p(x_i/y_j)$; it must go one step further and make a decision in favor of one x_i or another and pass on to the destination the symbol represented by this signal. Clearly, if the frequency of errors is to be made as small as possible, the receiver should consistently select the most likely of the transmitted symbols, i.e., that i for which $p(x_i/y_j)$ is the highest.

1.2 The Case of Additive White Gaussian Noise

The probability-computing operation of the receiver takes a particularly convenient physical form for the case in which the effect of the channel is to add white gaussian noise to the transmitted signals. This type of interference is defined by saying that it is a stationary random function of time having a power density spectrum flat over any frequency range in which signal components are present and that its multiple-order probability distributions are all multivariate gaussian. The assumption that the channel is characterized

only by additive white gaussian noise can often only be regarded as a first approximation to actual conditions, but in a great many cases it is a completely adequate model.

If the power density of this noise is N_0 (watts-per-cycle-per-second) it can be shown that the a posteriori symbol probability $p(x_i/y_j)$ after reception of a given waveform $y(t)$ is

$$p(x_i/y) = \frac{Kp(x_i)e^{-\frac{1}{N_0} \int_0^T [x_i(t)-y(t)]^2 dt}}{p(y)}, \quad (1.3)$$

where T is the signal duration, K is a constant, and $x_i(t)$ is the explicit form of the i -th transmitted signal. This expression defines the following operations at the receiver: Upon reception of a $y(t)$, the mean-square-difference between received signal and a locally-available copy of each $x_i(t)$ is computed. If the x_i are equally likely (as we shall assume them), the decision is made in favor of the i for which this quantity is the smallest, (otherwise an appropriate weighting of these differences with the logarithm of the $p(x_i)$ is seen to be necessary). It is seen that the channel conversion probabilities -- $p(y_j/x_i)$ in Section 1 but actually densities, say $w(y/x_i)$ here -- need not appear as explicitly stored data but may appear implicitly as the reference copies of signals $x_i(t)$ and the mean-square difference operation.

A receiver performing these operations is schematized in Figure 1.2. By rewriting the mean-square difference expression, we have

$$\int_0^T x_i^2(t) dt + \int_0^T y^2(t) dt - 2 \int_0^T x_i(t)y(t) dt, \quad (1.4)$$

where the first two terms are recognized as the energies of $x_i(t)$ and $y(t)$ and the last as -2 times the crosscorrelation between $x_i(t)$ and $y(t)$. This is the familiar crosscorrelation function $\phi_{xy}(\tau)$ evaluated at the origin, where

$$\phi_{xy}(\tau) = \int_0^T x(t)y(t+\tau)dt \quad . \quad (1.5)$$

Therefore, if the $x_i(t)$ all have equal energy, the minimum mean square difference criterion for decision can be replaced by that of maximum cross-correlation. In practice this is somewhat more convenient since the mean-square difference operation requires that the reference copies of the $x_i(t)$ all have the same amplitude as those that would be received in the absence of channel noise, while this amplitude requirement is not present with crosscorrelation detection. All that is required is that the reference waveforms have the proper amplitude relative to each other.

1.3 Crosscorrelation Detection

The use of crosscorrelation techniques for the detection of signals in noise has received quite some attention in recent years, and several practical methods have been evolved for implementing this operation. The types most directly connected with the present study are depicted in Figure 1.3 with appropriate nomenclature, and will be described here and analyzed more thoroughly in Chapter II.

It should be noted that the output of these detectors corresponding to each $x_i(t)$ is not a waveform, but a number. These numbers are compared in making the decision.

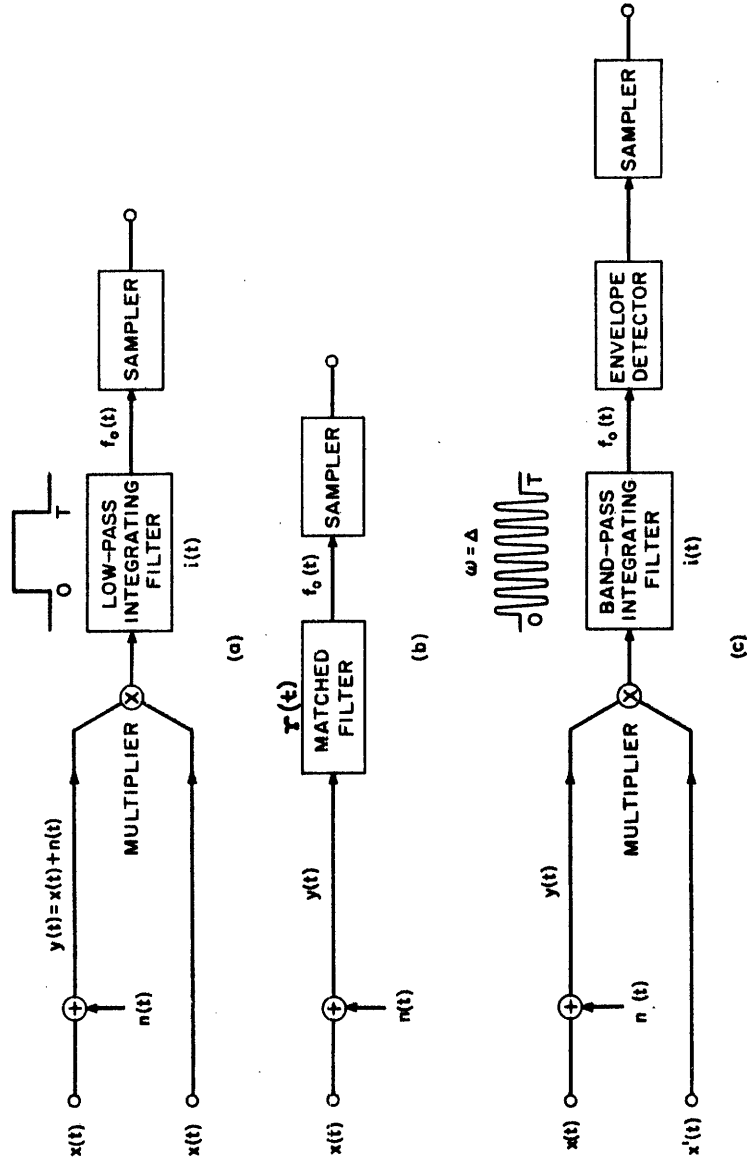


Fig.1.3. Correlation detectors (a) low-pass type (b) matched filter type (c) band-pass type.

In low-pass correlation detection the signals $x(t)$ and $y(t)$ are multiplied and passed through an integrating circuit. (For convenience the representation x_1 will now be written simply x since attention will center on a typical correlator-and-signal combination.) If the action of this circuit is to perform exactly the integration of the product from $t=0$ to $t=T$ (as would be the case for the rectangular filter impulse response given in the figure), the output sampled at T is

$$f_o(T) = \int_0^T x(t)y(t)dt \quad (1.6)$$

the desired crosscorrelation. We will refer to the rectangular type of integrator characteristic as ideal. If the impulse response of the integrator does not have this rectangular form but is instead some arbitrary $i(t)$, the process is spoken of as non-ideal integration and the output function of time is given by

$$f_o(t) = \int_{-\infty}^t x(\tau)y(\tau)i(t-\tau)d\tau \quad (1.7)$$

The operation of matched filter detection involves a linear system whose impulse response $r(t)$ is (apart from a constant time shift) the time reverse of $x(t)$, say

$$r(t) = x(T-t) \quad (1.8)$$

The output function of time will be

$$f_o(t) = \int_{-\infty}^{\infty} y(\tau)r(t-\tau)d\tau = \int_{-\infty}^{\infty} y(\tau)x(T-t+\tau)d\tau \quad (1.9)$$

which is the crosscorrelation function ϕ_{xy} (of Equation 1.5) in real time with origin at time T . If $x(t)$ is defined as nonzero only in the time

interval $(0, T)$, the output sampled at time T is seen to be mathematically identical with that given in Equation 1.6 for low-pass detection.

In effecting band-pass correlation detection the incoming $y(t)$ is multiplied not by $x(t)$ but by a function $x'(t)$ which is different from $x(t)$ only in that all its frequency components are displaced by a constant frequency Δ from those of $x(t)$. That is, if we express $x(t)$ for example as

$$x(t) = e(t)\cos(pt + \phi(t)) , \quad (1.10)$$

thus describing $x(t)$ by the two time functions $e(t)$ and $\phi(t)$ and the frequency parameter p , then the last has a new value $p-\Delta$ in

$$x'(t) = e(t)\cos((p-\Delta)t + \phi(t)) . \quad (1.11)$$

The product function is passed through a band-pass filter which is termed ideal if its impulse response has a rectangular envelope as depicted in Figure 1.3 and non-ideal otherwise. The envelope detector registers the envelope of the filtered difference frequency tone appearing in the output $f_o(t)$ due to interaction of $x(t)$ and $x'(t)$. Writing

$$y(t) = d(t)\cos(pt + \theta(t)) , \quad (1.12)$$

the output at time T from an ideal filter (of impulse response $\cos \Delta t$ in the range $(0, T)$ and zero elsewhere) is

$$f_o(T) = \int_0^T \cos \Delta t e(t)d(t)\cos((p-\Delta)t + \phi(t))\cos(pt+\theta(t))dt \quad (1.13)$$

which is

$$\frac{1}{2} \int_0^T e(t)d(t)\cos(pt + \phi(t))\cos(pt + \theta(t))dt = \frac{1}{2} \int_0^T x(t)y(t)dt \quad (1.14)$$

for the usual condition $p \gg \Delta \gg 1/T$. The function of the envelope detector and sampler in operating on $f_0(t)$ is discussed in more detail in Chapter II.

The use of the correlation function in studying random time functions first gained real prominence in the works of Wiener on the power density spectra of such functions² (1930) and on the filtration of random signals by linear systems³ (1942). (It appears now that part of the former theory was employed by Michelson⁴ on a heuristic basis as early as 1891.)

The possibilities of auto- and cross-correlation techniques for the detection of signals in noise was recognized by Lee and others⁵ in their investigations of the practical ramifications of Wiener's theories. They used still a different type of correlation detector from those considered above, namely the sampling correlator, in which a number of readings are made by sampling the functions $x(t)$ and $y(t)$ simultaneously. Products of corresponding samples then are added to approximate the desired integral of the product. This type of correlator is generally inapplicable in practice to the detection problem defined here because of the greater equipment complexity required.

The low-pass type of correlation was first studied by Fano⁶ and Davenport⁷ using a point of view different from that defined above for this type of correlator. It will be noted that in the previous discussion, the function $x_i(t)$ was considered to be the same waveform every time the symbol i is sent. The situation studied by Fano and Davenport

is that in which the observations are made not on the same explicitly defined signal function (of specified duration T), but on different portions of an indefinitely long function specified only on a statistical basis. This type of operation, which is sometimes very convenient in practical communication systems, will be termed continuous operation throughout the remainder of this paper. The term fixed operation will be used to describe the situation in which $x_i(t)$ is the same waveform segment each time the symbol i is sent.

The use of low-pass and band-pass type correlation detectors in the continuous sense for the detection of signals in noise was discussed by Fano.⁸ The notion of using a matched filter for signal detection is not new, but its implementation into a system of the type outlined in Section 1.1 was first suggested, also by Fano, in 1952.⁹ (Incidentally, it should be clear that "continuous" operation of the matched filter is not defined since the filter is constructed to have a fixed impulse response.)

1.4 NOMAC Systems

In the next chapter it will be found that a certain signal-to-noise ratio which is a central parameter in specifying the frequency of symbol errors, depends principally on the ratio of energy in each of the set of signal waveforms to the noise density N_0 so that the explicit form of the waveforms is to a great extent arbitrary. Because of this, it is possible to choose them so that their effectiveness against additive noise is supplemented by effectiveness in situations in which waveform structure is important. Such a situation is the military environment in which the systems of the present paper are required to operate.

[REDACTED]

A military communication operation is characterized by a tactical conflict between the transmitter-receiver combination whose purpose was described in Section 1.1 as the transmission of a succession of symbols (in private, it should be added) and a third party in the person of the enemy. His purposes are to detect the communication and either disrupt it or recover the message for himself. The desirable characteristics then of the communication are, first, that its very existence be as difficult to detect as possible, and second, that if intercept is inevitable, the transmission be of such a type that jamming, analysis, or imitation be as difficult as possible. By choosing as the signalling waveforms ones which have an even distribution of the energy in time and frequency, the first of these requirements is served, since by doing so the possibility that the ambient noise will conceal the transmission is enhanced. The wide bandwidth feature is also desirable as protection against random noise jamming, as will be seen in Section 2.6. If, in addition, the waveforms have to the outside observer a complex and "unpredictable" structure, the system has a better chance against cryptanalysis and deception.

These requirements have suggested the use of signals in the form of segments of random noise, and communication systems using noise-like signals detected by crosscorrelation have been termed NOMAC systems (for NOise Modulation And Correlation). In the present discussion we will call noise-like any signals which fit the above requirements of deliberate complexity and even energy distribution in time and frequency, whether or not they actually derived from such a source as thermal or shot noise. Physically, NOMAC systems may be divided into several clear-cut categories, the division being according to the method by which reference copies of the $x(t)$ are supplied.

[REDACTED]

In the transmitted reference system the reference signals are all sent to the receiver concurrently with the message transmission over a separate "auxiliary channel" (as contrasted with the "intelligence channel" bearing the message). In the stored reference system the signals are actually stored separately at transmitter and receiver as originally assumed. There is a subdivision into two types of stored-reference system, the stored-signal type in which the waveforms are stored as functions of time and read out of storage in synchronism with the incoming signal, and the matched filter type in which they are stored as the time-reversed impulse responses of a set of linear systems. Detection in the last type is by definition matched filter detection, whereas the stored signal type may use either low-pass or band-pass detection. It is customary to employ band-pass detection for the transmitted reference type since the intelligence and auxiliary channels must usually be separated in frequency.


The idea of using noise-like signals in a correlation type communication system seems to have originated in "Project Hartwell,"¹⁰ a study project conducted at M.I.T. in 1950, at which time the transmitted reference type was suggested by Wiesner and the stored reference type by DeRosa and Adams. One of the recommendations of this study project was that the possibilities of such systems be looked into. Subsequent work on the subject has centered principally in Lincoln Laboratory, M.I.T. A detailed exploration of much of the underlying theory, particularly the subject of error probability, has been made by Basore.¹¹ A number of versions of the transmitted reference system have been built and used in actual communication circuits,¹² and some exploratory work has been done on physical matched filters.¹³

1.5 The Storage Problem

That attention in system development would center first on the transmitted reference system is only natural, since problems of signal storage and synchronization are circumvented by this type of operation. The transmitter signals may be currently chosen segments of the noise output of a gas tube, for example.

However, this equipment convenience is bought at the expense not only of error probability (since much of the transmitter power is used to send the reference signals, and since the receiver must perform its correlation and decision operations using faulty, noisy reference signals), but also at the expense of security. Since the signal waveforms are no longer known only to transmitter and receiver, but are available to anyone having access to the channel, the hoped-for advantages against intercept, analysis, jamming, and deception are lost. Once the principle of operation of the system is found out by the enemy, detection of the transmission and recovery of the message are simple, since the set of reference signals, the "key," is available with no "cryptanalysis" necessary. Jamming and deception are easily effected by supplying the receiver with bogus intelligence and reference signals which it cannot differentiate from the legitimate ones.

These inadequacies of the present transmitted reference type system are so serious as to constitute a strong argument for the development of workable stored-reference systems, in spite of more difficult equipment realization problems. The stored-reference system is the point of emphasis of most of the remainder of this paper, the problem of actual equipment realization being dealt with in Chapter IV. This is preceded by a formulation



of the output signal-to-noise ratio parameter and an analysis of the effect upon it of various factors peculiar to the stored-reference system. The effect of multipath conditions on both types of NOMAC systems is dealt with in Chapter V.

CHAPTER II

OUTPUT SIGNAL-TO-NOISE RATIO

2.1 Significance and Definition of Output Signal-to-Noise Ratio

It has been mentioned that the task of the communication systems considered here is to convey a sequence of symbols to the destination with as few errors as possible. Thus the significant quantity specifying the degree to which the system performs this task is the probability of error.

The results of previous studies¹¹ of probability of error applicable to low-pass and matched filter detection can be stated in terms of 1) the number of equally-likely transmitter signals, 2) certain orthogonality relationships between these signals, and 3) a suitably defined output signal-to-noise power ratio from any one correlator.

For fixed operation of the low-pass correlator, where $x(t)$ is an explicitly determined time function, the output signal-to-noise ratio $(S/N)_0$ is defined in terms of the following hypothetical experiment: the crosscorrelation operation (Figure 1.3a) is performed once using each member of an infinite ensemble of additive noise waveforms of the specified statistical character. The output signal-to-noise ratio is defined as the ratio of mean output squared to output variance:

$$(S/N)_0 = \overline{f_0(T)}^2 / \sigma^2 [f_0(T)] \quad (2.1)$$

(Throughout this paper the bar will represent an ensemble average.) The mean output is the ensemble average of the numerical readings which the

correlator registers at its output, and the variance is the ensemble average of the squared difference between each reading and the mean output. The definition of $(S/N)_0$ is applicable to the probability of error studies only when this difference is gaussianly distributed over the ensemble.

For continuous operation of the low-pass correlator, the function $x(t)$ will be defined on a statistical basis only, and not as an explicit waveform. The output signal-to-noise ratio will then be the mean output voltage squared divided by the power in the output voltage fluctuations, this time the average being taken over the ensemble of infinitely long noise and signal functions. Again the probability of error studies require that the output fluctuations be gaussian.

For band-pass detection the pertinent studies of probability of error¹⁴ require that the signal-to-noise ratio be treated somewhat differently. Reference to Figure 1.3c shows that the numerical quantity delivered from the detector is not a reading of the filtered product waveform, but a reading of the envelope of this waveform. The probability of error is specified in terms of quantities identical to the three enumerated above for low-pass and matched filter detection, except that the last of these, the signal-to-noise ratio is that at the envelope detector input. It is defined for continuous signals as the ratio of the square of the average amplitude of the filtered difference frequency tone, divided by the power in the fluctuation component of the output. This fluctuation component is presumed to have the character of filtered random noise. The use of a band-pass correlation detector under fixed conditions will not be discussed in the present paper.

In the remaining sections of this chapter the output signal-to-noise ratio will be computed for conditions somewhat more general than those implicit in the original communication system model in which arbitrary signal and white gaussian noise were assumed. Figure 2.1 depicts the modifications to the block diagrams of Figure 1.3. The additive gaussian channel noise will be allowed to have an arbitrary spectrum, and independent additive noises will be assumed present in both multiplier inputs for the case of band-pass detection, thus treating the situation encountered in the transmitted-reference system (which customarily employs band-pass detection for frequency separation of the intelligence and reference channels.) Further, in all three detector types, one channel will be assumed to have in cascade an arbitrary linear two-terminal pair system. The precise character of this linear system will remain unspecified for the present analysis. In later chapters its presence in the signal-to-noise ratio expressions will be exploited in determining the influence of certain factors, such as multipath, on system performance.

2.2 Low-Pass Fixed Detection

The noise $n(t)$ indicated in Figure 2.1a is assumed to be a stationary and ergodic random function having a zero mean and power density spectrum $N(\omega)$. The function $u(t)$ is given by

$$u(t) = \int_0^T x(\tau)h(t-\tau)d\tau \quad . \quad (2.2)$$

Assuming the integrator characteristic ideal,

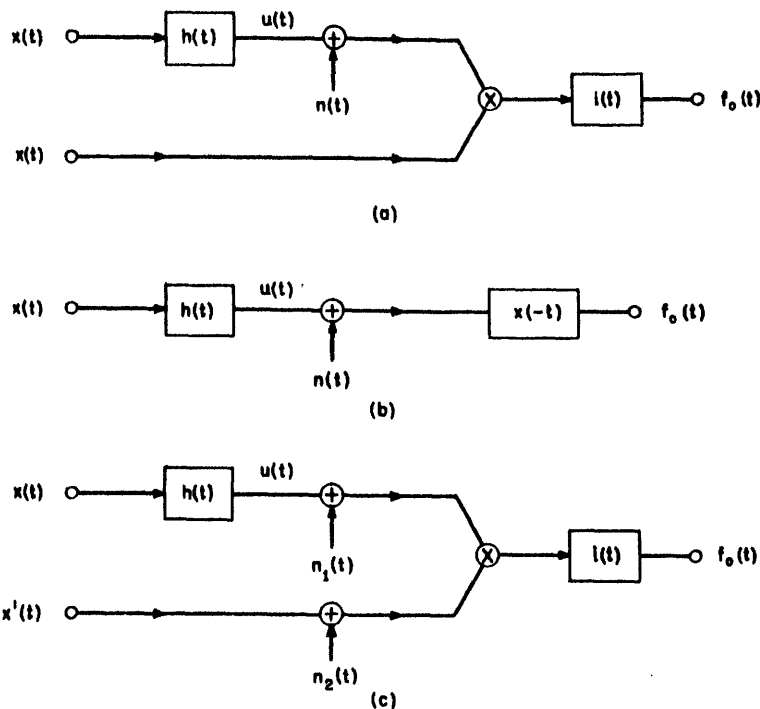


Fig.2.1. Correlation detectors of Fig.1.3 modified for $(S/N)_0$ calculation.

- (a) low-pass type
- (b) matched filter type
- (c) band-pass type.

Fig.2.2. Spectra involved in low-pass continuous $(S/N)_0$ computation.

- (a) power spectrum of $x(t)$
- (b) power spectrum of $u(t)$
- (c) power spectrum of $n(t)$
- (d) $X \times U$ multiplier input term
- (e) $X \times N$ multiplier input term
- (f) integrating filter characteristic $|I(\omega)|^2$.

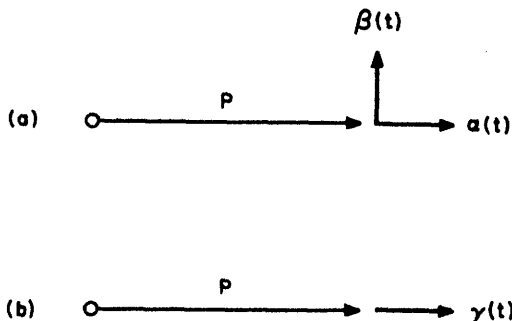
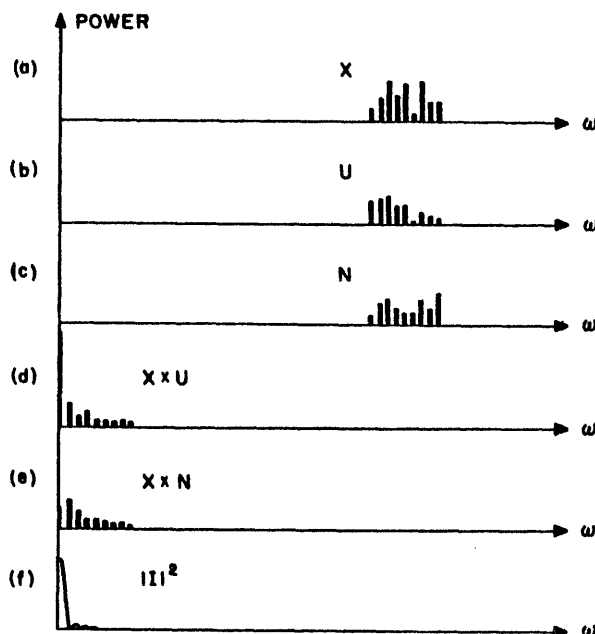


Fig.2.3. Vector diagrams representing output signal and noise for band-pass continuous detection.

$$f_o(T) = \int_0^T x(t) [u(t) + n(t)] dt \quad (2.3)$$

so that

$$\overline{f_o(T)} = \int_0^T [x(t)u(t) + x(t)\overline{n(t)}] dt = \int_0^T x(t)u(t) dt \quad (2.4)$$

since $\overline{n(t)}=0$. If the Fourier transform of $x(t)$ is

$$X(\omega) = \int_{-\infty}^{\infty} x(t)e^{-j\omega t} dt, \quad (2.5)$$

and similarly for $U(\omega)$ the transform of $u(t)$, then by the Parseval theorem,

$$\overline{f_o(T)} = \int_{-\infty}^{\infty} X^*(\omega)U(\omega) d\omega \quad (2.6)$$

But

$$U(\omega) = X(\omega)H(\omega), \quad (2.7)$$

so that

$$\overline{f_o(T)} = \int_{-\infty}^{\infty} |X(\omega)|^2 H(\omega) d\omega \quad (2.8)$$

The energy density spectrum of the signal $X(\omega)$ is defined as

$$X(\omega) = |X(\omega)|^2 \quad (2.9)$$

Substituting this in the last expression and recognizing that it is even, whereas the imaginary part of $H(\omega)$, written $\text{Im}[H(\omega)]$, is odd we have



$$\overline{f_o(T)} = \int_{-\infty}^{\infty} X(\omega) \text{Re} [H(\omega)] d\omega \quad (2.10)$$

The denominator of equation 2.1 is

$$\sigma^2(f_o(T)) = \overline{f_o^2(T)} - \overline{f_o(T)}^2 = \int_0^T \int_0^T x(t)x(\tau) \overline{n(t)n(\tau)} dt d\tau. \quad (2.11)$$

Since $n(t)$ is assumed stationary, the ensemble average $\overline{n(t)n(\tau)}$ can be replaced by $\overline{n(t')n(t' + \tau - t)}$ where t' is any value of time while t and τ are those in the expression to be evaluated. But because of the assumed ergodic character, this ensemble average may be replaced by the time average

$$\lim_{\theta \rightarrow \infty} \frac{1}{\theta} \int_{-\theta/2}^{\theta/2} n(t')n(t' + \tau - t) dt', \quad (2.12)$$

which is the autocorrelation function $\phi_n(\tau-t)$ of the random function $n(t)$. By the Wiener-Khintchine theorem² on such functions this is the inverse Fourier transform of $N(\omega)$, the power density spectrum of $n(t)$. So the denominator becomes

$$\frac{1}{2\pi} \int_{-\infty}^{\infty} N(\omega) d\omega \int_0^T \int_0^T x(t)x(\tau) e^{-j\omega(t-\tau)} dt d\tau \quad (2.13)$$

which is

$$\frac{1}{2\pi} \int_{-\infty}^{\infty} X(\omega)N(\omega) d\omega \quad (2.14)$$

so that the output signal-to-noise ratio is



$$\left(\frac{S}{N}\right)_0 = \frac{\left[\int_{-\infty}^{\infty} X(\omega) \operatorname{Re} [H(\omega)] d\omega \right]^2}{\int_{-\infty}^{\infty} X(\omega) N(\omega) d\omega} \quad (2.15)$$

For the case of $H(\omega)$ identically unity and $N(\omega) = N_0 / 2$ (that is, N_0 for a single-sided frequency scale) in the region of nonzero $X(\omega)$ we have

$$\left(\frac{S}{N}\right)_0 = \frac{2}{N_0} \int_{-\infty}^{\infty} X(\omega) d\omega = \frac{2 \times \text{signal energy}}{N_0} \quad (2.16)$$

as was mentioned in Section 1.4.

2.3 Matched Filter Detection

The mathematical expression for $f_0(T)$, the quantity registered at the output of a matched filter detector, Equation 1.6, was found to be identical with that for $f_0(T)$ from the low-pass correlator for fixed operation using an ideal integrator. Therefore the above results, Equations 2.15 and 2.16, apply to the matched filter as well.

2.4 Continuous Operation of the Low-Pass Detector

To compute $(S/N)_0$ in this case we proceed as follows: an ensemble of stationary gaussian noise and signal functions all θ seconds long is considered, where $\theta \gg T$. Each is expanded in a Fourier series and the spectrum at the multiplier output is computed for a representative ensemble member in terms of the unspecified Fourier coefficients. The ensemble average power spectrum at the multiplier output is then gotten from this

based on known statistical properties of these coefficients. Then Θ is allowed to grow without limit whereupon certain summations become integrals involving power density spectra. The power spectrum of the filter output is the input power spectrum multiplied by the squared-magnitude of the filter frequency response. The signal-to-noise ratio is the ratio of the square of the d.c. component in the filter output to the remainder of the power, representing fluctuation.

For each member of the ensemble of signal and noise functions we have the following Fourier expansions

$$\begin{aligned}
 x(t) &= \sum_{i=1}^{\Theta W} \xi_i \cos(\omega_i t + \phi_i) \\
 n(t) &= \sum_{i=1}^{\Theta W} \nu_i \cos(\omega_i t + \gamma_i) \\
 u(t) &= \sum_{i=1}^{\Theta W} \xi_i h_i \cos(\omega_i t + \phi_i + \eta_i)
 \end{aligned} \tag{2.17}$$

where ω_i represents the lower edge of a band of width W cycles-per-second placed to include all signal and noise components, and h_i and η_i are $|H(\omega_i)|$ and $\text{arc}[H(\omega_i)]$, respectively. It is known¹⁵ that when $x(t)$ is a stationary gaussian random process having power density spectrum $X(\omega)$ (in considering fixed operation this symbol was used to represent an energy density) each ξ_i has a Rayleigh distribution over the ensemble with

$$\overline{\xi_i^2} = 2 X_i \frac{2\pi}{\Theta} = 2 X_i \Delta\omega \tag{2.18}$$

and

$$\overline{\xi_i^4} = 2(\overline{\xi_i^2})^2 = 8 X_i^2 (\Delta\omega)^2 \quad (2.19)$$

where X_i is defined by $\lim_{\theta \rightarrow \infty} X_i = X(\omega_i)$. The phase angle ϕ_i has a probability distribution which is flat from $-\pi$ to $+\pi$. Similar statements hold for $n(t)$ in relation to ν_i , γ_i , and the power density spectrum $N(\omega)$.

At the multiplier output there will be two distinct contributions from the product $x(t)[u(t) + n(t)]$ which we will denote as the (X x U) and (X x N) contributions, respectively, using the subscripts I and II. Figure 2.2 depicts the line spectrum of the power of one ensemble member of $x(t)$, $u(t)$, and $n(t)$ and shows how the operation of the multiplier produces the (X x U) and (X x N) components. (There are also components about the double frequency which will be ignored since they lie outside the filter passband.) The large d.c. output signal resulting from the coherence between $x(t)$ and $u(t)$ will be noted in the (X x U) term of Figure 2.2d. For the wideband signals of interest, the signal bandwidth W will be large compared to that of the integrating filter. This is depicted in Figure 2.2f.

When the signals $x(t)$ and $u(t)$ are multiplied, the voltage at $\omega=0$ is

$$V_I(0) = \frac{1}{2} \sum_{i=1}^{BW} \xi_i^2 h_i \cos \eta_i \quad (2.20)$$

and the power is

$$P_I(0) = V_I^2(0) = \frac{1}{4} \sum_i \xi_i^4 h_i^2 \cos^2 \eta_i + \frac{1}{4} \sum_i \xi_i^2 h_i \cos \eta_i \sum_{j \neq i} \xi_j^2 h_j \cos \eta_j \quad (2.21)$$

Taking the ensemble average of this and then going to the limit as $\theta \rightarrow \infty$,

we have

$$\lim_{\theta \rightarrow \infty} \overline{P_I(0)} = \lim_{\theta \rightarrow \infty} \frac{2\pi}{\theta} \int_0^{\infty} X^2(\omega) |H(\omega)|^2 \cos^2 \eta(\omega) d\omega + \left[\int_0^{\infty} X(\omega) |H(\omega)| \cos \eta(\omega) d\omega \right]^2 \quad (2.22)$$

Similarly the $(X \times N)$ term at zero frequency is

$$V_{II}(0) = \frac{1}{2} \sum_i \nu_i \xi_i \cos(\phi_i - \gamma_i) \quad (2.23)$$

from which

$$P_{II}(0) = \frac{1}{4} \sum_i \nu_i^2 \xi_i^2 \cos^2(\phi_i - \gamma_i) + \frac{1}{4} \sum_i \nu_i \xi_i \cos(\phi_i - \gamma_i) \sum_{j \neq i} \nu_j \xi_j \cos(\phi_j - \gamma_j) \quad (2.24)$$

and

$$\lim_{\theta \rightarrow \infty} \overline{P_{II}(0)} = \lim_{\theta \rightarrow \infty} \frac{1}{2} \frac{2\pi}{\theta} \int_0^{\infty} N(\omega) X(\omega) d\omega \quad (2.25)$$

since ϕ_i and γ_i are independent and uniformly distributed from $-\pi$ to π .

In the case of terms at output frequencies different from zero,

$\omega = 2\pi n/\theta$, $n=1, 2, \dots, \theta W$, we have for the $(X \times U)$ term

$$V_I\left(\frac{2\pi n}{\theta}\right) = \frac{1}{2} \sum_i \xi_i \xi_{i+n} h_{i+n} \cos\left(\frac{2\pi n t}{\theta} + \phi_{i+n} + \eta_{i+n} - \phi_i\right) + \frac{1}{2} \sum_i \xi_{i+n} \xi_i h_i \cos\left(\frac{2\pi n t}{\theta} + \phi_i + \eta_i - \phi_{i+n}\right) \quad (2.26)$$

$$\begin{aligned}
&= \frac{1}{2} \cos \frac{2\pi n t}{\theta} \sum_i \xi_i \xi_{i+n} h_{i+n} \cos(\phi_{i+n} + \eta_{i+n} - \phi_i) + \xi_{i+n} \xi_i h_i \cos(\phi_i + \eta_i - \phi_{i+n}) \\
&+ \frac{1}{2} \sin \frac{2\pi n t}{\theta} \sum_i \dots \sin(\dots) + \dots \sin(\dots) \quad (2.27)
\end{aligned}$$

Since the integrating filter bandwidth is much smaller than W , we are really interested only in the multiplier output spectral lines for which $n \ll W\theta$. If $H(\omega)$ is a reasonably continuous function, we have, for small n , that $h_k \approx h_{k+n}$ and $\eta_k \approx \eta_{k+n}$. The second term above is thus negligible.

$$P_I\left(\frac{2\pi n}{\theta}\right) = \frac{1}{2} \left[\sum_i \xi_i \xi_{i+n} h_{i+n} \cos(\phi_{i+n} + \eta_{i+n} - \phi_i) \right]^2 \quad (2.28)$$

for sufficiently large θ , and

$$\lim_{\theta \rightarrow \infty} \overline{P_I\left(\frac{2\pi n}{\theta}\right)} = \lim_{\theta \rightarrow \infty} \frac{4\pi}{\theta} \int_0^{\infty} X(\omega) X\left(\omega + \frac{2\pi n}{\theta}\right) |H\left(\omega + \frac{2\pi n}{\theta}\right)|^2 \cos^2 \eta(\omega) d\omega \quad (2.29)$$

The $(X \times N)$ term is

$$\begin{aligned}
V_{II}\left(\frac{2\pi n}{\theta}\right) &= \frac{1}{2} \sum_i \xi_{i+n} \nu_i \cos\left(\frac{2\pi n t}{\theta} + \phi_{i+n} - \gamma_i\right) + \xi_i \nu_{i+n} \cos\left(\frac{2\pi n t}{\theta} + \phi_i - \gamma_{i+n}\right) \\
&= \frac{1}{2} \cos \frac{2\pi n t}{\theta} \sum_i \xi_{i+n} \nu_i \cos(\phi_{i+n} - \gamma_i) + \xi_i \nu_{i+n} \cos(\phi_i - \gamma_{i+n}) \\
&+ \frac{1}{2} \sin \frac{2\pi n t}{\theta} \sum_i \dots \sin(\dots) + \dots \sin(\dots) \quad (2.30)
\end{aligned}$$

from which

$$\lim_{\theta \rightarrow \infty} \overline{P_{II}(\frac{2\pi n}{\theta})} = \frac{1}{2} \lim_{\theta \rightarrow \infty} \left[\frac{2\pi}{\theta} \int_0^{\infty} N(\omega) X(\omega + \frac{2\pi n}{\theta}) d\omega + \frac{2\pi}{\theta} \int_0^{\infty} N(\omega + \frac{2\pi n}{\theta}) X(\omega) d\omega \right]. \quad (2.31)$$

Those terms that will pass through the integrating filter are for $n \ll \theta W$, so with reasonably continuous spectra we may write

$$\lim_{\theta \rightarrow \infty} \overline{P_{II}(\frac{2\pi n}{\theta})} = \lim_{\theta \rightarrow \infty} \frac{2\pi}{\theta} \int_0^{\infty} X(\omega) N(\omega) d\omega \quad (2.32)$$

$n=0, 1, \dots$

and

$$\lim_{\theta \rightarrow \infty} \overline{P_I(\frac{2\pi n}{\theta})} = \lim_{\theta \rightarrow \infty} \frac{4\pi}{\theta} \int_0^{\infty} X^2(\omega) |H(\omega)|^2 \cos^2 \eta(\omega) d\omega \quad n \neq 0 \quad (2.33)$$

For $n=0$, the second term of $\lim_{\theta \rightarrow \infty} \overline{P_I(0)}$ predominates, representing the signal output. If we now form the ratio $(S/N)_0$ as the quotient of this term divided by all others, we have

$$\left(\frac{S}{N}\right)_0 = \frac{\left[\int_0^{\infty} X(\omega) |H(\omega)| \cos \eta(\omega) d\omega \right]^2}{\int_0^{\infty} X^2(\omega) |H(\omega)|^2 \cos^2 \eta(\omega) d\omega + \frac{1}{2} \int_0^{\infty} X(\omega) N(\omega) d\omega} \frac{1}{W_f} \quad (2.34)$$

Here use has been made of the definition for W_f the effective noise bandwidth¹⁶ of the filter

$$2\pi W_f = \int_{-\infty}^{\infty} |I(\omega)|^2 d\omega / |I_{\max}(\omega)|^2, \quad (2.35)$$

which in this case is

$$\lim_{\theta \rightarrow \infty} \left[1 + 2 \sum_{\substack{\text{passband} \\ \text{except zero}}} \frac{|I(\omega)|^2}{|I(0)|^2} \frac{2\pi}{\theta} \right] \quad (2.36)$$

in which

$$I(\omega) = \int_{-\infty}^{\infty} i(t) e^{-j\omega t} dt \quad (2.37)$$

If $H(\omega)$ is defined on the basis of a double-sided frequency scale, $(S/N)_0$ can be written in a form more easily compared with equation 2.1.

$$\left(\frac{S}{N}\right)_0 = \frac{\left[\int_0^{\infty} X(\omega) \operatorname{Re}[H(\omega)] d\omega \right]^2}{2 \int_0^{\infty} X^2(\omega) \operatorname{Re}^2[H(\omega)] d\omega + \int_0^{\infty} X(\omega) N(\omega) d\omega} \frac{2}{W_f} \quad (2.38)$$

2.5 Continuous Operation of the Band-Pass Detector

The analysis for band-pass continuous operation (Figure 2.1c) proceeds in a fashion almost identical with the preceding work for the low-pass case except that here the spectra of $x(t)$ and $u(t)$ are shifted apart by Δ , which we will assume larger than the signal bandwidth. Therefore we seek as $(S/N)_0$ the ratio of the squared amplitude of the difference-frequency sinusoid passed by the filter to the remaining power, representing fluctuations.

Independent additive gaussian noises having power density spectra $N_1(\omega)$ and $N_2(\omega)$ are assumed added to the upper and lower correlator inputs of Figure 2.1c, respectively, so as to include the condition of operation of the transmitted reference type of system.

The Fourier expansions which will be dealt with are now

$$\begin{aligned}
 u(t) &= \sum_{i=1}^{GN} \xi_i h_i \cos(\omega_i t + \phi_i + \eta_i) \\
 n_1(t) &= \sum_i v_i \cos(\omega_i t + \gamma_i) \\
 x'(t) &= \sum_i \xi_i \cos[(\omega_i - \Delta)t + \phi_i] \\
 n_2(t) &= \sum_i \mu_i \cos[(\omega_i - \Delta)t + \delta_i].
 \end{aligned}
 \tag{2.39}$$

Again we will compute the power in the various lines at the multiplier output, which in this case will be examined in the neighborhood of the difference frequency Δ . There are four sets of lines to be considered, $(X' \times U)$, $(X' \times N_1)$, $(U \times N_2)$, and $(N_1 \times N_2)$ for which the subscripts I, II, III, and IV will be used, respectively.

When $x'(t)$ and $u(t)$ are multiplied, the voltage at the difference frequency is

$$V_I(\Delta) = \frac{1}{2} \sum_i \xi_i^2 h_i \cos(\Delta t + \eta_i)
 \tag{2.40}$$

and the power is the time average of $V_I^2(\Delta)$ which is

$$\begin{aligned}
 P_I(\Delta) &= \frac{1}{8} \left[\sum_i \xi_i^2 h_i \cos \eta_i \right]^2 + \frac{1}{8} \left[\sum_i \xi_i^2 h_i \sin \eta_i \right]^2 \\
 &= \frac{1}{8} \sum_i \xi_i^4 h_i^2 + \frac{1}{8} \sum_i \xi_i^2 h_i \cos \eta_i \sum_{j \neq i} \xi_j^2 h_j \cos \eta_j \\
 &\quad + \frac{1}{8} \sum_i \xi_i^2 h_i \sin \eta_i \sum_{j \neq i} \xi_j^2 h_j \sin \eta_j.
 \end{aligned}
 \tag{2.41}$$

The limit of the ensemble average of this expression as θ approaches infinity is

$$\begin{aligned} \lim_{\theta \rightarrow \infty} \overline{P_I(\Delta)} &= \lim_{\theta \rightarrow \infty} \frac{1}{2} \frac{2\pi}{\theta} \int_0^{\infty} X^2(\omega) |H(\omega)|^2 d\omega \quad (2.42) \\ &+ \frac{1}{2} \left[\int_0^{\infty} X(\omega) |H(\omega)| \cos \eta(\omega) d\omega \right]^2 + \frac{1}{2} \left[\int_0^{\infty} X(\omega) |H(\omega)| \sin \eta(\omega) d\omega \right]^2. \end{aligned}$$

The contribution at $\omega = \Delta$ of the $(X \times N_1)$ term is

$$V_{II}(\Delta) = \frac{1}{2} \sum_i \xi_i \nu_i \cos(\Delta t - \phi_i + \gamma_i) \quad (2.43)$$

from which

$$P_{II}(\Delta) = \frac{1}{8} \left[\sum_i \xi_i \nu_i \cos(\phi_i - \gamma_i) \right]^2 + \frac{1}{8} \left[\sum_i \xi_i \nu_i \sin(\phi_i - \gamma_i) \right]^2 \quad (2.44)$$

and

$$\lim_{\theta \rightarrow \infty} \overline{P_{II}(\Delta)} = \lim_{\theta \rightarrow \infty} \frac{1}{2} \frac{2\pi}{\theta} \int_0^{\infty} X(\omega) N_1(\omega) d\omega \quad (2.45)$$

Similarly we find the $(U \times N_2)$ and $(N_1 \times N_2)$ terms at $\omega = \Delta$ to be

$$\lim_{\theta \rightarrow \infty} \overline{P_{III}(\Delta)} = \lim_{\theta \rightarrow \infty} \frac{1}{2} \frac{2\pi}{\theta} \int_0^{\infty} X(\omega) |H(\omega)|^2 N_2(\omega - \Delta) d\omega \quad (2.46)$$

and

$$\lim_{\theta \rightarrow \infty} \overline{P_{IV}(\Delta)} = \lim_{\theta \rightarrow \infty} \frac{1}{2} \frac{2\pi}{\theta} \int_0^{\infty} N_1(\omega) N_2(\omega - \Delta) d\omega \quad (2.47)$$

respectively.

By repeating these four calculations to find the contributions to the power at other frequencies we find at $\omega = \Delta = 2\pi n/\Theta$ where $n = \pm 1, \pm 2, \dots$

$\pm \Theta W$ that

$$\lim_{\Theta \rightarrow \infty} \overline{P_{\text{I}}\left(\frac{2\pi n}{\Theta} + \Delta\right)} = \lim_{\Theta \rightarrow \infty} \frac{1}{2} \frac{2\pi}{\Theta} \int_0^{\infty} X(\omega) X\left(\omega + \frac{2\pi n}{\Theta}\right) H\left(\omega + \frac{2\pi n}{\Theta}\right)^2 d\omega \quad (2.48)$$

$$\lim_{\Theta \rightarrow \infty} \overline{P_{\text{II}}\left(\frac{2\pi n}{\Theta} + \Delta\right)} = \lim_{\Theta \rightarrow \infty} \frac{1}{2} \frac{2\pi}{\Theta} \int_0^{\infty} X(\omega) N\left(\omega + \frac{2\pi n}{\Theta}\right) d\omega \quad (2.49)$$

$$\lim_{\Theta \rightarrow \infty} \overline{P_{\text{III}}\left(\frac{2\pi n}{\Theta} + \Delta\right)} = \lim_{\Theta \rightarrow \infty} \frac{1}{2} \frac{2\pi}{\Theta} \int_0^{\infty} X(\omega) H(\omega)^2 N_2\left(\omega - \Delta + \frac{2\pi n}{\Theta}\right) d\omega \quad (2.50)$$

and

$$\lim_{\Theta \rightarrow \infty} \overline{P_{\text{IV}}\left(\frac{2\pi n}{\Theta} + \Delta\right)} = \lim_{\Theta \rightarrow \infty} \frac{1}{2} \frac{2\pi}{\Theta} \int_0^{\infty} N_1(\omega) N_2\left(\omega - \Delta + \frac{2\pi n}{\Theta}\right) d\omega \quad (2.51)$$

Again with the integrating filter bandwidth much less than W , and for reasonably well-behaved signal and noise spectra, only those fluctuations components close to $\omega = \Delta$ will pass through the filter. The desired output signal-to-noise ratio is the ratio of twice the power in the difference frequency tone (the squared amplitude is twice the power) divided by the fluctuation power, and so collecting terms we have

$$\left(\frac{S}{N}\right)_0 = \frac{\left[\int_0^\infty X(\omega) \operatorname{Re}[H(\omega)] d\omega \right]^2 + \left[\int_0^\infty X(\omega) \operatorname{Im}[H(\omega)] d\omega \right]^2}{\int_0^\infty X^2(\omega) |H(\omega)|^2 d\omega + \int_0^\infty X(\omega) N(\omega) d\omega + \int_0^\infty X(\omega) |H(\omega)|^2 N_2(\omega-\Delta) d\omega + \int_0^\infty N_1(\omega) N_2(\omega-\Delta) d\omega} \quad \frac{2}{W_f}$$

(2.52)

where here the effective bandwidth of the integrating filter is written

$$2\pi W_f = \lim_{\theta \rightarrow \infty} \sum_{\text{passband}} \frac{|I(\omega)|^2}{|I(\Delta)|^2} \frac{2\pi}{\theta} \quad (2.53)$$

and where, as before, the channel filter characteristic $H(\omega)$, is rephrased in terms of a double-sided spectral representation. The noise spectra may be regarded as either all single- or all double-sided without the expression being altered, since it is a ratio of powers. However, it must be carefully noted that the range of the integrals must include only the half-range 0 to infinity, because of the second numerator term.

2.6 Interpretation and Remarks

If one compares the expression for $(S/N)_0$ for fixed operation (equation 2.15) with those for continuous operation (equations 2.38 and 2.52), one is struck by the presence of the extra denominator term in the latter, a term which does not involve the channel noise. This part of the fluctuation power is called the self-noise. In continuous type operation since measurements of the energy, equation 1.6, are made on different portions of the same signal function, instead of the same portion as with fixed

operation, there is this fluctuation in the energy which is seen to decrease as the observation interval widens.^{7,17} In the low-pass detection case, this self-noise can be assumed to have the required gaussian distribution by virtue of the small bandwidth of the filter compared to the bandwidth of the self-noise spectrum before filtering.¹⁸

When the self-noise term becomes the predominant denominator term in the band-pass expression (equation 2.52) for $(S/N)_0$, it must be used with some caution in determining the probability of error. This is because the pertinent probability of error expressions¹⁴ are based on the assumption that the output noise power is narrow band gaussian noise representable as¹⁹

$$f(t) = \alpha(t)\cos \Delta t + \beta(t)\sin \Delta t \quad (2.54)$$

where $\alpha(t)$ and $\beta(t)$ are independent and gaussianly distributed with zero mean and variance equal to that of $f(t)$. The last three denominator terms may be expected to have this behavior because of the small bandwidth of the integrating filter and because there is no coherent structure in the filter input spectra giving these three terms. However, if one sets $H(\omega) = a$ constant and examines the self-noise spectrum in the derivation of $(S/N)_0$, it is found to be symmetrical about $\omega = \Delta$ so that even though the self-noise output may also be considered approximately gaussian due to narrow filter bandwidth, it cannot be expressed in the above way, but instead as

$$f(t) = \gamma(t) \cos \Delta t \quad (2.55)$$

(which is seen to be non-stationary) the difference being in the absence of any phase modulation.

It turns out that when $H(\omega) = \text{a constant}$, the $(S/N)_o$ expression (2.52) is still correct for the high output signal-to-noise ratios used in practice if the self-noise term is multiplied by two. This can be shown as follows (Figure 2.3): The large horizontal vector of length P represents the signal sinusoid. The narrow band gaussian noise of equation 2.54 is then represented by the resultant of the two small vectors having length (positive or negative) equal to $\alpha(t)$ and $\beta(t)$, Figure 2.3a. The envelope detector will register the length of the signal-plus-noise vector which is

$$(P + \alpha) / \cos \theta$$

where

$$\theta = \sin^{-1}(\beta/P + \alpha).$$

For sufficiently high signal-to-noise ratio, $\beta \ll P$ and the vector length is $P + \alpha(t)$. The variance of $\alpha(t)$ is the same as that of $f(t)$. In Figure 2.3b the case of equation 2.55 is depicted, and here the variance of $\gamma(t)$ can be shown to be twice that of $f(t)$. Therefore in determining the effect on the envelope, the self-noise power must be multiplied by two when the complex self-noise spectrum is symmetrical about the difference frequency Δ .

When $H(\omega)$ is not a constant, then it is not clear just what the behavior corresponding to Figure 2.3 will be, since the self-noise spectrum is neither even, nor are the parts on opposite sides of the carrier completely unrelated. It is conceivable that the orientation of the vector representing output self-noise power be more perpendicular on the average than parallel to the signal vector, thus reducing the probability of error. In the absence of more investigation of this

problem, the safest thing to do is to compute probability of error on the pessimistic assumption that all the self-noise power is concentrated in the orientation of Figure 2.3b. Equation 2.52, modified by inserting a factor of two in the first denominator term, still stands, but it must be remembered that when self-noise is predominant and $H(\omega)$ is not a constant, the probability of error may actually be lower than computed.

Expressions 2.15, 2.38, and 2.52 are somewhat unwieldy in their generalized form as they stand, and it is useful to rewrite them for certain particular situations of frequent occurrence.

First, if the noises and signal all have the same spectral shape, and if $H(\omega) = \text{constant}$, then the reciprocal of $(S/N)_o$ is

$$\left(\frac{N}{S}\right)_o = \frac{K}{2TW_x} \left(\frac{N}{S}\right)_i \quad (2.56)$$

for low-pass fixed operation or matched filter detection (equation 2.15). Here $(N/S)_i$ is the ratio of average noise power to average signal power at the correlator input, T is the symbol duration as before, W_x is the effective bandwidth of the signal energy density spectrum $X(\omega)$, and K is a spectrum form factor

$$K = \frac{\int_0^{\infty} X^2(\omega) d\omega}{X_{\max}(\omega) \int_0^{\infty} X(\omega) d\omega} \quad (2.57)$$

a few representative values of which are given in Table I. For low-pass continuous operation (equation 2.38), we have

$$\left(\frac{N}{S}\right)_o = \frac{W_f}{W_x} K \left(1 + \frac{1}{2} \left(\frac{N}{S}\right)_i\right) \quad (2.58)$$

where W_x and K are computed from the power density spectrum $X(\omega)$. For band-pass continuous operation,

$$\left(\frac{N}{S}\right)_o = \frac{W_f}{W_x} K \left(\frac{1}{2} + \frac{1}{2} \left(\frac{N}{S}\right)_1 + \frac{1}{2} \left(\frac{N}{S}\right)_2 + \frac{1}{2} \left(\frac{N}{S}\right)_1 \left(\frac{N}{S}\right)_2 \right) \quad (2.59)$$

Type of Spectrum	$X(\omega)$	K
Rectangular	$\begin{cases} 1 \text{ for } \omega \text{ in bandwidth } \Omega \\ 0 \text{ otherwise} \end{cases}$	1
Triangular	$\begin{cases} 1 - \frac{ \omega - \omega_c }{\Omega/2} \text{ for } \omega - \omega_c < \Omega/2 \\ 0 \text{ otherwise} \end{cases}$	2/3
Gaussian	$e^{-(\omega - \omega_c)^2}$	$1/\sqrt{2}$
Exponential	$e^{- \omega - \omega_c }$	1/2
1 st order Butterworth ("Optical" or "Cauchy")	$\frac{1}{1 - (\omega - \omega_c)^2}$	1/2
n th order Butterworth	$\frac{1}{1 - (\omega - \omega_c)^{2n}}$	$1 - 1/2n$

TABLE I: Spectrum Form Factor K

where $(N/S)_1$ and $(N/S)_2$ are the noise-to-signal power ratios at the two correlator inputs.

For the case of white channel noise, with $H(\omega)=1$, we have the result of equation 2.16 for fixed operation, and for low-pass continuous operation,

$$\left(\frac{N}{S}\right)_o = \frac{W_f}{W_x} \left(K + \frac{N_o}{2 X_{max}} \right) \quad (2.60)$$

For band-pass continuous operation

$$\left(\frac{N}{S}\right)_o = \frac{W_f}{W_x} \left(\frac{K}{2} + \frac{N_{O1}}{2X_{max}} + \frac{N_{O2}}{2X_{max}} + \frac{1}{2} \frac{N_{O1} N_{O2}}{X_{max}^2} \frac{W'}{W_x} \right) \quad (2.61)$$

where N_{O1} and N_{O2} are the spectral densities of noise at the two correlator inputs, and W' is the bandwidth of these white (rectangular spectrum) noises, W' being assumed large enough to include all of $X(\omega)$. These expressions are seen to be somewhat similar to the preceding except that the input noise-to-signal ratios are redefined in terms of power densities.

Equations (2.59) and (2.61) point up a fundamental disadvantage of the transmitted-reference system compared to the stored-reference system, namely the much lower output signal-to-noise ratio for a given input signal-to-noise ratio. Specifically if the channel signal-to-noise ratio is a quantity ρ somewhat less than unity, $(S/N)_o$ for the stored-reference system is ρ times $2 W_x / KW_f$. However, for the transmitted-reference system with a small signal-to-noise ratio ρ in intelligence and auxiliary channels, $(S/N)_o$ is ρ^2 times $2 W_x / KW_f$.

Although in the analysis of fixed type operation, the character of the signal was arbitrary, it will be recalled that it was specified as a gaussian random function for the case of continuous operation. (Sections 2.4 and 2.5) A review of this analysis will disclose that except for the self-noise denominator terms, the results (equations 2.38 and 2.52) are still correct for non-gaussian signals. All that is required is that, as in equation 2.18, a constant ratio exist between the second moment $\overline{\xi_i^2}$ of the Fourier coefficient ξ_i and the power density spectrum $X(\omega)$. (The behavior of the fourth moment $\overline{\xi_i^4}$ is seen to enter only in the self-noise term, and the phase ϕ_i not at all.) This condition exists in general for well-behaved functions of time, since if it is valid to expand in a Fourier series segment of the function θ seconds long, as $\theta \rightarrow \infty$ the average power contained in any one Fourier spectral line at ω_i must become identical with the power in that part of the power density spectrum from $\omega_i - \pi/\theta$ to $\omega_i + \pi/\theta$, which is asymptotically

$$X(\omega_i) \frac{2\pi}{\theta} = X(\omega_i) \Delta\omega \quad . \quad (2.62)$$

It is of collateral interest to use the general expressions for $(S/N)_0$ in determining the effect of noise jamming on NOMAC system performance. Specifically, we might ask what spectral shape $N(\omega)$ of jamming power will be most effective in reducing $(S/N)_0$ for a given jamming power. For the stored-reference system (equations 2.15 and 2.38 with $H(\omega)=1$, and 2.52 with $H(\omega)=1$, $N_2=0$, and $N_1=N(\omega)$) this means maximizing

$$\int_0^{\infty} X(\omega)N(\omega) d\omega \quad (2.63)$$

while constraining

$$\int_0^{\infty} N(\omega) d\omega = P_N \quad (2.64)$$

If $X(\omega)$ has a maximum value X_{\max} at some frequency ω_1 , the $N(\omega)$ should be an impulse (of value P_N) at this frequency, whereupon

$$\int_0^{\infty} X(\omega)N(\omega) d\omega = P_N X_{\max} \quad (2.65)$$

If instead $N(\omega)$ is for example rectangular with width Ω and therefore height P_N/Ω , then we must have

$$\int_0^{\infty} X(\omega)N(\omega) d\omega \leq \frac{P_N}{\Omega} X_{\max} \Omega \quad (2.66)$$

since no values of X in Ω are greater than X_{\max} . (The equality sign holds if $X=X_{\max}$ everywhere in Ω .) The output signal-to-jamming ratio is (from equation 2.52)

$$\left(\frac{S}{J}\right)_o = \frac{2W_x}{W_f} \left(\frac{S}{J}\right)_i \quad (2.67)$$

where $(S/J)_i$ and $(S/J)_o$ are the input and output signal-to-jamming power ratios. Thus it is seen that no distribution of jamming power is more effective than an extremely narrow concentration of power in frequency, and this jamming frequency should be adjusted to coincide with the frequency of maximum signal power. The advantage of wide-band signals against jamming is now apparent since if the best the jammer can do

is expressed by equation 2.65, the logical defense is to spread the signal spectrum, making its maximum value as small as possible.

For the transmitted-reference system, two independent noise jamming signals $N_1(\omega)$ and $N_2(\omega)$ separated by a frequency difference Δ would have the effect given by the last denominator term of equation 2.52. However, a more harmful jamming can be effected by employing two signals, identical except for their center frequency. Let $N'(\omega)$ and $N'(\omega-\Delta)$ be their power density spectra. Then, so long as these two spectra lie within the acceptance band of the receiver, the jamming power at the correlator output can be deduced by treating the jamming as a signal in equation 2.52. The ratio of signal-to-jamming power at the correlator output is then

$$\left(\frac{S}{J}\right)_o = \frac{\left[\int_0^{\infty} X(\omega) d\omega\right]^2}{\left[\int_0^{\infty} N(\omega) d\omega\right]^2} = \left(\frac{S}{J}\right)_i^2 \quad (2.68)$$

the square of the input signal-to-jamming power ratio, irrespective of the form of $N(\omega)$. In this calculation we have assumed the output jamming power to be the square of the amplitude of the difference frequency tone produced by jamming along. It has also been assumed that the input signal-to-jamming ratio is small enough so that the output jamming power is produced predominantly by the interaction of the two jamming signals, and not by interaction between them and the two intended signals.

The contrast between the performance of the stored and transmitted-reference systems as given in equations 2.67 and 2.68 is striking. In the former, the jamming can be effectively combatted by widening the spectrum. In the latter there is no corresponding defense.

CHAPTER III

PROBLEMS OF STORAGE

3.1 Introduction

In contemplating the task of carrying a system conception to the point of physical realization, it is important to know not only what the desired parameter values are, but also how closely they must be adhered to in order to preserve a given system performance. In NOMAC systems there are a number of factors which in practice may cause a deviation of the various important quantities from their nominal values. Previous studies of these matters have been limited to questions of the departure from ideal performance resulting from the use of non-ideal integrators (which were discussed in Chapter II) and non-ideal multipliers.¹¹ In this chapter these studies will be extended by an investigation of the effects on output signal-to-noise ratio of distortions of various kinds in the signalling waveforms themselves.

In the transmitted-reference type of system, the environments of the intelligence and reference signals are much the same, so that both will be disturbed in a similar manner. However, in the stored-reference system, the completely different environments of the received and stored signals make the problem of dissimilar perturbations of great importance. Discrepancies between waveforms will cause a change not only in output signal-to-noise ratio but also in the input signal-to-noise ratio.

It is of interest to determine the effect on the ratio of output (S/N) to input (S/N) when distortions are introduced in the waveforms.

This chapter will therefore deal with expressions for the quantity

$$R^2 = \frac{(S/N)_o / (S/N)_i \text{ with distorted waveforms}}{(S/N)_o / (S/N)_i \text{ with undistorted waveforms}} = \frac{(S/N)_o' / (S/N)_i'}{(S/N)_o / (S/N)_i} \quad (3.1)$$

as a function of parameters describing the important types of distortions. (The primed quantities are those evaluated with distortion present.) This expression can be rewritten

$$R^2 = \frac{S_o' N_o S_i N_i'}{S_o N_o' S_i' N_i} \quad (3.2)$$

thus placing in evidence how the effect of signalling waveform distortions on the various signal and noise powers influences R^2 .

When the two signals are undistorted we have the situation originally depicted in Figure 1.3. We will refer to the correct version of the signal as $x(t)$ and will call this the nominal signal. When imperfections are present in the two signals shown entering at the left in Figure 1.3, we will rewrite them as $x_1(t)$ and $x_2(t)$, respectively, and call these the actual signals. In using the signal-to-noise ratio expressions from Chapter II, the transfer function $H(\omega)$ of the linear cascade of Figure 2.1 will be set equal to unity unless otherwise noted.

3.2 Desynchronization

Lack of agreement between the time scales of the two functions to be correlated is one of the most important respects in which the functions may differ. This condition will be referred to as desynchronization. Ideally, the two correlator inputs should have exactly the same time origin and the juxtaposition of the two time scales should be preserved exactly throughout the entire signal duration. The degree to which this requirement is violated can be represented by writing the two functions as

$$x_1(t) = x(t + D_1(t))$$

(3.3)

and

$$x_2(t) = x(t + D_2(t))$$

where $x(t)$ is the function in its undistorted form and $D_1(t)$ and $D_2(t)$ are the distortions of the two time scales.

In considering "fixed" operation, it is convenient to write

$$D_1(t) = a_0 + a_1 t$$

(3.4)

and

$$D_2(t) = b_0 + b_1 t.$$

In limiting the analysis to a two-term description of the time-scale distortions the assumption has been made that a storage medium will be used having a time scale of very high "inertia." The major portion of the time scale disagreement then arises from either the improper starting time of one signal with respect to the other or a stretching or compression of one time scale relative to the other, and not from

higher order time-scale fluctuations. The discrepancy between the two time scales will be described by calling $(a_0 - b_0) = \tau$ the time desynchronization, and $(a_1 - b_1) = \rho$ the rate desynchronization. The latter includes the effect of possible Doppler conditions in which the time scale at the transmitter is different from that at the receiver due to relative motion of the two. ($\rho = 1.72$ parts in 10^6 per 1000 knots radial relative velocity.)

In treating the case of continuous operation, the situation is somewhat different. Here successive readings are taken on portions of a pair of time functions $x_1(t)$ and $x_2(t)$, and $(S/N)_0$ has been computed (Sections 2.4 and 2.5) on the premise that the functions last an infinite time. If rate desynchronization is present, it is seen that the two signals will be properly synchronized for a negligible fraction of the time and the time-average output will therefore be negligible compared to the noise. Consequently, in discussing the effect of desynchronization on continuous operation, the rate term will be omitted.

In evaluating R (Equation 3.2) the input noise power is, of course, unaffected by desynchronization of the signals, and therefore (N'_i/N_i) is unity. We will now show that for usual orders of magnitude of desynchronization, neither the input signal power nor that part of the noise output power due to channel noise is changed significantly from the nominal values, so that (N_o/N'_o) and (S_i/S'_i) are substantially unity. Thus for small input signal-to-noise ratios (where self-noise is not the predominant output noise component), R^2 will be the ratio (S'_o/S_o) of output signal powers. (The effect of desynchronization on the self-noise term will be discussed later at the appropriate point.)

DECLASSIFIED

In equations 2.15, 2.38, and 2.52 for $(S/N)_o$ a typical term representing the output noise power resulting from interaction of signal and channel noise can be written

$$Q = \int_{-\infty}^{\infty} X(\omega)N(\omega) d\omega \quad (3.5)$$

when the signal has its distortionless form $x(t)$. Since finite time shifts of the signal have no effect on $X(\omega)$ time desynchronization is seen to have no effect on Q . The input signal, which is proportional to the integral of $X(\omega)$ over frequency, is seen to be likewise independent of time desynchronization. As for the rate desynchronization term arising in fixed operation, the spectrum corresponding to one of the signals, say $x_1(t) = x(t+a_1 t)$ is

$$X_1(\omega) = \frac{1}{(1+a_1)^2} X\left(\frac{\omega}{1+a_1}\right) \quad (3.6)$$

When the noise spectrum $N(\omega)$ is flat with density $N_o/2$,

$$Q = \frac{N_o}{2} \int_{-\infty}^{\infty} X(\omega) d\omega \quad (3.7)$$

when rate desynchronization is absent, and

$$Q_1 = \frac{N_o}{2} \int_{-\infty}^{\infty} X_1(\omega) d\omega = Q/1+a \quad (3.8)$$

when it is present. Thus if we may assume that a_1 and b_1 are $\ll 1$, rate desynchronization too is seen to have a negligible effect on output noise

DECLASSIFIED

power. Clearly, for a_1 and $b_1 \ll 1$, the effect on the input signal power is negligible, too.

As the analysis proceeds, the condition a_1 and $b_1 \ll 1$ will be recognized as completely realistic since very small values of the quantity $|a_1 - b_1|$ will be found capable of causing severe decreases in R . In the present discussion we will exclude the possibility that a_1 and b_1 are both an appreciable fraction of unity, have the same sign, and are very nearly equal. This singular condition would hardly arise in normal operating conditions, but would have to be produced deliberately under unusual circumstances.

A. Low-Pass Detection of Fixed Low-Pass Signals

For the present treatment of fixed operation, we will define the nominal signal $x(t)$ as being appreciably different from zero only in the time interval $(-T/2, T/2)$. The output power will then be nominally $f_0^2(T/2)$ where

$$f_0(T/2) = \int_{-T/2}^{T/2} x^2(t) dt = \int_{-\infty}^{\infty} x^2(t) dt \quad . \quad (3.9)$$

With desynchronization present, we have instead

$$f_0'(T/2) = \int_{-\infty}^{\infty} x_1(t)x_2(t) dt \quad . \quad (3.10)$$

These will be abbreviated f_0 and f_0' . As discussed above, we may consider the quantity R^2 to be given by the ratio of signal powers. In the present case of a low-pass fixed signal, the calculation of these quantities requires

an explicit expression for the particular waveform in use. Rather than choose some arbitrary function and make calculations from it, we will investigate instead the average behavior over an ensemble of signal functions representing segments of white gaussian noise of bandwidth W . This procedure will be more appropriate for the treatment of NOMAC system performance. Instead of calculating R as a ratio of output voltages f_o for a specific $x(t)$, we will calculate instead the ratio of ensemble average output voltages

$$R_1 = \overline{f_o'} / \overline{f_o} \quad . \quad (3.11)$$

A function which is band-limited to the frequency range 0 to W can be expressed as a sum of $\sin(2\pi Wt)/(2\pi Wt)$ functions $1/2W$ seconds apart where each is multiplied by a coefficient proportional to the signal voltage at that time.²⁰ We will express our nominal function $x(t)$ in this way. (Because of the limitation to a confined frequency range, $x(t)$, which will be chosen from an ensemble of low-pass white gaussian noises of bandwidth W , will not be limited entirely to the time interval $(-T/2, T/2)$. It will have some energy outside this interval, but this will be a negligible fraction of the total if the time-bandwidth product is large.)

We represent the function $x(t)$ in terms of the voltage samples α_n at times $n/2W$ as

$$x(t) = \sum_{n=-TW}^{TW} \alpha_n \frac{\sin \pi(2Wt-n)}{\pi(2Wt-n)} \quad . \quad (3.12)$$

If there is no desynchronization present, the output will be

$$f_o = \int_{-\infty}^{\infty} x^2(t) dt \quad , \quad (3.13)$$

which may be visualized as the integral of the product of the two waveforms of Figure 3.1a. Since the α 's are not functions of time, this can be written

$$f_o = \sum_{n=-TW}^{TW} \sum_{m=-TW}^{TW} \alpha_m \alpha_n \int_{-\infty}^{\infty} \frac{\sin \pi(2Wt-n)}{\pi(2Wt-n)} \frac{\sin \pi(2Wt-m)}{\pi(2Wt-m)} dt = \sum_{n=-TW}^{TW} \sum_{m=-TW}^{TW} \alpha_m \alpha_n I_{m,n} \quad , \quad (3.14)$$

where $I_{m,n}$ is the integral within the summation.

We now determine the ensemble average $\overline{f_o}$ making use of the following known statistical properties of the α 's: They are independent and gaussianly distributed with mean zero and the same variance $\overline{\alpha^2}$, that is, $\overline{\alpha_m} = 0$, $\overline{\alpha_m \alpha_n} = \delta_{mn} \overline{\alpha^2}$.

We thus have

$$\overline{f_o} = \sum_{n=-TW}^{TW} \overline{\alpha^2} I_{n,n} = T \overline{\alpha^2} \quad . \quad (3.16)$$

since $I_{m,n}$ is not a random variable.

When desynchronization is present, we have the situation pictured in Figure 3.1b for which

$$f_o' = \sum_{n=-TW}^{TW} \sum_{m=-TW}^{TW} \alpha_m \alpha_n I'_{m,n} \quad , \quad (3.17)$$

where

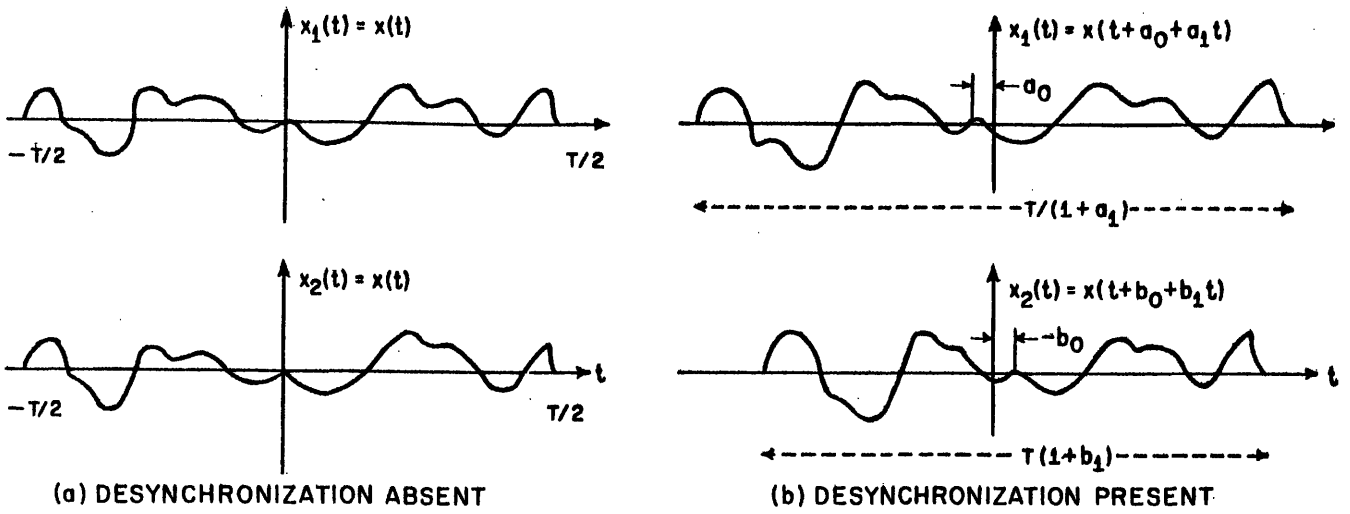


Fig. 3.1. Effect of desynchronization on fixed low-pass signals.

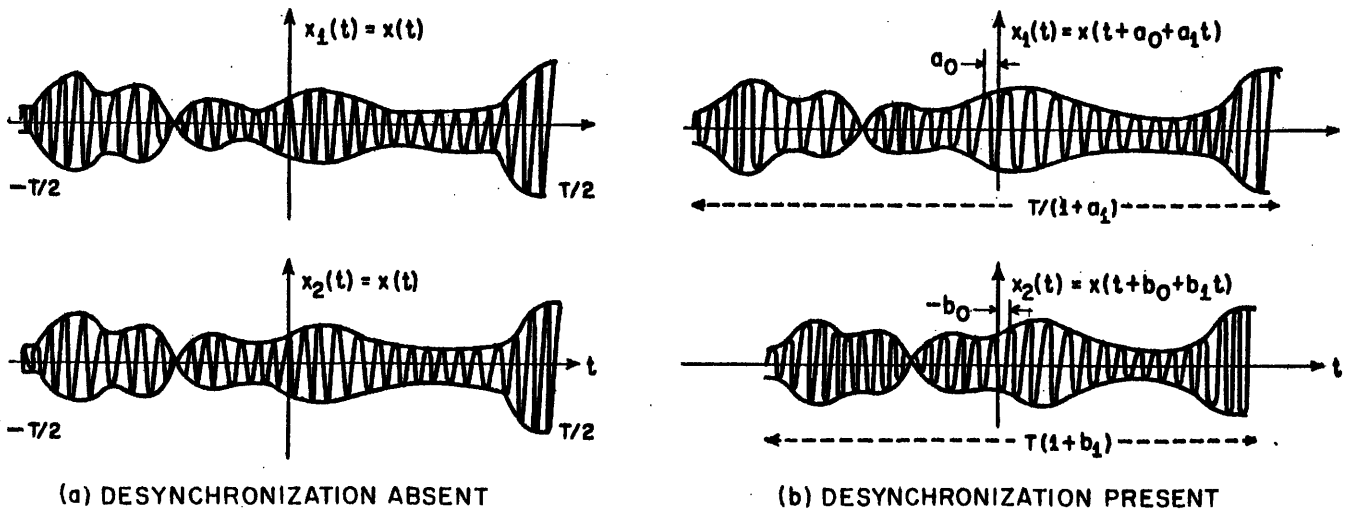


Fig. 3.2. Effect of desynchronization on fixed band-pass signals.



$$I'_{m,n} = \int_{-\infty}^{\infty} \frac{\sin \pi [2Wt(1+a_1) - m + 2Wa_0]}{\pi [2Wt(1+a_0) - m + 2Wa_0]} \frac{\sin \pi [2Wt(1+b_1) - n + 2Wb_0]}{\pi [2Wt(1+b_1) - n + 2Wb_0]} dt \quad (3.18)$$

Again we take the ensemble average of f_o' , and since $I'_{m,n}$ is not a random variable, we have

$$f_o' = \sum_{n=-TW}^{TW} \overline{\alpha^2} I'_{n,n} \quad (3.19)$$

Making the change of variable

$$t' = t - (n - 2Wa_0) / 2W(1+a_1) \quad (3.20)$$

the integral $I'_{n,n}$ becomes

$$I'_{n,n} = \int_{-\infty}^{\infty} \frac{\sin 2\pi W(1+a_1)t'}{2\pi W(1+a_1)t'} \frac{\sin 2\pi W [(1+b_1)t' + \sigma_n]}{2\pi W [(1+b_1)t' + \sigma_n]} dt' \quad (3.21)$$

where

$$\sigma_n = \frac{1}{2W} \left[\frac{1+b_1}{1+a_1} (n - 2Wa_0) - n + 2Wb_0 \right] \approx \frac{n}{2W} (b_1 - a_1) + (b_0 - a_0) = -\frac{np}{2W} - \tau \quad (3.22)$$

This integral can be readily evaluated by the Parseval theorem, by which the integral of the product of two time functions is the integral of the product of the Fourier transform of one times the complex conjugate of the Fourier transform of the other. In the present case, the first integrand



factor transforms into a rectangle centered on zero frequency, with height $1/(1+a_1)$ and width $2W(1+a_1)$. The transform of the second factor is a rectangle centered on zero frequency with height $1/(1+b_1)$, phase angle $\omega\sigma_n$ and width $2W(1+b_1)$. The product of the second times the conjugate of the first is a third rectangle of height $1/(1+a_1)(1+b_1)$, phase angle $\omega\sigma_n$ and width $2W(1+\epsilon)$, where ϵ is either a_1 or b_1 , whichever has the smaller algebraic value. The integral of this third rectangle is the inverse Fourier transform

$$\int_{-W(1+\epsilon)}^{W(1+\epsilon)} \frac{e^{j\omega\sigma_n}}{(1+a_1)(1+b_1)} d\omega = \frac{1+\epsilon}{2W(1+a_1)(1+b_1)} \frac{\sin 2\pi W(1+\epsilon)\sigma_n}{2\pi W(1+\epsilon)\sigma_n} \approx \frac{\sin 2\pi W\sigma_n}{(2W)2\pi W\sigma_n} \quad (3.23)$$

As $2TW \rightarrow \infty$ with $1/2W = \Delta u \rightarrow du$, and $n/2W = u$, the summation in

$$\lim_{2TW \rightarrow \infty} \overline{f'_0} = \lim_{2TW \rightarrow \infty} \frac{\overline{a^2}}{2W} \sum_{n=-TW}^{TW} \frac{\sin 2\pi W(\tau + n\rho/2W)}{2\pi W(\tau + n\rho/2W)} \quad (3.24)$$

approaches the integral

$$\int_{-T/2}^{T/2} \frac{\sin 2\pi W(\tau + \rho u)}{2\pi W(\tau + \rho u)} du \quad , \quad (3.25)$$

and so, in the limit, R_1 as a function of ρ and τ is

$$R_1(\rho, \tau) = \overline{f'_0} / \overline{f_0} = \frac{\text{Si } 2\pi W(\tau + \rho T/2) - \text{Si } 2\pi W(\tau - \rho T/2)}{2\pi W\rho T} \quad , \quad (3.26)$$

where

$$S_{i\lambda} = \int_0^\lambda \frac{\sin q}{q} dq \quad . \quad (3.27)$$

As a function of time desynchronization τ alone, this becomes

$$R(0, \tau) = \frac{\sin 2\pi W\tau}{2\pi W\tau} \quad , \quad (3.28)$$

which, as would be expected, is identical with the autocorrelation function corresponding to an energy spectrum flat from $\omega=0$ to $2\pi W$, and zero elsewhere.

As a function of rate desynchronization ρ alone,

$$R(\rho, 0) = \frac{\text{Si } \pi W\rho T}{\pi W\rho T} \quad , \quad (3.29)$$

which is plotted in Figure 3.3.

B. Low-Pass Detection of Fixed Band-Pass Signals

When a gaussian signal is limited to a bandwidth W much smaller than its center frequency it is expressible as

$$f(t) = \alpha(t)\cos pt + \beta(t)\sin pt \quad , \quad (2.54)$$

where p is a radian frequency near the band center and the functions $\alpha(t)$ and $\beta(t)$, which will be termed amplitude functions, are independent gaussianly-distributed variables with the same variance and zero mean. The signal has the character of a sinusoid of radian frequency p which has been randomly amplitude- and phase-modulated. Rice²¹ has shown that the quantity $(\alpha^2 + \beta^2)^{1/2}$ has an average fluctuation rate on the order of the bandwidth, from which we

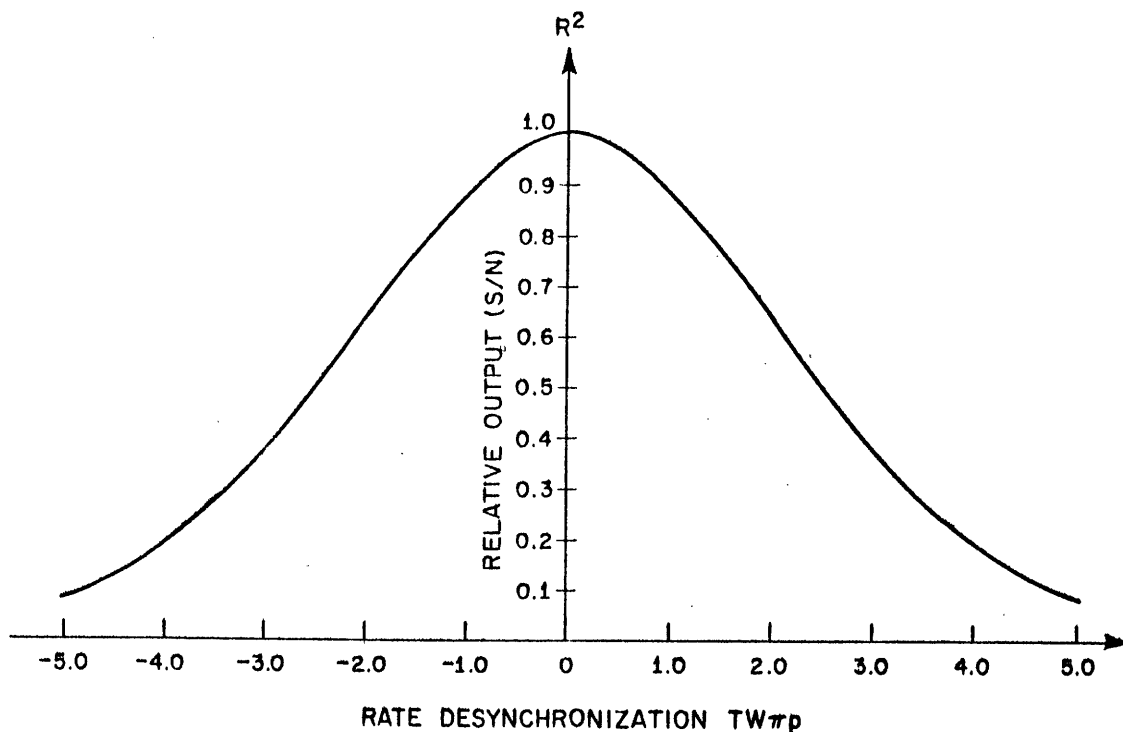


Fig. 3.3. Effect of rate desynchronization on output signal-to-noise ratio for low-pass or matched-filter detection of low-pass rectangular-band signal

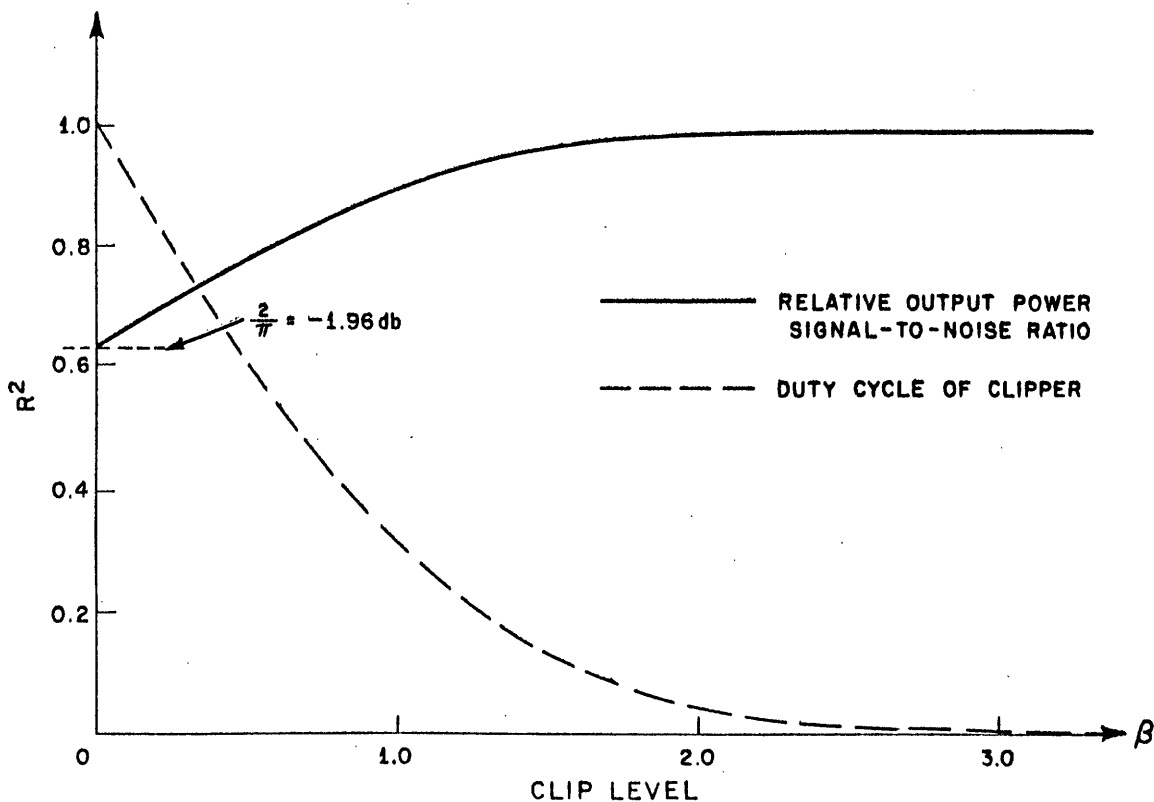


Fig. 3.4. Relative correlator output signal-to-noise ratio and clipper duty cycle for symmetrical peak clipping of one of two Gaussian signals

may conclude that, $\alpha(t)$ and $\beta(t)$ being independent, they will each have average fluctuation rates of about this order of magnitude.

We will consider as $x(t)$ a portion T seconds long of such a narrow band gaussian function, as depicted in Figure 3.2a, and will assume that $p \gg W \gg 1/T$. Under these conditions, the "carrier" goes through many cycles during one cycle of fluctuation of either amplitude function. Further, the amplitude functions undergo many alternations during the signal duration. As before, when desynchronization is present, as in Figure 3.2b, the output, which can be visualized as the area under the product waveform derived from multiplying the two signals, will be diminished from its value for the condition of Figure 3.2a. It is seen that rate desynchronization is much more serious here than in the low-pass case depicted in Figure 3.1, since a significant loss in output results if the signal durations differ by so much as a cycle or two of the "carrier." Time desynchronization is also more critical since the time origins of the two signals must coincide within a fraction of a carrier cycle.

Let us assume at the outset that the rate parameter p is less than, say, $6\pi/pT$. We will find at the end of the analysis that it may not even be this large before a prohibitively large loss in output occurs. Similarly, let us take τ as less than several carrier cycles, say three, so that $\tau \ll 6\pi/p$.

The effect of rate desynchronization on the amplitude functions will thus have a negligible influence on the output compared to its effect on the carrier. Therefore, in writing

$$f_o' = \int_{-T/2}^{T/2} \left[\alpha(t+a_o) \cos p(t+a_1 t+a_o) + \beta(t+a_o) \sin p(t+a_1 t+a_o) \right] \times \left[\alpha(t+b_o) \cos p(t+b_1 t+b_o) + \beta(t+b_o) \sin p(t+b_1 t+b_o) \right] dt \quad (3.30)$$

the rate term is omitted from $\alpha(t)$ and $\beta(t)$. Expanding,

$$f_o' = \frac{1}{2} \int_{-T/2}^{T/2} [\alpha(t+a_o)\alpha(t+b_o) + \beta(t+a_o)\beta(t+b_o)] \cos p(\tau+pt) dt$$

$$+ \frac{1}{2} \int_{-T/2}^{T/2} [\alpha(t+b_o)\beta(t+a_o) - \alpha(t+a_o)\beta(t+b_o)] \sin p(\tau+pt) dt \quad ,$$
(3.31)

the double-frequency terms being ignored in comparison to those for which the trigonometric argument is the very much smaller $(a_1 - b_1)pt = pt\rho$. Then

$$f_o' = \frac{1}{2} \cos p\tau \left\{ \int [\alpha(t+a_o)\alpha(t+b_o) + \beta(t+a_o)\beta(t+b_o)] \cos pt \rho dt \right.$$

$$\left. + \int [\alpha(t+b_o)\beta(t+a_o) - \alpha(t+a_o)\beta(t+b_o)] \sin pt \rho dt \right\}$$

$$+ \frac{1}{2} \sin p\tau \left\{ - \int [\alpha(t+a_o)\alpha(t+b_o) + \beta(t+a_o)\beta(t+b_o)] \sin pt \rho dt \right.$$

$$\left. + \int [\alpha(t+b_o)\beta(t+a_o) - \alpha(t+a_o)\beta(t+b_o)] \cos pt \rho dt \right\} \quad .$$
(3.32)

where the limits of integration are $-T/2$ and $T/2$.

Each integrand is the product of two factors, the first varying many times in the signal interval, and the second a low-frequency sinusoid independently executing at most three alternations during the interval. (ρ was assumed $\ll 6\pi/pT$). We therefore rewrite the integrand as the first factor times the average of the second factor over the interval, giving

$$f_o' = \frac{1}{2} \cos p\tau \frac{\sin pT\rho/2}{pT\rho/2} \int [\alpha(t+a_o)\alpha(t+b_o) + \beta(t+a_o)\beta(t+b_o)] dt \quad (3.33)$$

$$+ \frac{1}{2} \sin p\tau \frac{\sin pT\rho/2}{pT\rho/2} \int [\alpha(t+b_o)\beta(t+a_o) - \alpha(t+a_o)\beta(t+b_o)] dt$$

$$= \frac{1}{2} \cos p\tau [\phi_{\alpha\alpha}(\tau) + \phi_{\beta\beta}(\tau)] \frac{\sin pT\rho/2}{pT\rho/2} \quad (3.34)$$

$$- \frac{1}{2} \sin p\tau [\phi_{\beta\alpha}(\tau) - \phi_{\alpha\beta}(\tau)] \frac{\sin pT\rho/2}{pT\rho/2} ,$$

in which a representative correlation term ϕ is

$$\phi_{\alpha\beta}(\tau) = \int_{-T/2}^{T/2} \alpha(t) \beta(t+\tau) dt \approx \int_{-T/2}^{T/2} \alpha(t+b_o) \beta(t+a_o) dt \quad (3.35)$$

for values of a_o and $b_o \ll T$.

The amplitude functions $\alpha(t)$ and $\beta(t)$ have identical statistical properties over an ensemble of functions $x(t)$ with the specified spectrum. Thus if the present analysis were a calculation of ensemble average effects, we would have

$$\phi_{\alpha\alpha}(\tau) = \phi_{\beta\beta}(\tau) \quad \text{and} \quad \phi_{\alpha\beta}(\tau) = \phi_{\beta\alpha}(\tau) . \quad (3.36)$$

We would like to deal, however, with only one member function of the ensemble. In the absence of an explicit description of the function $x(t)$, we can only say that when its duration is very large compared to the average fluctuation

period of $\alpha(t)$ and $\beta(t)$, their time average properties will begin to converge to the ensemble statistical properties. So, for large TW , we are able to rewrite f_o' as approximately

$$f_o' = \phi_{aa}(\tau) \cos p\tau \frac{\sin pT\rho/2}{pT\rho/2}, \quad (3.37)$$

so that the ratio of this to f_o , which is f_o' evaluated for $\tau=\rho=0$, is

$$\frac{f_o'}{f_o} = R(\rho, \tau) = \frac{\phi_{aa}(\tau)}{\phi_{aa}(0)} \cos p\tau \frac{\sin pT\rho/2}{pT\rho/2}. \quad (3.38)$$

As a function of time desynchronization alone this has the form of a slowly decaying cosine wave, as is to be expected from the known character of the correlation function of a narrow-band function, and in particular when $\rho=0$

$$R(0, \tau) = \frac{\phi_{aa}(\tau)}{\phi_{aa}(0)} \cos p\tau. \quad (3.39)$$

As a function of rate desynchronization alone equation 3.38 has the form of a $\sin x/x$ function, and in particular when $\tau=0$,

$$R(\rho, 0) = \frac{\sin pT\rho/2}{pT\rho/2}. \quad (3.40)$$

C. Matched Filter Detection

For the matched filter operated as in Figure 1.3b, with sampling occurring at the exact instant representing the termination of the nominal

signal $x(t)$, the behavior with time and rate desynchronization present is that given in Equations 3.26 and 3.38. ($r(t)$ is now $x(T/2 - t)$ and the output is $f_0(T/2)$.)

However, it is possible that the operation of this type of detector might be modified so that the output peak is observed whenever this happens to be. The effect of time desynchronization is then absent entirely, and the pertinent equations are now 3.29 and 3.40. This is the peculiar advantage of the matched filter type of detection. Since the output waveform will always be the crosscorrelation function of the input voltage and the filter impulse response reversed, different times of occurrence of the input result in different times of occurrence of this output, but not in any diminution of it such as is the effect in low-pass or band-pass detection. One pays for this advantage, however, by having to observe the output not at a particular instant, but over a period of time during which noise is allowed to pass through together with the momentary signal peak.

D. Low-Pass Continuous Detection

The effect of the time desynchronization term on the output of this type of detector can be derived by suitably defining the cascaded arbitrary linear system which was assumed present in one correlator input (Figure 2.1a). Since the signal is assumed stationary, the time desynchronization a_0 in one input and b_0 in the other may be lumped as $(a_0 - b_0) = \tau$ in one input, $H(\omega)$ then being specified as $e^{j\omega\tau}$.

For input signal-to-noise ratios small enough so that output self-noise is not a factor, we have seen that the quantity R^2 is the ratio of signal

output power with desynchronization to that without desynchronization. In this case these powers are directly available as the numerator of equation 2.38 evaluated for these two conditions. We thus have

$$R^2(\tau) = \frac{\left[\int_0^\infty X(\omega) \cos \omega \tau d\omega \right]^2}{\left[\int_0^\infty X(\omega) d\omega \right]^2} = \frac{\phi_x^2(\tau)}{\phi_x^2(0)} \quad (3.41)$$

whether or not the signal is gaussian. On the other hand, if the input signal-to-noise ratio is high, whereupon the self-noise is the predominant output fluctuation term, we see from equation 3.2 that R^2 is the ratio of $(S/N)_o$ of equation 2.38 evaluated with desynchronization present to $(S/N)_o$ with it absent. In both cases only the self-noise term is retained in the denominator of equation 2.38. The result is

$$R^2(\tau) = \frac{\phi_x^2(\tau) \int_0^\infty X^2(\omega) d\omega}{\phi_x^2(0) \int_0^\infty X^2(\omega) \cos^2 \omega \tau d\omega} \quad (3.42)$$

The self-noise denominator is seen to decrease from

$$\int_0^\infty X^2(\omega) d\omega$$

to one-half this value as τ is increased from zero to sufficiently high values. This can be explained by returning to the derivation of $(S/N)_o$ of Section 2.4. Examination of equation 2.26 for $V_I(2\pi n/\theta)$ shows that for $\tau=0$ (that is, $h_i = \text{constant}$, $\eta_i = 0$) there is a voltage addition of two

sets of difference frequency terms, whereas, for large τ , they add incoherently on a power basis. The distinction between the two sets of terms is that if a two-sided frequency scale had been used, one set would lie at the negative of the frequency of the other set.

E. Band-Pass Continuous Detection

Here for low input signal-to-noise ratios we have from equation 2.52

$$R^2(\tau) = \frac{\left[\int_0^{\infty} X(\omega) \cos \omega\tau \, d\omega \right]^2 + \left[\int_0^{\infty} X(\omega) \sin \omega\tau \, d\omega \right]^2}{\left[\int_0^{\infty} X(\omega) \, d\omega \right]^2} \quad (3.43)$$

whether the signal is gaussian or not. For high input signal-to-noise ratio and a gaussian signal the result is the same since the self-noise power is actually independent of τ . But as we have seen in Section 2.6, the character of the self-noise changes with τ . A given amount of self-noise power is twice as effective when the complex self-noise spectrum is symmetrical about the difference frequency (as is the case when $\tau=0$) as when the spectrum is that of a filtered random noise (equation 2.55) (as it will be when τ is sufficiently large so that $x(t)$ and $x(t+\tau)$ are independent). So, in spite of the constant self-noise power with τ , the situation is much the same as for low-pass continuous detection. The effect of the self-noise is twice as great for very small τ as for very large τ .

It is interesting to note that the numerator of equation 3.43 is simply the square of the envelope of the correlation function of $x(t)$, $\phi(\tau)$. This may be shown most easily by recognizing that the envelope of

DECLASSIFIED

$\phi(\tau)$ is the square root of the sum of the squares of $\phi(\tau)$ and its Hilbert transform (which we may write $\phi'(\tau)$). The latter represents the imaginary part of a hypothetical rotating vector the real part of which is $\phi(\tau)$. The first squared term in the numerator of equation 3.43 is seen to be $\phi(\tau)$ and the second $\phi'(\tau)$.

A corollary to this is that since the correlation function of the envelope is independent of the center frequency of $X(\omega)$, if $X(\omega)$ is even about some center frequency ω_1 , then the numerator of equation 3.43 can be easily evaluated by choosing the frequency origin at ω_1 , whereupon the second term vanishes.

3.3 Amplitude Distortion

A second important respect in which the actual correlator inputs $x_1(t)$ and $x_2(t)$ may differ from the nominal $x(t)$ is in their amplitudes. In this section we will treat the effect on R (equation 3.1) of amplitude distortion. This is defined as a time invariant effect on $x(t)$ which maps the voltage levels of $x(t)$ uniquely onto voltage levels for, say, $x_1(t)$, but for which corresponding levels are not necessarily related by a simple constant of proportionality. For example, the action of a stage with limited dynamic range might be to make all levels of the output equal to those levels of the input less than a certain maximum, and equal to this maximum value for higher input voltages.

We will now compute R from equation 3.2 by first determining individually the three quantities (S_o'/S_o) , (N_o'/N_o) , and (S_i'/S_i) . Since signal

DECLASSIFIED



distortions cannot affect the input noise power, we have for the fourth factor $(N_i'/N_i)=1$ as before.

A. Low-Pass and Matched Filter Detection

In the analysis of Sections 2.2 and 2.3 it was seen that the output signal component is given by the autocorrelation $\phi_{xx}(0)$ of the signal $x(t)$. If one or both of the actual correlator input signals is an amplitude-distorted version of $x(t)$, this output signal component will be changed, as will the output noise component.

With $x(t)$ being the undistorted signal, we write

$$x_1(t) = V_1 [x(t)] \tag{3.44}$$

and

$$x_2(t) = V_2 [x(t)] \tag{3.45}$$

for the distorted signals, where $V_1(x)$ and $V_2(x)$ are time invariant single-valued functions of the amplitude x . An amplitude density function $W(x)$ is here defined for both fixed and continuous operation by saying that

$$\int_{-\infty}^a W(x) dx$$

is the fraction of the time duration of $x(t)$ that $x \leq a$.

When distortion is impressed on the nominal function of $x(t)$, the output signal power is changed by a factor

$$(S_o'/S_o) = \left[\int_a^b x_1(t)x_2(t)dt \right]^2 / \left[\int_a^b x^2(t)dt \right]^2 \tag{3.46}$$



where the range of the integral is from $\alpha=0$ to $\beta=T$ for fixed operation. For continuous operation, the range is $\alpha=-\theta/2$ to $\beta=\theta/2$ and the integrals are evaluated by dividing each by θ and allowing $\theta \rightarrow \infty$. For both fixed and continuous operation this factor can be rewritten in terms of the amplitude scale as

$$(S_o' / S_o) = \left[\int_{-\infty}^{\infty} V_1(x) V_2(x) W(x) dx \right]^2 / \left[\int_{-\infty}^{\infty} x^2 W(x) dx \right]^2 \quad (3.47)$$

The power in the signal $x_1(t)$ is changed by a factor

$$(S_i' / S_i) = \int_{-\infty}^{\infty} V_1^2(x) W(x) dx / \int_{-\infty}^{\infty} x^2 W(x) dx \quad (3.48)$$

by the distortion operation.

At low values of input signal-to-noise ratio the term (N_o' / N_o) involves only the effect of channel noise. We will not consider the case of continuous type operation at high input signal-to-noise ratios, for which the self-noise (also a function of signal distortion²²) predominates in the output. If it is $x_1(t)$ to which the channel noise has been added, and this noise is gaussian and white, of spectral density $N_o/2$, the noise output power is altered by a factor

$$\begin{aligned} (N_o' / N_o) &= \int_{-\infty}^{\infty} X_2(\omega) \frac{N_o}{2} d\omega / \int_{-\infty}^{\infty} X(\omega) \frac{N_o}{2} d\omega \\ &= \int_{\alpha}^{\beta} x_2^2(t) dt / \int_{\alpha}^{\beta} x^2(t) dt = \int_{-\infty}^{\infty} \frac{V^2(x) W(x) dx}{2} / \int_{-\infty}^{\infty} x^2 W(x) dx \end{aligned} \quad (3.49)$$

(where $X(\omega)$ is an energy density spectrum for fixed operation and a power density spectrum for continuous operation).

From equations 3.2, 3.46, 3.48, and 3.49 we have for R^2 as a function of the functions $V_1(x)$, $V_2(x)$, and $W(x)$

$$R^2(V_1, V_2, W) = \frac{\left[\int_{-\infty}^{\infty} V_1(x)V_2(x)W(x) dx \right]^2}{\int_{-\infty}^{\infty} V_1^2(x)W(x) dx \int_{-\infty}^{\infty} V_2^2(x)W(x) dx} \quad (3.50)$$

The application of this formula is of course a matter of specific calculation for choices of V_1 , V_2 , and W appropriate to a particular situation. As a representative case of some interest a computation has been made for the situation in which the signal is nominally gaussian and one correlator input signal has been symmetrically peak-clipped. This case is of practical importance in practical NOMAC systems since it represents cases in which either the receiver storage medium or the transmitter has a symmetrical amplitude limitation. The assumptions are that $W(x)$ is gaussian with mean zero and that the amplitudes of only one of the two signals x_1 or x_2 are different from those of x , this difference being that a clipping at plus and minus β times the standard deviation has taken place. From equation 3.50

$$R^2(\beta) = \frac{\left[\frac{2}{\sqrt{2\pi}} \int_0^\beta x^2 e^{-x^2/2} dx + \frac{2}{\sqrt{2\pi}} \int_\beta^\infty \beta x e^{-x^2/2} dx \right]^2}{\left[\frac{2}{\sqrt{2\pi}} \int_0^\beta x^2 e^{-x^2/2} dx + \frac{2}{\sqrt{2\pi}} \int_\beta^\infty \beta^2 e^{-x^2/2} dx \right]} x_1 \quad (3.51)$$

This expression is plotted in Figure 3.4 together with

$$\frac{2}{\sqrt{2\pi}} \int_\beta^\infty e^{-x^2/2} dx \quad (3.52)$$

the fraction of the time that the clipper is actuated. It is seen that R^2 drops off at about the same rate as the clipper duty cycle increases, but that the minimum value of R^2 (occurring at the "completely clipped" condition $\beta=0$) is $2/\pi$, or -1.96 decibels.

For the effect of other types of distortions of one of a pair of gaussian signals, the reader is referred to a study by Bussgang²³ which treats a variety of cases. With suitable renormalization, the results are directly applicable to the above equation 3.50.

B. Band-Pass Detection

The interaction of two band-pass signals in producing a difference-frequency tone when one or both have been amplitude distorted is not as amenable to analysis as the preceding case in which the instantaneous voltages of the two time functions are multiplied and the product waveform integrated.

Certain specific cases can be analyzed however, and one of these is the case of symmetrical peak-clipping which was just discussed. We write the nominal function as

$$x(t) = e(t)\cos (pt + \phi(t)) \quad (1.10)$$

for one correlator input and

$$x'(t) = e(t)\cos [(p+\Delta)t + \phi(t)] \quad (1.11)$$

for the other. We now suppose that one of the actual functions, say $x_1(t)$, is the undistorted $x(t)$, but $x'(t)$ has been completely peak-clipped, so that only the zero-crossing configuration has been preserved, and not the

envelope fluctuations. Although the clipped function is a "square-wave," the harmonics of the "carrier" will usually be removed by filtering in a practical system. The function actually entering the second correlator input can thus be considered a phase-modulated sine wave of constant amplitude, say P.

We thus have

$$x_1(t) = e(t) \cos (pt + \phi(t)) \quad (3.53)$$

and

$$x_2(t) = P \cos [(p+\Delta)t + \phi(t)] \quad (3.54)$$

The infinite-time-averaged amplitude of the difference-frequency tone (the output signal) is nominally

$$\lim_{\theta \rightarrow \infty} \frac{1}{2\theta} \int_{-\theta/2}^{\theta/2} e^2(t) dt = \frac{1}{2} \int_0^{\infty} e^2 W(e) de \quad (3.55)$$

where $W(e)$ is the amplitude density distribution of the nominal envelope function $e(t)$, defined in precisely the same way that $W(x)$ was defined before for the entire function $x(t)$. So when distortion is present, the output signal power is changed by a factor

$$(S_0'/S_0) = \left[\int_0^{\infty} PeW(e) de \right]^2 / \left[\int_0^{\infty} e^2 W(e) de \right]^2 \quad (3.56)$$

The power in $x_1(t)$ has not been altered from its nominal value, so $(S_1'/S_1)=1$. Assuming that the (white) channel noise is added to $x_1(t)$, then the output noise contribution from this cause is altered by a factor

$$(N_o' / N_o) = P^2 / \int_0^{\infty} e^2 W(e) de \quad , \quad (3.57)$$

as determined in a manner similar to equation 3.49.

So we have

$$R^2 = \left[\int_0^{\infty} e W(e) de \right]^2 / \int_0^{\infty} e^2 W(e) de \quad . \quad (3.58)$$

The result would have been the same had it been $x_2(t)$ to which the channel noise was added, since (N_o' / N) would be unity and (S_1' / S_1) would be the same as equation 3.57.

For the case of $x(t)$ a gaussian signal, $W(e)$ is the Rayleigh distribution for which equation 3.58 (the ratio of the square of the first moment to the second moment) gives

$$R = \pi/4, \quad \text{or} \quad -1.06 \text{ db}$$

A direct comparison of this figure and the 1.96 db obtained for low-pass detection is not strictly appropriate since in the above result it was assumed that the clipped band-pass function was filtered to remove the harmonics. In the analysis of low-pass detection, this filtering was absent.

In a practical system using band-pass signals the filtering will usually occur, and it is of interest to know the effect for low-pass detection. The calculation is identical to that of equations 3.53 through 3.58, equation 3.55 now representing a d.c. level rather than the amplitude of the difference-frequency tone. The result for gaussian signals is again that complete clipping of one signal causes a loss in relative output signal-to-noise ratio of 1.06 decibels.

The fact that output signal-to-noise ratio for the same input signal-to-noise ratio is only one or two decibels less when one signal is completely clipped than it would be if it were a perfect replica of the nominal signal is quite significant. It means that as long as the amplitude distortion is of this particular kind, the system performance might not be significantly impaired. As a matter of fact, one might be very willing to trade the one or two decibels loss in $(S/N)_o$ for the convenience of storing or transmitting a constant amplitude signal.

3.4 Frequency Distortion

The term "frequency distortion" is usually used to describe the alteration of the amplitude spectrum of a signal, and "phase distortion" the alteration of the phase spectrum. Here frequency distortion means the alteration of the complex spectrum (the real part of which is the magnitude spectrum, and the imaginary part the phase spectrum). This type of distortion might be caused, for example, by dissimilar filtering of the two correlator inputs somewhere in the system. The particular case in which multipath effects can be described in terms of a filtering operation on the signals will be discussed in detail in Chapter V.

The output signal-to-noise ratio expressions 2.15, 2.38, and 2.52 can be used to deduce the effect of frequency distortion on the correlator output when the quantity $H(\omega)$ represents the difference in the complex spectra of the two correlator inputs.

A detailed analysis of this type of distortion, leading to a precise expression for R (equation 3.2) will not be carried out here. For a particular case, the calculation can be quickly made using the signal-to-noise

ratio expressions. Here it will merely be pointed out that the effect will not be of significant proportions if 1) the magnitude spectra of filters used in the system are not such as to remove an appreciable fraction of the total spectrum $X(\omega)$, and 2) the slopes of the phase spectra at correlator inputs do not differ by more than some quantity τ_{\max} over that portion of the bandwidth occupied by the predominant part of $X(\omega)$. The quantity τ_{\max} is roughly the time desynchronization (Section 3.2) necessary for severe loss in output, and depends on the type of correlator. These rule-of-thumb conditions are fairly simple to observe in a physical system particularly if one chooses a type of operation where τ_{\max} is given by the reciprocal of the signal bandwidth, rather than the signal center frequency. (See Section 3.5.)

3.5 Conclusions

We have examined the more important sources of possible dissimilarities in the two waveforms to be correlated. From the analyses we may conclude that, of these, the problem of desynchronization will probably be the most troublesome in the realization of a stored-reference system. Reasonable amplitude and frequency distortion effects were found to cause only moderate decreases in system performance.

The magnitude of the synchronization requirement was seen to be very much a function of the type of correlation detector used. Table II compares the requirements on time and rate tolerances to maintain less than a 3 db loss in output signal-to-noise ratio when rectangular-band signals of

bandwidth W cycles-per-second are used. The center frequency (in cycles-per-second) of band-pass signals of this type is written f_c here.

Type Detector	Type Signal	Equation No.	Maximum τ	Maximum ρ
Low-pass ideal	Fixed low-pass white gaussian	3.26	.25/W	.79/TW
Low-pass ideal	Fixed band-pass gaussian	3.38	.125/ f_c	.50/ $f_c T$
Low-pass	Continuous low-pass	3.41	.25/W	0
Low-pass	Continuous band-pass	3.41	.125/ f_c	0
Matched filter	Fixed low-pass white gaussian	3.29	----	.79/TW
Matched filter	Fixed band-pass gaussian	3.40	----	.50/ $f_c T$
Band-pass	Continuous band-pass	3.43	.50/W	0

TABLE II

Maximum tolerable time desynchronization (τ) and rate desynchronization (ρ) to maintain $R > .707$.

The analysis shows that for low-pass detection of low-pass signals, time desynchronization of the pair of signals must not be greater than the order of the reciprocal of the bandwidth, whereas for band-pass signals, the tolerance allowed is only of the order of the reciprocal of the

center frequency; that is, a "phase lock" is required between the two signals. However, for band-pass detection, (for which band-pass signals are used by definition) time desynchronization need be kept only within the reciprocal of the bandwidth.

In a radio communication link, the transmitted signals must be of a band-pass character. To convert these at the receiver to low-pass signals would mean either a difficult synchronous detection operation or a nonlinear detection with its consequent loss in signal-to-noise ratio. (Specifically, for small receiver input signal-to-noise ratios, the nonlinear detection process produces a new power signal-to-noise ratio which is approximately the square of the predetection power signal-to-noise ratio).²⁵ By using a band-pass correlation detection one achieves the same latitude in time synchronization as if the signal were a low-pass function. Therefore, the band-pass type detection is the detection method preferred in devising a physical stored signal system. This is fortunate in that previous studies¹¹ have shown that one of the simplest correlation schemes, a mixer tube followed by a band-pass filter is as good as is usually required. In low-pass detection, it is not possible to use such a simple multiplier as a mixer tube because of quiescent components and undesired cross-product components about zero frequency.

As for the matched filter type of stored-reference system, if one can devise a flexible system of sampling at the output peak regardless of its time of occurrence, the time synchronization requirement is absent by definition. This is the situation assumed in Table II. However, attention must still be given to the possibility of desynchronization in rate. If

a low-pass matched filter is used, the rate factor ρ must be kept within the order of the reciprocal of the time-bandwidth product. However, for the more desirable band-pass type of signal, this figure becomes the reciprocal of the time-center frequency product. This may mean a troublesome stability requirement on the matched filter's impulse response.

CHAPTER IV

AN EXPERIMENTAL STORED-SIGNAL SYSTEM

4.1 Introduction

The choice between the matched filter and stored-signal types for a physical realization of the stored-reference type of NOMAC system hinges principally on the two questions of synchronization and storage.

The synchronization problem is potentially much simpler in the matched filter type of system. However the problem of storing a wide-band noise-like signal as the impulse response of a linear system is a very difficult one and a satisfactory solution does not appear imminent.¹³ On the other hand, the possibilities for storage as a function of time are a good bit more encouraging, since there exist a number of fairly well-developed storage methods of this type.

In view of the difficulty of suitable matched filter realization, it was decided to devote attention to the design and construction of an operating laboratory model of the stored-signal type of system. A particular form of experimental system has been built, and will now be described in detail, giving the reasons for attacking the problem in this particular way. Pertinent experimental results will be presented and compared with theory, and recommendations will be made for further refinement for actual operating use.

4.2 Requirements on the Storage Medium

Certain equipment techniques already in use¹² with transmitted-reference type NOMAC systems may be taken over intact in the design of a

stored signal system -- specifically methods of performing the modulation of intelligence onto the noise at the transmitter, and the correlation operation at the receiver. However, the problem of providing a synchronized noise-like signal having suitable characteristics is another matter. There are a number of requirements on the storage operation of varying degrees of severity.

Time Scale Stability: The results of Section 3.2 indicate the orders of magnitude of the synchronization requirement when various types of correlator are employed as the detector. To qualify for consideration, the available time scale stability of a proposed storage method must meet this requirement. In conjunction with this, the system must also be capable of a convenient initial synchronization followed by periodic re-synchronizations. The re-synchronization operation should be required as infrequently as possible, and should cause a minimum in interruption of the information flow. Thus it is clear that the storage medium must not only preserve an accurate time scale, but must be easy to start or reset. One might express these two requirements by saying that the time scale of the system should be capable of displaying a "low inertia" when readjustment is desired, and a "high inertia" during normal operation.

Capacity: The results of Chapter II show that the crucial system parameter describing the signal-to-noise ratio improvement is the time-bandwidth product of the waveforms or waveform segments used as symbols. This places a corresponding requirement on the capacity of the storage medium. The symbol duration is usually fixed by the prime source of

[REDACTED]

data from which the system operates and the bandwidth by frequency allocation considerations although it is possible that synchronization requirements may also dictate upper bounds on symbol duration and bandwidth.

The presence of multipath or echo conditions in the propagation path can cause intersymbol interference if the stored signal is repeated with a period shorter than the total spread of propagation times of the various paths. Interference results when two of the transmission paths differ in propagation time by very nearly the signal repetition period. Then every received signal has mixed with it an interfering signal which is the preceding symbol. There are situations, therefore, in which a lower limit might be imposed on the repetition period of the waveform being stored; this lower limit is equal to the spread in time of all propagation paths. This figure is very seldom more than ten milliseconds.

Random Character: As a countermeasure against undesired interception and jamming, the signal should be as difficult to analyze and reproduce as possible, as pointed out in Chapter I. The need for security of the reference signal is a third reason for making it of long duration.

It should be convenient to change the stored reference at will. To a certain extent, ability to change the signal at frequent intervals (or in the language of the cryptographer, change the key) can be traded for difficulty of analysis, since the latter can be expressed in terms of the length of time operation may be continued before the key must be considered insecure. An assumption which is customarily made in such cases is that the enemy has a complete version of the equipment, save for the key, so

that the burden of security falls on the key itself and not on the ingenuity or complexity of the equipment.

A number of possible storage methods were examined in the light of these requirements. Among presently employed storage schemes are such methods as

- 1) Magnetic recording on tape or drums
- 2) Optical recording on film
- 3) Cathode ray tube function generators
- 4) Storage tubes
- 5) Sonic delay line storage
- 6) Galactic noise
- 7) Digital storage registers

In one way or another the first six of these have serious limitations in their present suitability to the problem. In any of the mechanical methods it is possible in principle to lock the mean speed of the prime mover to some stable frequency source such as a crystal oscillator. Even when this is done, however, there remain fluctuations about the mean velocity of the medium past the record or playback point. In tape and film recording this is quite severe, and at the present state of the art the minimum fluctuation seems to be one part in 10^4 rms speed deviation.²⁵ For magnetic drums the figure is lower,²⁶ the difference being due to the greater rigidity with which the magnetic medium is attached to a high inertia member.

The storage capacity of magnetic recording techniques is adequate, bandwidths of the order of a megacycle being attainable. The capacity

[REDACTED]

of cathode ray tube function generators²⁷ on the other hand is quite limited. This together with the difficulty of providing an extremely close tolerance on the sweeping waveform constitutes a serious objection to their use. This type of function generator as well as the storage tube method does have the advantage of being relatively inertialess and it is the lack of this feature which is one of the principle indictments of any mechanical storage system.

Both storage tube²⁸ and delay²⁹ line memories have the disadvantage of storing information in a "volatile" way, that is, the storage is not permanent, but a re-recording at intervals is necessary. This makes these two methods, especially the latter, very vulnerable to temporary component or power failures.

In 1951, J.B. Wiesner suggested using as the reference signal certain noise-like radiations which have been observed to emanate from various regions of outer space.³⁰ If it is found that such galactic noise signals are strong and constant enough and near enough alike at different locations on the earth's surface, they might provide very reliable reference signals. Because these signals would be gotten from highly directional antennas they would be very difficult to jam. If the present rate of discovery of new regions of high galactic noise activity continues, the choice of possible reference signals will be large enough to make analysis difficult.

At the present writing, the investigations necessary to explore thoroughly the possibilities of this type of reference signal have hardly begun, so that the technique must be considered unavailable for some time yet. Certain studies have been made³¹ of the coherence between galactic

signals received at two different points on the earth's surface from the same region of outer space. Although the results are seemingly negative (in that very little correlation between the two received signals was found), they must be regarded as quite inconclusive, since the data were taken on the signal level averaged over several seconds, and not on the "r.f." fine structure of the signals. The amplitude levels were apparently affected separately by the local terrestrial atmospheric conditions intervening between the source and each receiver. These conditions may be found to change slowly enough so that any coherence in the two signals is not destroyed.

In contrast to these findings on other types of storage are the potentialities inherent in a digital storage scheme. The possibilities of high stability are limited only by the clocking source itself. The bandwidth limitation may be considered to reside in the upper limit of available counting speeds. The key by which the waveform is constructed is permanent. When a synchronization is desired, the entire waveform can be restarted in a length of time on the order of microseconds.

These considerations have led to the conclusion that a digital method should be sought which derived a complex pseudo-random waveform from the output of a stable oscillator, and which did so according to a key which could be conveniently changed.

4.3 Description of the Experimental System

The decision to use a crystal controlled oscillator as the time base for a noise-like signal poses the question: How can one derive a signal

with an apparently random character from something as "unrandom" as a constant-frequency sinusoid? One answer is to generate from this sinusoid a second signal, of required bandwidth, which is also periodic, but whose period is so long as to constitute a formidable amount of waveform for an enemy analyst to have to reconstruct. This principle is implemented in the signal generator schematized in Figure 4.1. The blocks in Figure 4.1 correspond to units occupying the same position beginning at the top of each relay rack shown in Figure 4.2.

The system derives a band-pass noise-like signal having a repetition time of 10.4 seconds from a quartz crystal oscillator operating at 200 kilocycles. The signal has an effective bandwidth of some 30 kilocycles and can be reset to its beginning in 20 microseconds.

The method of operation is as follows: 200 kilocycle clock pulses are fed into each of three electronic commutators. In the first of these, a predetermined arbitrary three out of every 129 clock pulses are passed on to output number 1. A different three occur at output number 2, and so forth for outputs 3, 4, and 5. Each output thus consists of a train of 3 pulses repeating every 129 clock pulses. When each output is combined with similar outputs from the other two commutators, repeating once every 128 and 127 clock pulses, respectively, the result is a pulse train whose repetition period is

$$127 \times 128 \times 129 / 200 \times 10^3 = 10.4 \text{ seconds,}$$

since the largest common division of 127, 128, and 129 is unity. There are five such waveforms, all different, and each is used to shock excite a parallel R-L-C resonant circuit. The five resonators are stagger-tuned

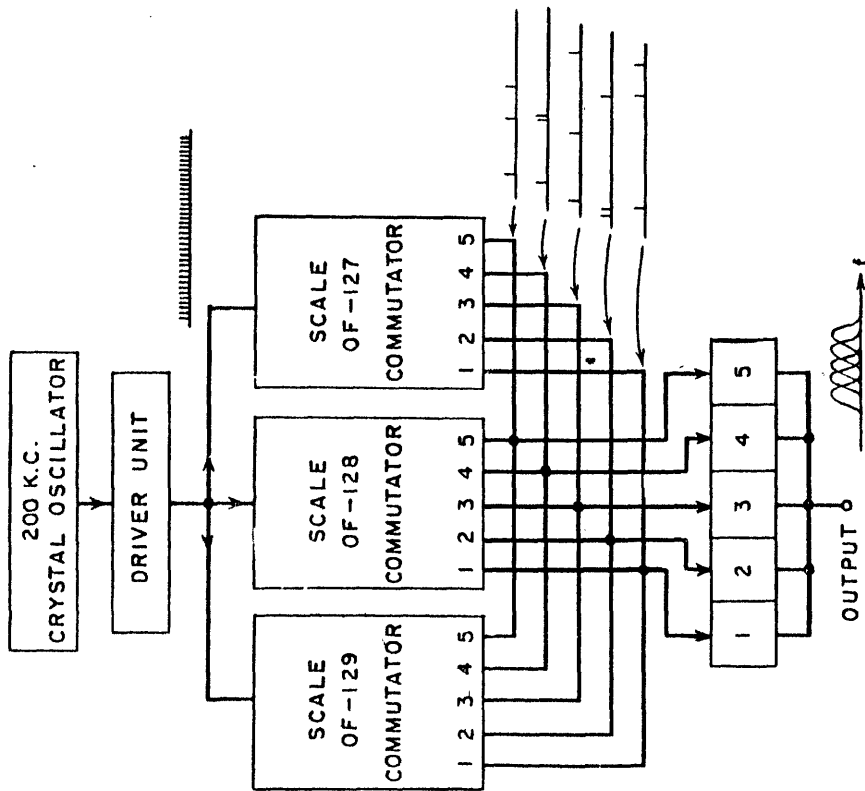


Fig. 4.1. Block diagram of digital signal generator.

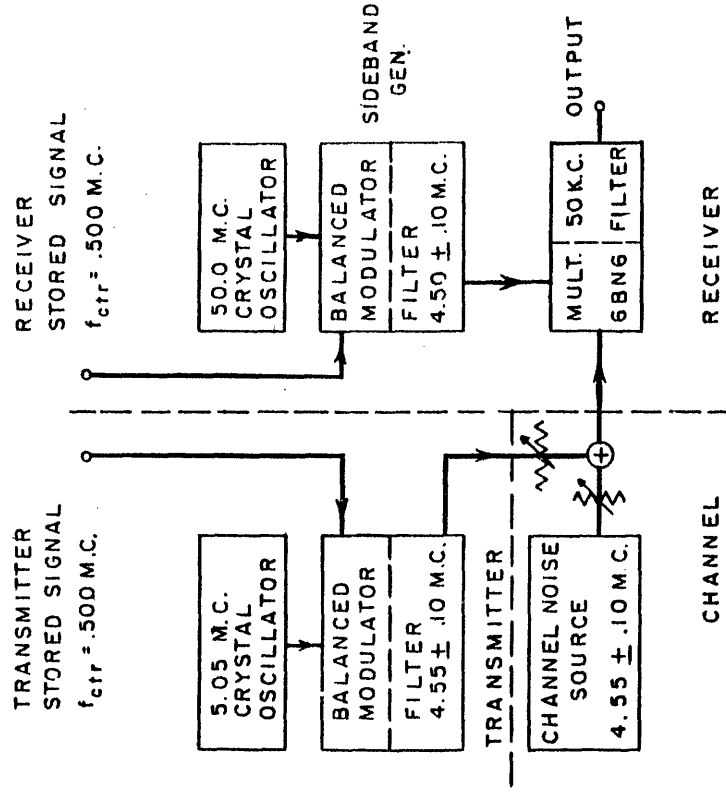


Fig. 4.4. Block diagram of experimental system using stored signal generator of Fig. 4.1.

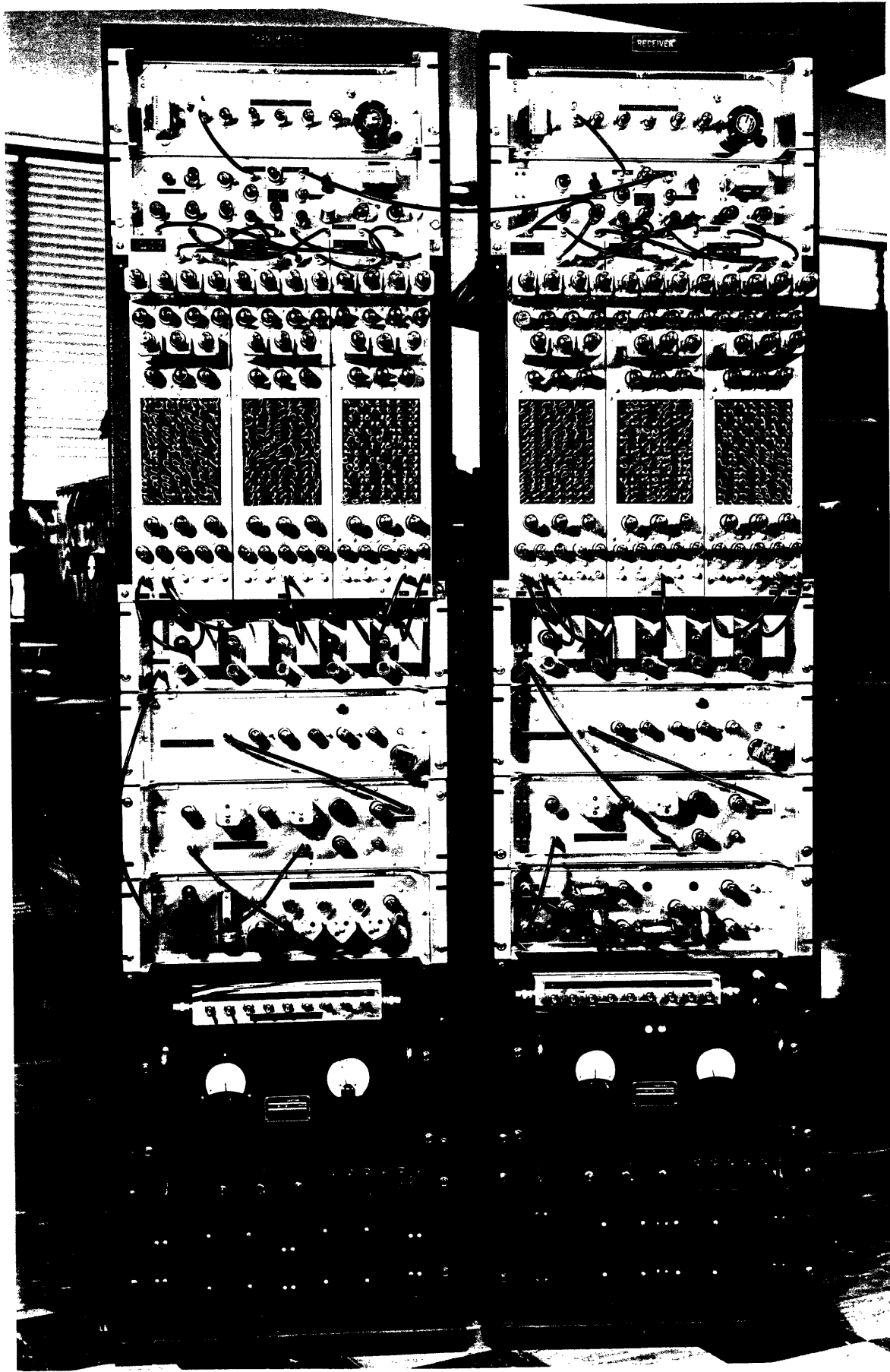


Fig. 1.2 Experimental Stored-Signal System

to provide a band-pass configuration. The sum of all five resonator responses constitutes the signalling waveform.

Before proceeding to a description of the remainder of the system, it is appropriate to discuss in a general way the operation of each of the units in the block diagram. The appropriate schematic circuit diagrams are to be found in Appendix I.

The 200 kilocycle oscillator uses an oven-controlled crystal in a Meacham bridge³² circuit, for high stability.

The driver unit performs several functions. First, it provides an uninterrupted train of sharp 1 microsecond pulses which are supplied to the gate tubes of the commutator units. A second waveform consisting of high-amplitude 200 kilocycle square-waves is fed to the commutator inputs, and this waveform may be periodically interrupted for 20 microseconds for re-synchronization purposes. This 20 microsecond gate is initiated either manually or automatically by an appropriate input to the "resync" circuit. During this gate period, not only are the commutator inputs removed, but the commutators are reset to zero by means of the "Reset" connection.

Each commutator³³ consists of a chain of seven binary counters feeding a crystal diode matrix, as shown in Figure 4.2. The seven "columns" are fed from the plates of the counter tubes, and the fifteen "rows" correspond to the (5 x 3) outputs.

To cause a particular pulse of the 128 to appear at the output corresponding to a given row, the digit is spelled out in binary form by feeding from one counter plate for a "0" and the other for a "1." This is illustrated in the schematic diagram for the digit 75 (decimal notation)=

1001011 (in binary notation). For a given setting of a row, an output in the form of a negative pulse occurs when and only when the proper configuration of on and off conditions exists in all seven counter tubes. Thus each row specifies one digit out of $2^7 = 128$. Each negative pulse from the matrix is inverted and fed to a gate tube so that a clock pulse is gated through to the output whenever this digit occurs.

The operation of the scale-of-127 and 129 commutators differs from this only in that a feedback connection is inserted between certain counters as shown in the schematic diagram. For the 127 connection this has the effect of causing the first counter to step ahead prematurely by one count for every complete cycle of the last counter. For the 129 connection the first counter again steps ahead by one count, but the action of the second is to delay the counting by two clock pulses.

The "0" and "1" settings of the matrix elements are randomly prescribed, for example, by flipping a coin, or by using a random number table. Physically, the settings are made using a plugboard arrangement for each commutator. In this way, the entire key can be changed quickly. One figure of merit of a cryptographic system, of which this might be considered an example, is the key size.³⁴ When specified in binary digits or bits, this is the base-two logarithm of the number of possible key settings, for all keys equally-likely. For the present system, the key size in bits is seen to be the same as the number of matrix elements, which is $3 \times 15 \times 7 = 315$ bits, a figure which compares favorably with conventional cryptographic systems.

The resonator unit contains five monostable multivibrators which convert the incoming pulse trains into a succession of $1/2$ microsecond pulses. Each of these causes a burst of charge to be injected into a parallel resonant circuit by a pentode which is cut off at other times. The resulting damped exponential waveforms are added to form the output signal, a portion of which is shown in Figure 4.3.

Figure 4.4 shows how two complete signal generators of the type described in the preceding paragraphs are used as part of the overall system (figure 4.2). As they emerge from the signal generator section, the transmitter and receiver signal spectra are both centered about 500 kilocycles. Each is then single-sideband-suppressed-carrier modulated to shift the center frequency to 4.505 and 4.500 megacycles, respectively, the transmitted signal being then passed to the receiver through a simulated "channel" involving the addition of gaussian noise having a flat spectrum over the range of significant signal components.

A transmitted frequency of at least 4 or 5 megacycles was felt desirable since this would give a much closer approach to common operating conditions than the low figure of 500 kilocycles. On the other hand, it was found inconvenient to build the resonators with sufficient stability and high enough Q to operate directly at 4 or 5 megacycles. Although the two heterodyning oscillators must be tuned so that their difference lies within the integrating filter pass-band, the tolerance on the tuning of the resonators is much less stringent than this. The loss of output voltage due to detuning of one resonator with its mate is given by the magnitude of the resonator's frequency response. By having the resonators

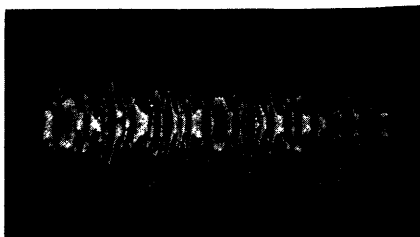


Fig. 4.3

1500- μ sec. section
of output noise-
like signal waveform



operate at the low frequency of 500 kilocycles instead of 5 megacycles, the stability requirement is concentrated in a place where it is conveniently met, namely in the frequency of the two heterodyning oscillators. The half-power bandwidth of the integrating filter is 135 cycles, so that the frequency of each heterodyning oscillator must be constant to about 1 part in 10^5 , a requirement easily within the capabilities of a Meacham bridge circuit much like that used for the 200 kilocycle clock pulse generator.

At the receiver the standard multiplying and filter integrating techniques have been employed. Everything seems to indicate that this is the most practical way to perform the correlation operation at the receiver. (Its preference from the synchronization standpoint has been discussed in Article 3.5.)

Nothing has been said up to this point about the stagger-tuning configuration of the resonator bank. There are several conflicting factors which govern the choice of parameters and a compromise must be made in practice according to the relative importance of these factors. In the first place there is the question of how rapid the decay constants of the resonator responses should be compared to the average repetition rate of the exciting pulses (70 kilocycles in the present case). If the decay is made too small, the signal bandwidth suffers, but on the other hand, too large a decay rate reduces the overlapping of successive outputs, making the system more vulnerable to cryptanalysis.

For a given choice of the bandwidths of the various resonator outputs, there is still the problem of stagger-tuning them to form the resultant total output spectrum. If they are separated by too large a frequency difference in order to give a high overall bandwidth, there will be tell-tale splitting in the spectrum which would allow the resonator outputs to be analyzed individually in deducing the form of each exciting pulse train. To consider the other extreme, if all the circuits are synchronously tuned, the process of cryptanalysis reduces to recovering one overall pulse train for one resonator rather than five pulse trains for five resonators. For intermediate orders of spacing, the overlap of individual spectra presents the analyst with a troublesome noise component if he attempts to determine the pulse train configuration for any one resonator.

4.4 Experimental Results

In view of the considerations just mentioned, the experimental system was adjusted to give three different output spectral configurations as shown in Figure 4.5. Each power density spectrum depicted there is the linear addition of the five individual power density spectra, using the appropriate frequency spacing. Additivity on a power basis was assumed as a result of the supposed independence between the excitation waveforms for the various resonators. This assumption was checked by measurements of the power in various combinations of the resonator outputs.

The three settings of the output spectrum were used to provide a check on the loss of output versus time desynchronization predicted by Equation 3.43.

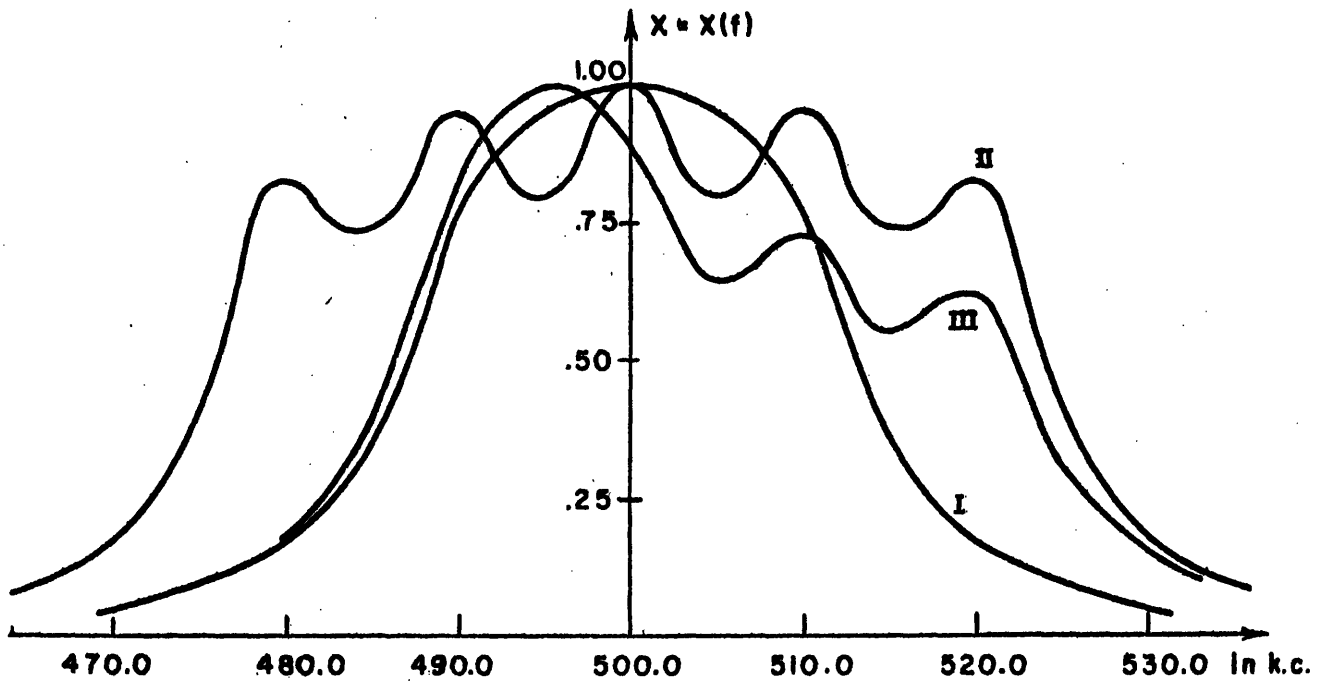


Fig. 4.5. Stored-signal normalized power density spectra for three different stagger-tuning configurations. Resonator $Q = 50.0$. I. Uniform separation = 5.0 kc. Effective total bandwidth = 32.7 kc. II. Uniform separation = 10.0 kc. Effective total bandwidth = 50.4 kc. III. Separation between resonators 1 and 2 and between 2 and 3 = 5.0 kc. Separation between resonators 3 and 4 and between 4 and 5 = 10.0 kc. Effective total bandwidth = 35.8 kc.

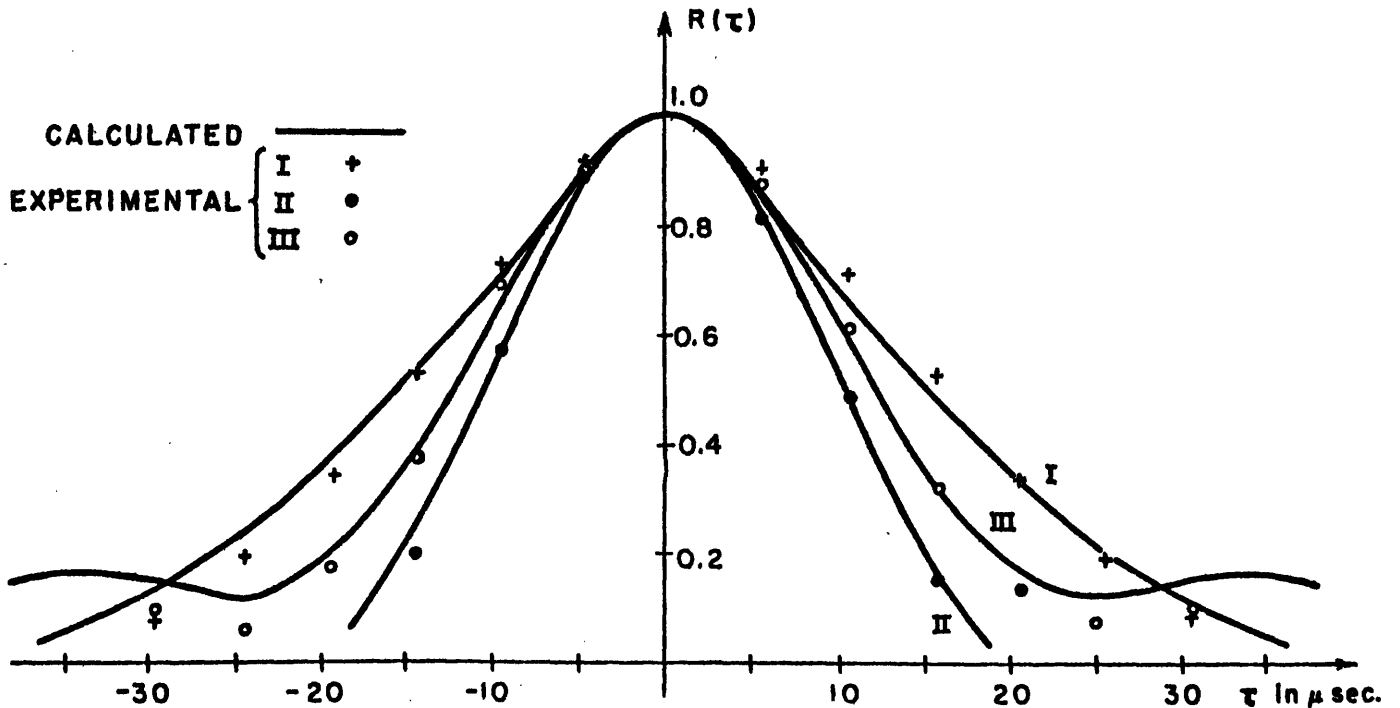


Fig. 4.6. Output voltage vs time desynchronization for experimental system.

The power density spectrum $X(\omega)$ is even for conditions I and II of Figure 4.5, and so determination of $R(\tau)$ need not involve the second numerator term. The asymmetrical spectral shape of condition III was chosen in order to provide a confirmation of the above expression in which both numerator terms were present. Plots of $R(\tau)$ computed from the above equation are given in Figure 4.6 together with corresponding experimental data. Because of the self-noise present in the integrating filter output, readings of the signal level were made with decreasing accuracy as the desynchronization time was increased.

Repeated runs of the actual equipment with the two signal generators driven separately from their respective clock oscillators have shown an average running time after readjustment of oscillator frequency into coincidence of 40 seconds before τ becomes 10 microseconds. This corresponds to a monotonic drift of one frequency with respect to the other of about 5 parts in 10^7 per minute.

Although no attempt was made to adjust the equipment for extreme reliability, it was observed to operate using a common clocking oscillator for periods up to three days without losing synchronization. A check on the identity of the two stored signals was made by driving the two channels (Figure 4.4) with the same stored signal. The output showed no noticeable difference from the separately driven condition.

According to equation 2.61, if the interfering gaussian noise is white, there should be a gain in signal-to-noise power ratio at the output over that in the channel given by twice the ratio of signal and integrator effective bandwidths, for small input signal-to-noise ratio. The

channel signal-to-noise ratio is defined in this equation as the ratio of power densities at the frequency of peak signal intensity. An observed value of 25.3 db was obtained for the spectrum configuration of condition I. The calculated value of bandwidth ratio is 26.8 db. For high input signal-to-noise ratios, equation 2.61 states that the output signal-to-noise ratio, for a gaussian signal, is twice the ratio of signal and integrator bandwidths divided by the spectrum form factor K, in this case 25.2 db. The observed value of $(S/N)_o$ is 22.1 db, the discrepancy being considered due to the departure of the actual signal amplitude distribution from the gaussian form. Ideally, if the ratio of resonator decay time constant to mean interval between excitations were made to increase without limit, the statistics of the waveform would approach gaussian.³⁵

4.5 The Synchronization Problem

Having described in detail how an actual storage system might be devised, we must now turn our attention to the principal obstacle between realization of satisfactory storage facilities and an operating system, namely the means for acquiring and preserving synchronization.

This problem is of rather unusual proportions in the environment in which a stored reference type NOMAC system is expected to be of the greatest immediate use. This environment is of a military nature in which the parties which are trying to communicate will be faced by a resourceful adversary who is presumed to have

- 1) A desire to actually decipher the message, if possible (for either intelligence or deception purposes), but also,

- 2) A willingness to be satisfied with merely interrupting the communication.
- 3) A power advantage at the receiver input which is offset by an appreciable signal-to-integration bandwidth ratio at the receiver. This ratio is assumed large enough so that the enemy will not be able to disrupt communication by his power advantage alone but will be required to use some subtlety.
- 4) An accurate idea of the method being used, up to and including a version of the equipment, but not the key in use.
- 5) All reasonable countermeasures such as recorders, repeaters time and frequency domain analyzers, and computers.

In addition to these conditions, the system should be prepared to operate under the following circumstances:

- 6) Its anti-jamming characteristics make this the only communication link available between transmitter and receiver.
- 7) Transmission will take place through the ionosphere under conditions in which Doppler effect due to changes in layer height, will produce frequency discrepancies of the order of 1 part in 10^7 .
- 8) The multipath configuration (which will be denoted $h(t)$ in Chapter V) characterizing the ionospheric propagation is changing slowly with time.
- 9) Communication must take place within a modest bandwidth allocation.
- 10) Temporary power or equipment failures will be unavoidable.

The situation described by the above list is seen to be entirely different from that accompanying most other forms of synchronized communication systems, such as teletype, facsimile, television, or speech scrambling systems. Not all these conditions will be in effect simultaneously, but it seems a realistic point of view to assume that they are and design the system accordingly. In the remaining few paragraphs of this chapter is presented an account of some ways of dealing with the problem, an appraisal of them in the light

of these conditions, and finally suggestions as to a particular practical procedure which it is felt represents a reasonable answer.

Assuming that signal bandwidths of the order of 5-50 kc are available, equation 3.43 shows that an adjustment of synchronization is required if the accumulated time scale time error is more than about 100 μ sec and 10 μ sec, respectively. With a time scale stability limitation of about 1 part in 10^7 imposed by condition (7) above, this means that resynchronization is required at least every 15 minutes and 1-1/2 minutes, respectively, no matter how accurate are the clocking oscillators at transmitter and receiver. Preliminary data on multipath effects which will be described in Chapter V more fully indicate that one may expect to have to re-synchronize on a different path as often as once every 30 seconds depending on various factors, such as time of day.

The information required to establish and then suitably readjust the time scale at the receiver may come from a) the transmitter (in the form of sync pulses, for example), b) the receiver itself (an "AFC" system), or c) some third party (for example, WWV or Loran stations). The last of these must be ruled out on the basis of condition (6) which amounts to the statement that if the third party were receiveable, the present system might be unnecessary.

The principal indictment of the use of characteristic synchronization signals is their vulnerability to such countermeasures as imitation and repeater techniques by which counterfeit signals could effect a false synchronization. These synchronization signals might be sent in the same band as the intelligence or perhaps transmitted on an entirely different frequency. The use of a separate frequency for the synchronization waveform could not long escape detection.

One argument for use of a separate synchronizing signal which ignores the countermeasures aspect is that this signal might be made to provide the receiver with an indication of the multipath characteristic $h(t)$. A sharp pulse for example would be received as a series of pulses and the stored signal could be automatically synchronized with the largest of these.

Some degree of protection against analysis of the synchronization waveforms would be gotten by suitably encoding them as well as the message. If this is done, the key size must be large, indeed in view of condition (2), it should probably be almost as large as that of the signal itself. The question of how much of the available key size and transmitter power to allot to synchronization and how much to the intelligence depends upon the relative predominance of conditions 1 or 2, that is, on whether the enemy is principally interested in the message or the synchronization.

All in all, the use of transmitted synchronizing waveforms is not a very satisfactory solution and one is led to inspect the possibilities of the third source of synchronizing information, the transmitted message signal itself. The key which describes this signal is the very information that only the transmitter and receiver possess. To the enemy the problem of reading the message and interrupting it now become of more equal difficulty.

In order to use the received message as a source of synchronization data, the system must somehow be synchronized in the first place. Because it is desirable not to have to rely on indefinite uninterrupted operation to maintain synchronization, means must be provided for acquiring and

re-acquiring proper synchronization at will. In short, the problem is one of devising some scheme of scanning the incoming signal for the proper reference signal timing to be used, and then shifting from this search phase through the operation of acquisition to a tracking phase (to use radar terminology) in which discrepancies between the incoming time scale and the reference signal result in correction of the latter.

On the basis of the factors discussed in the preceding paragraphs some thought has been given to a possible mechanism by which these operations might be carried out and such a method will now be briefly outlined.

The only quantity derivable from the incoming signal which could be used to indicate a correct synchronization is a significant integrating filter output. It is suggested, therefore, that the search phase involve a temporary timing of the reference signal from a clocking oscillator which is deliberately off in frequency; the stored and incoming signals will then slip past one another in time and eventually a large integrator output will signal a condition of synchronization. At this time, acquisition would be effected by resuming normal operation from the more stable clocking oscillator. The oscillator used in this search phase should be in error by a frequency difference large enough so that the average search through the incoming waveform would not last too long. On the other hand, if the frequency discrepancy is too large, a loss in output will result from the stretching or compression of one time scale relative to the other.

The operation of "tracking" involves a continual readjustment of the phase of the receiver clocking oscillator in maintaining the signal output power at or near its maximum value. The process is in many respects similar

to automatic frequency control except that it is the phase and not merely the frequency which must be adjusted. Also the indication of misadjustment in one direction or another is not an odd function (such as a discriminator characteristic) but the even function shown in Figure 4.6. A means must be provided for determining the sign of any time scale error. The desired odd function can be derived by working with the slope of this curve -- by sensing the difference between outputs for two slightly different values of clock oscillator phase (for example, by purposely jittering the phase back and forth between two values). When these two time values are symmetrically disposed about the signal peak, a zero difference will result, whereas a drift of the average phase to one side or the other will produce an error signal of corresponding sign from which a correction could be derived.

Periodically the tracking phase would have to be interrupted in order to search out a stronger received signal but this, of course, would not involve the long search times involved in the initial acquisition.

The synchronization scheme which has just been outlined is admittedly a rather complex one, and yet it is felt to be a reasonable compromise solution which could be made to perform satisfactorily even under the adverse conditions which were listed at the beginning of this section.

[REDACTED]

CHAPTER V
MULTIPATH EFFECTS

5.1 Introduction

The preceding chapters have discussed a communication system whose purpose is the transmission of a succession of symbols through gaussian noise under the conditions of a military environment. Unfortunately, in practical operation there arise situations in which the assumption of additive gaussian noise is an incomplete description of the perturbations of the transmitted signals as they pass through the channel. Besides the noise, an important perturbing factor in practice is multipath, a condition by which the transmitted signal is delivered to the receiver via a number of propagating paths. Perhaps the best known manifestation of the multipath phenomenon is in ionospheric propagation,³⁶ although it sometimes occurs due to local reflections from terrestrial objects in the vicinity of transmitter and receiver, or in a communication system using "polycasting" in which several separately located transmitters send the same signal at the same frequency.

In this chapter we will deal with the analysis of the effect of multipath on NOMAC systems. For a discussion of the synthesis problem in which a channel model is assumed and the desirable system properties deduced (as described in Section 1.2 for additive white gaussian noise in the channel), the reader is referred to the work of Price.³⁷

The specific problem to be dealt with here is the determination of output signal-to-noise ratio for the three types of NOMAC systems when a quasistationary multipath condition exists between transmitter and receiver. The impulse response $h(t)$ of the cascaded linear system of Figure 2.1 will be specified in such a way as to describe this multipath condition. By quasistationary we mean that fluctuations of the multiple path configuration occur at a rate which is slow compared to the symbol lengths so that $h(t)$ may be regarded as fixed over the symbol length. For the symbol durations usually used in practice (20 milliseconds or less) this assumption is valid since the fluctuation rate for the usual type of ionospheric transmission (below the "maximum usable frequency") is seldom more than several cycles per second³⁸ and is about the same for ionospheric scatter propagation³⁹ (above the MUF).

We also assume that the time difference between the first and last multiple path is smaller than the symbol length. Therefore the multipath condition will not produce inter-symbol interference due to the presence at the sampling time of one symbol of a delayed replica of the previous symbol. This condition, too, usually exists in practical NOMAC systems since the difference in arrival times of the various multipath signals is seldom more than ten milliseconds, and symbol durations as small as this are not used.

In actual operation, one transmits a succession of different symbols which are perturbed by a slowly varying $h(t)$. We will be interested, however, in the average effect of a particular multipath condition $h(t)$ on a

particular symbol. Under the assumptions of the preceding two paragraphs, we may treat this problem by considering a hypothetical situation in which the transmitter sends the same symbol repeatedly through a time-invariant $h(t)$. We will calculate the output signal-to-noise ratio, as defined in Chapter II, on this basis.

When fixed low-pass detection or matched filter detection is employed, it can be seen from equation 2.15 that the output noise term is not a function of $H(\omega)$ (the Fourier transform of $h(t)$) and is therefore unaffected by the multipath condition. This is true, of course, because the output noise is caused by interaction between channel noise and the stored version of the signal. Because of this, in comparing the the output signal-to-noise ratio for various multipath conditions we need only compute the effect on the numerator of equation 2.15, denoted by S_o .

For the case of continuous detection there is the self-noise term to consider. Not only is the signal output power affected by the multipath condition, but the self-noise is considerably aggravated by this condition, as we shall see. For high input signal-to-noise ratios we will use equations 2.38 and 2.52 to compute $(S/N_s)_o$, the ratio of output signal to self noise power. At low input signal-to-noise ratios the predominant output noise term (due to channel noise) is independent of the character of the multipath configuration. This is true for the stored-reference system by the same reasoning as in the preceding paragraph. For the transmitted-reference system, which we will consider as employing continuous band-pass detection, it is true because the predominant output noise term is the $(N_1 \times N_2)$ term, which is completely independent of both signals.

We now proceed to a calculation of S_o when fixed low-pass or matched filter detection is used, and $(S/N_s)_o$ for continuous detection. In computing the latter, we will be careful to keep numerator and denominator separate throughout the calculation so that the numerator S_o can be examined alone to determine multipath effects at low input signal-to-noise ratios. It is appropriate to insert a reminder at this point that for band-pass detection the self-noise power must be used with care in inserting the (S/N_s) expression into calculations for the probability of error. As mentioned in Section 2.6, due to the anomalous behavior of the self-noise, there is the possibility that the probability of error may be lower than that calculated on the basis of the power in the self-noise.

The calculation will be carried out by first transforming to the time domain the appropriate expressions from Chapter II. This will allow the inclusion of the multipath condition as $h(t)$, which will be somewhat easier to deal with than $H(\omega)$. The transmission path impulse response will then be specified as consisting of N impulses, of various values and delay times, representing the N paths by which the transmitted signal is delivered to the receiver. The signal spectrum will be assumed to be of a rectangular band-pass type, with bandwidth W (radians-per-second) and center radian frequency ω_o .

5.2 Stored-Signal System (Continuous Signals)

A. Band-Pass Detection

From the numerator and first denominator terms of equation 2.52, we have for the output signal-to-self-noise ratio:

$$\left(\frac{S}{N_s}\right)_o = \frac{2}{W_f} \frac{A_1^2 + B_1^2}{C_1} \quad (5.1)$$

where

$$\begin{aligned} A_1 &= \int_0^{\infty} X(\omega) \operatorname{Re} [H(\omega)] d\omega \\ &= \int_0^{\infty} X(\omega) d\omega \int_{-\infty}^{\infty} h(t) \cos \omega t dt \\ &= 2\pi \int_{-\infty}^{\infty} h(t) \phi(t) dt \end{aligned} \quad (5.2)$$

$$B_1 = \int_0^{\infty} X(\omega) \operatorname{Im} [H(\omega)] d\omega = 2\pi \int_{-\infty}^{\infty} h(t) \phi'(t) dt \quad (5.3)$$

in a similar manner, and

$$\begin{aligned} C_1 &= \int_0^{\infty} X^2(\omega) |H(\omega)|^2 d\omega \\ &= \int_{-\infty}^{\infty} h(\mu) d\mu \int_{-\infty}^{\infty} h(\sigma) \left[(\phi_{\phi}(\mu-\sigma) + j\phi'_{\phi}(\mu-\sigma)) d\mu \right] \\ &= 2\pi \int_{-\infty}^{\infty} \phi_{\phi}(t) \phi_{hh}(t) dt \end{aligned} \quad (5.4)$$

Here use has been made of the definitions

$$\phi(t) = \frac{1}{2\pi} \int_0^{\infty} X(\omega) \cos \omega t \, d\omega \quad , \quad (5.5)$$

$$\phi'(t) = \frac{1}{2\pi} \int_0^{\infty} X(\omega) \sin \omega t \, d\omega \quad , \quad (5.6)$$

$$\phi_{\phi\phi}(t) = \frac{1}{2\pi} \int_0^{\infty} X^2(\omega) \cos \omega t \, d\omega = \int_{-\infty}^{\infty} \phi(\tau)\phi(\tau+t) \, d\tau \quad , \quad (5.7)$$

$$\phi_{\phi\phi}'(t) = \frac{1}{2\pi} \int_0^{\infty} X^2(\omega) \sin \omega t \, d\omega \quad , \quad (5.8)$$

and

$$\phi_{hh}(t) = \int_{-\infty}^{\infty} h(\tau)h(\tau+t) \, d\tau \quad . \quad (5.9)$$

These time domain formulations will now be used in the specific case where $h(t)$ is assumed to consist of N impulses of value a_i occurring at times T_i , $i=1, 2, \dots, N$. This function

$$h(t) = \sum_{n=1}^N a_n \delta(t-T_n) \quad (5.10)$$

is depicted at the top of Figure 5.1 together with its even and odd parts

$$h_e(t) = \sum_{n=1}^N \frac{a_n}{2} [\delta(t-T_n) + \delta(t+T_n)] \quad (5.11)$$

and

DECLASSIFIED

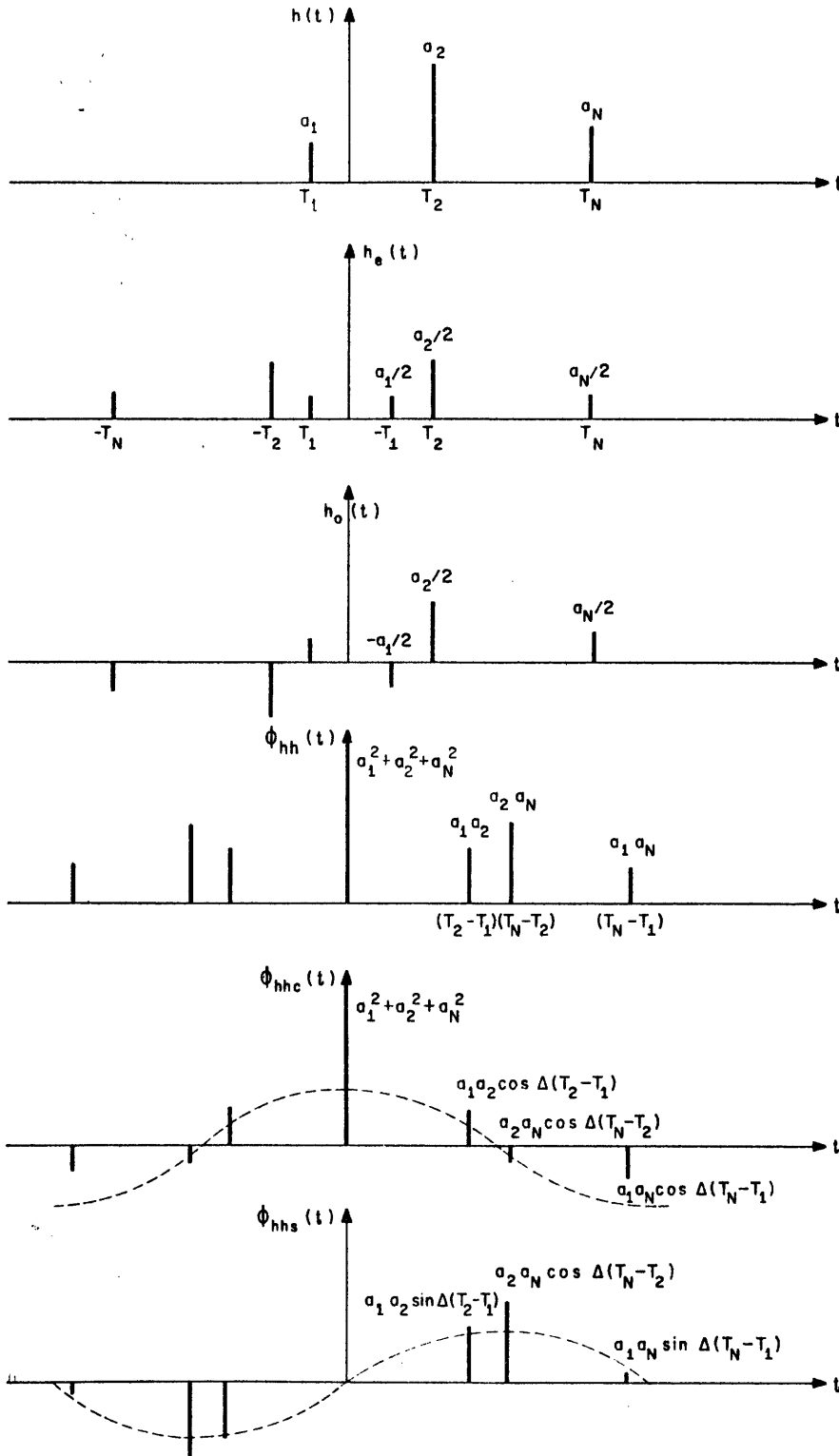


Fig. 5.I. Transmission path impulse response and related functions



DECLASSIFIED

$$h_o(t) = \sum_{n=1}^N \frac{a_n}{2} [\delta(t-T_n) - \delta(t+T_n)] \quad (5.12)$$

(Also illustrated in this figure are certain other quantities derived from $h(t)$ which will be needed for later calculations.) From the assumption that the signal spectrum $X(\omega)$ is rectangular, of width W radians-per-second, height $1/W$, and center frequency ω_o , we have

$$\phi(t) = \cos \omega_o t \frac{\sin \frac{Wt}{2}}{\frac{Wt}{2}} \quad (5.13)$$

$$\phi'(t) = \sin \omega_o t \frac{\sin \frac{Wt}{2}}{\frac{Wt}{2}} \quad (5.14)$$

$$\phi_{\phi}(t) = \frac{1}{W} \cos \omega_o t \frac{\sin \frac{Wt}{2}}{\frac{Wt}{2}} \quad (5.15)$$

and

$$\phi_{\phi}'(t) = \frac{1}{W} \sin \omega_o t \frac{\sin \frac{Wt}{2}}{\frac{Wt}{2}} \quad (5.16)$$

For this choice of spectrum and channel impulse response $h(t)$, we have for A_1 , B_1 , and C_1

$$A_1 = 2\pi \int_{-\infty}^{\infty} h_e(t)\phi(t)dt = 2\pi \sum_{n=1}^N a_n \cos \omega_o T_n \frac{\sin \frac{WT_n}{2}}{\frac{WT_n}{2}} \quad (5.17)$$

DECLASSIFIED

$$B_1 = 2\pi \int_{-\infty}^{\infty} h_o(t) \phi'(t) dt = 2\pi \sum_{n=1}^N a_n \cos \omega_o T_n \frac{\sin \frac{WT_n}{2}}{\frac{WT_n}{2}}, \quad (5.18)$$

and

$$C_1 = 2\pi \int_{-\infty}^{\infty} \frac{1}{W} \cos \omega_o t \frac{\sin \frac{Wt}{2}}{\frac{Wt}{2}} \sum_{m,n=1}^N a_m a_n \delta(t-T_m+T_n) dt$$

$$= \frac{2\pi}{W} \sum_{m,n=1}^N a_m a_n \cos \omega_o (T_m - T_n) \frac{\sin \frac{W(T_m - T_n)}{2}}{\frac{W(T_m - T_n)}{2}}, \quad (5.19)$$

from which (equation 5.1).

$$\left(\frac{S}{N}\right)_o = \frac{4\pi W}{W_f} \frac{\sum_{m,n=1}^N a_m a_n \cos \omega_o (T_m - T_n) \frac{\sin \frac{WT_m}{2}}{\frac{WT_m}{2}} \frac{\sin \frac{WT_n}{2}}{\frac{WT_n}{2}}}{\sum_{m,n=1}^N a_m a_n \cos \omega_o (T_m - T_n) \frac{\sin W(T_m - T_n) / 2}{W(T_m - T_n) / 2}} \quad (5.20)$$

B. Low-Pass Detection

From equation 2.38, we have for the output signal-to-self-noise ratio

$$\left(\frac{S}{N}\right)_{s o} = \frac{1}{W_f} \frac{A_1^2}{D} \quad (5.21)$$

where A_1 is the same as before (equation 5.2) and D is determined following a procedure similar to that used for C_1 , (equation 5.4):

$$D = \int_0^{\infty} X^2(\omega) \operatorname{Re}^2 [H(\omega)] d\omega \quad (5.22)$$

$$= \frac{2\pi}{W} \int_0^{\infty} h(\mu) d\mu \int_0^{\infty} h(\nu) d\nu [\delta_{\delta\delta}(\mu+\nu) + \delta_{\delta\delta}(\mu-\nu)] .$$

For the particular choice of $h(t)$ and $X(\omega)$ in use, we have

$$A_1^2 = \left[\sum_{n=1}^N a_n \cos \omega_0 T_n \frac{\sin WT_n/2}{WT_n/2} \right]^2 \quad (5.23)$$

and

$$D = \frac{1}{2W} \sum_{m,n=1}^N a_m a_n \cos \omega_0 (T_m - T_n) \frac{\sin W(T_m - T_n)/2}{W(T_m - T_n)/2} + \frac{1}{2W} \sum_{m,n=1}^N a_m a_n \cos \omega_0 (T_m + T_n) \frac{\sin W(T_m + T_n)/2}{W(T_m + T_n)/2} \quad (5.24)$$

from which (equation 5.21)

$$\left(\frac{S}{N_s}\right)_{\omega_0} = \frac{2\pi W}{W_f} \frac{\sum_{m,n=1}^N a_m a_n \cos \omega_0 T_m \frac{\sin WT_m/2}{WT_m/2} \frac{\sin WT_n/2}{WT_n/2}}{\frac{1}{2} \sum_{m,n=1}^N a_m a_n \cos \omega_0 (T_m + T_n) \frac{\sin W(T_m + T_n)/2}{W(T_m + T_n)/2}} . \quad (5.25)$$

In this last equation, the abbreviation \pm represents that the summation is to be taken twice, once with $\pm = +$ throughout, and again with $\pm = -$ throughout.

5.3 Transmitted-Reference System (Continuous Signals)

The $(S/N)_o$ expressions 2.38 and 2.52 were applicable as they stand to the stored-signal type system where, just as in Figure 2.1, $X(\omega)$ is the signal spectrum and $H(\omega)$ is the complex transfer characteristic of the single channel. To investigate the transmitted-reference system in which multipath conditions exist in both channels, we must carry out a modification of equation 2.52 to include the condition of a cascaded linear system in both correlator inputs. Specifically, the quantities in the $(S/N)_o$ expression are to be redefined so that one multiplier input is the signal perturbed by the multipath, and the other multiplier input is the same signal displaced in frequency by Δ , and perturbed by the same multipath condition. If one re-examines the derivation of $(S/N)_o$ given in Section 2.5, and substitutes for $x'(t)$ the following quantity describing the presence of the linear cascade in the second channel

$$u'(t) = \sum_{i=1}^{M} h_i \cos [(\omega_i - \Delta)t + \theta_i + \gamma_{i-\Delta}] , \quad (5.26)$$

it follows by direct calculation that the signal-to-self-noise ratio is given by

$$\left(\frac{S}{N}\right)_o = \frac{\left[\int_0^{\infty} X(\omega) \operatorname{Re} [H(\omega) H^*(\omega - \Delta)] d\omega \right]^2 + \left[\int_0^{\infty} X(\omega) d\omega \operatorname{Im} [H(\omega) H^*(\omega - \Delta)] d\omega \right]^2}{\int_0^{\infty} X^2(\omega) |H(\omega)|^2 |H(\omega - \Delta)|^2 d\omega} = \frac{A_2^2 + B_2^2}{W_f C_2} \frac{2}{W_f} \quad (5.27)$$

The assumption that the ionosphere impulse response is not appreciably different at the frequencies of the intelligence and auxiliary channels appears to be a reasonable one for the bandwidths W and channel separations Δ usually employed. Although it is not known how great a frequency difference is required before the ionosphere multiple path configuration and its fluctuations become unrelated at the two frequencies of observation, there is very good reason to believe that it is large enough to be an immaterial factor for the present calculation. (See, for example, Reference 36, p. 726.)

Transforming equation 5.27 to the time domain, the quantities $A_2, B_2,$ and C_2 are determined as follows:

$$\begin{aligned}
 A_2 &= \int_0^{\infty} X(\omega) \operatorname{Re} [H(\omega) H^*(\omega-\Delta)] d\omega \\
 &= \int_0^{\infty} X(\omega) d\omega \operatorname{Re} \left[\int_{-\infty}^{\infty} d\mu \int_{-\infty}^{\infty} d\sigma h(\mu) h(\sigma) e^{-j\omega\mu} e^{j(\omega-\Delta)\sigma} \right] \\
 &= \int_0^{\infty} X(\omega) d\omega \int_{-\infty}^{\infty} d\mu \int_{-\infty}^{\infty} d\sigma h(\mu) h(\sigma) [\cos \Delta\sigma \cos \omega(\mu-\sigma) - \sin \Delta\sigma \sin \omega(\mu-\sigma)] \\
 &= 2\pi \int_{-\infty}^{\infty} \phi(t) \phi_{\text{hnc}}(t) dt - 2\pi \int_{-\infty}^{\infty} \phi'(t) \phi_{\text{hns}}(t) dt \quad (5.28)
 \end{aligned}$$

and

$$\begin{aligned}
 B_2 &= \int_0^{\infty} X(\omega) d\omega \operatorname{Im} [H(\omega) H^*(\omega-\Delta)] d\omega \\
 &= \int_0^{\infty} X(\omega) d\omega \int_{-\infty}^{\infty} d\mu \int_{-\infty}^{\infty} d\sigma h(\mu) h(\sigma) [-\sin \Delta\sigma \cos \omega(\mu-\sigma) - \cos \Delta\sigma \sin \omega(\mu-\sigma)] \\
 &= -2\pi \int_{-\infty}^{\infty} \phi(t) \phi_{\text{hns}}(t) dt - 2\pi \int_{-\infty}^{\infty} \phi'(t) \phi_{\text{hnc}}(t) dt \quad (5.29)
 \end{aligned}$$

in which

$$\phi_{\text{hnc}}(t) = \int_{-\infty}^{\infty} h(\sigma)h(\sigma+t)\cos \Delta\sigma \, d\sigma \quad (5.30)$$

and

$$\phi_{\text{hns}}(t) = \int_{-\infty}^{\infty} h(\sigma)h(\sigma+t)\sin \Delta\sigma \, d\sigma \quad (5.31)$$

The denominator is

$$C_2 = \int_0^{\infty} X^2(\omega) |H(\omega)|^2 |H(\omega-\Delta)|^2 \, d\omega \quad (5.32)$$

$$= \int_{-\infty}^{\infty} h(\mu) \, d\mu \int_{-\infty}^{\infty} h(\nu) \, d\nu \int_{-\infty}^{\infty} h(\rho) \, d\rho \int_{-\infty}^{\infty} h(\sigma) \, d\sigma \int_0^{\infty} e^{j\omega(\mu-\nu)} e^{j(\omega-\Delta)(\rho-\sigma)} X^2(\omega) \, d\omega$$

Since the entire expression is real, the imaginary part of the last integral is known to be zero so that

$$C_2 = 2\pi \int_{-\infty}^{\infty} h(\mu) \, d\mu \int_{-\infty}^{\infty} h(\nu) \, d\nu \int_{-\infty}^{\infty} h(\rho) \, d\rho \int_{-\infty}^{\infty} h(\sigma) \, d\sigma \left[\cos \Delta(\sigma-\rho) \phi_{\text{hnc}}(\mu-\nu+\rho-\sigma) - \sin \Delta(\sigma-\rho) \phi_{\text{hns}}(\mu-\nu+\rho-\sigma) \right] \quad (5.33)$$

Evaluating ϕ_{hnc} and ϕ_{hns} for our particular choice of $h(t)$ and $X(\omega)$, we have

$$\phi_{\text{hnc}}(t) = \int_{-\infty}^{\infty} h(\sigma) \cos \Delta\sigma h(\sigma+t) \, d\sigma = \sum_{m,n=1}^N a_m \cos(\Delta T_m) a_n \delta(t - T_n + T_m) \quad (5.34)$$

$$\phi_{hhs}(t) = \int_{-\infty}^{\infty} h(\sigma) \sin \Delta \sigma h(\sigma + t) d\sigma = \sum_{m,n=1}^N a_m \sin(\Delta T_m) a_n \delta(t - T_n + T_m) \quad (5.35)$$

From these

$$A_2 = 2\pi \sum_{m,n=1}^N a_m a_n \cos \omega_0 (T_n - T_m) \cos \Delta T_m \frac{\sin \frac{W}{2}(T_n - T_m)}{\frac{W}{2}(T_n - T_m)} \quad (5.36)$$

$$- 2\pi \sum_{m,n=1}^N a_m a_n \sin \omega_0 (T_n - T_m) \sin \Delta T_m \frac{\sin \frac{W}{2}(T_n - T_m)}{\frac{W}{2}(T_n - T_m)}, \quad (5.37)$$

$$B_2 = 2\pi \sum_{m,n=1}^N a_m a_n \cos \omega_0 (T_n - T_m) \sin \Delta T_m \frac{\sin \frac{W}{2}(T_n - T_m)}{\frac{W}{2}(T_n - T_m)} \quad (5.38)$$

$$- 2\pi \sum_{m,n=1}^N a_m a_n \sin \omega_0 (T_n - T_m) \cos \Delta T_m \frac{\sin \frac{W}{2}(T_n - T_m)}{\frac{W}{2}(T_n - T_m)}, \quad (5.39)$$

and

$$C_2 = \frac{2\pi}{W} \int_{-\infty}^{\infty} h(\mu) d\mu \int_{-\infty}^{\infty} h(\nu) d\nu \int_{-\infty}^{\infty} h(\rho) d\rho \int_{-\infty}^{\infty} h(\sigma) d\sigma \quad X$$

$$\left[\cos \Delta(\sigma - \rho) \cos \omega_0 (\mu - \nu + \rho - \sigma) \frac{\sin \frac{W}{2}(\mu - \nu + \rho - \sigma)}{\frac{W}{2}(\mu - \nu + \rho - \sigma)} - \sin \Delta(\sigma - \rho) \sin \omega_0 (\mu - \nu + \rho - \sigma) \frac{\sin \frac{W}{2}(\mu - \nu + \rho - \sigma)}{\frac{W}{2}(\mu - \nu + \rho - \sigma)} \right]$$

$$= \frac{2\pi}{W} \sum_{m,n,r,s=1}^N a_m a_n a_r a_s \cos \left[(T_m - T_n) \omega_o + (T_r - T_s) (\omega_o + \Delta) \right] \frac{\sin \frac{W}{2} (T_m - T_n + T_r - T_s)}{\frac{W}{2} (T_m - T_n + T_r - T_s)} .$$

(5.40)

Finally,

$$\left(\frac{S}{N} \right)_o = \frac{\frac{4\pi W}{W_f} \left[\sum_{m,n=1}^N a_m a_n \cos [T_n \omega_o - T_m (\omega_o - \Delta)] \frac{\sin \frac{W}{2} (T_n - T_m)}{\frac{W}{2} (T_n - T_m)} \right]^2 + \left[\sum_{m,n=1}^N a_m a_n \sin [T_n \omega_o - T_m (\omega_o - \Delta)] \frac{\sin \frac{W}{2} (T_n - T_m)}{\frac{W}{2} (T_n - T_m)} \right]^2}{\sum_{m,n,r,s=1}^N a_m a_n a_r a_s \cos \left[(T_m - T_n) \omega_o + (T_r - T_s) (\omega_o + \Delta) \right] \frac{\sin \frac{W}{2} (T_m - T_n + T_r - T_s)}{\frac{W}{2} (T_m - T_n + T_r - T_s)}} .$$

(5.41)

5.4 Matched Filter System, and Stored-Signal System Using Fixed Signals

Equation 2.15 gives the output signal-to-noise ratio for both matched filter and low-pass fixed detection operation of the stored-signal system.

The numerator S_o of equation 2.15 is identical with the numerator of equation 5.21 except that $X(\omega)$ is an energy density spectrum in the former and a power density spectrum in the latter. Because of this identity in the expressions, the desired S_o (the signal output power) for matched filter and low-pass fixed type detection is available as the numerator summation of equation 5.25.

It was mentioned in Section 3.2-C that the matched filter type of detection gives an output from the filter whenever an input occurs, although one still has a time synchronization problem in sampling the output waveform at the correct point. Under the conditions of multipath operation, the matched filter output function of time due to the signal alone takes the form of the sum of N replicas of the correlation function $\phi(t)$. That is, if T is the sampling instant, as in equation 1.6, we have

$$f_o(t) = \sum_{n=1}^N a_n \cos(t-T-T_n) \frac{\sin W(t-T-T_n)/2}{W(t-T-T_n)/2} \quad (5.42)$$

It has been suggested that matched filter detection might provide good performance in the presence of multipath conditions if a means could be devised of observing only the peaks of the various correlation function replicas of equation 5.42. In this way one would be using signal energy delivered to the receiver by all multiple paths instead of merely the one in synchronism with the stored reference.

5.5 A Comparison of System Performance

Generally speaking, the expressions 5.20, 5.25, and 5.41 are too unwieldy to give a good picture of multipath conditions without going to particular cases. In this section we will make a comparison of the performance of the various types of systems on the basis of a simple but revealing particular case, that in which there are two paths having delay time $T_1=0$ and $T_2=\tau$, and strength $a_1=1$ and $a_2=a$. That is,

$$h(t) = \delta(t) + a\delta(t-\tau) \quad (5.43)$$

Under this condition, we have for the stored-signal system using band-pass detection, the following expression for normalized $(S/N_s)_o$ (from equation 5.20)

$$\left(\frac{S}{N_s}\right)' = \frac{W_f}{4\pi W} \left(\frac{S}{N_s}\right)_o = \frac{1 + 2a \cos \omega_o \tau + a^2 \left(\frac{\sin W\tau/2}{W\tau/2}\right)}{\left[1 + 2a \cos \omega_o \tau \frac{\sin W\tau/2}{W\tau/2} + a^2\right]} \quad (5.44)$$

Figure 5.2 shows both the signal power (the numerator S_o') and the normalized signal-to-self-noise ratio $(S/N_s)'_o$ as a continuous function of τ for various values of a . These plots describe the behavior of output signal-to-noise ratio when the input signal-to-noise ratio is much less than unity and much greater than unity, respectively. Because the functions are even in τ , only the positive τ -axis is included.

For the stored-signal system using low-pass integration, the expression is

$$\left(\frac{S}{N_s}\right)' = \frac{W_f}{2\pi W} \left(\frac{S}{N_s}\right)_o = \frac{\left[1 + a \cos \omega_o \tau \frac{\sin W\tau/2}{W\tau/2}\right]^2}{1 + 2a \cos \omega_o \tau \frac{\sin W\tau/2}{W\tau/2} + \frac{a^2}{2}(1 + \cos 2\omega_o \tau) \frac{\sin W\tau}{W\tau}} \quad (5.45)$$

from equation 5.25, and the corresponding plots are given in Figure 5.3.

For the transmitted-reference system, we have from equation 5.41

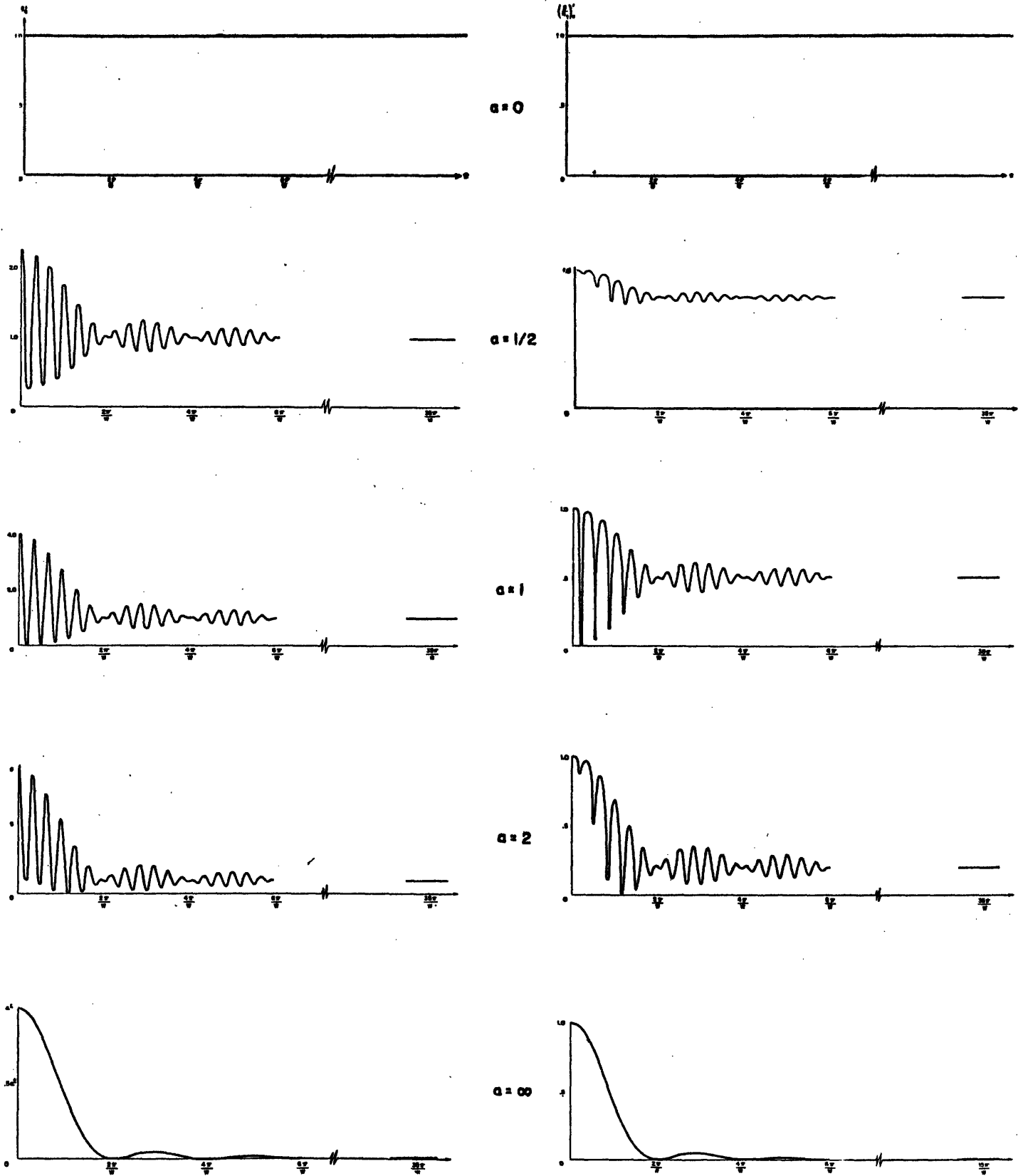


Fig. 5.2. Normalized signal output power (left curves) and output signal-to-self-noise ratio (right curves) for stored signal system using band-pass continuous type detection.

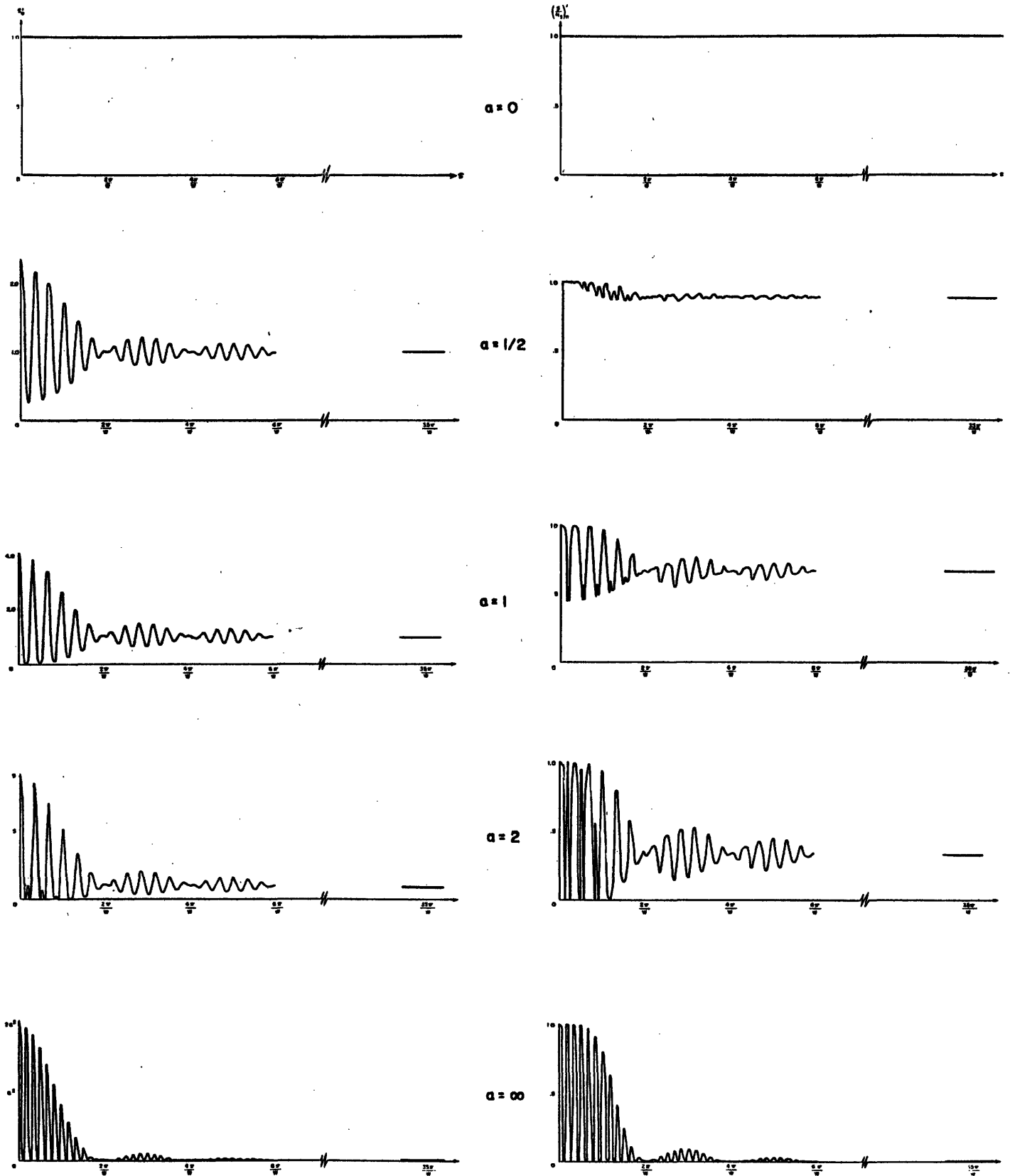


Fig. 5.3. Normalized signal output power (left curves) and output signal-to-self noise ratio (right curves) for stored signal system using low-pass continuous type detection. α = relative strength of second path and τ = path time separation.

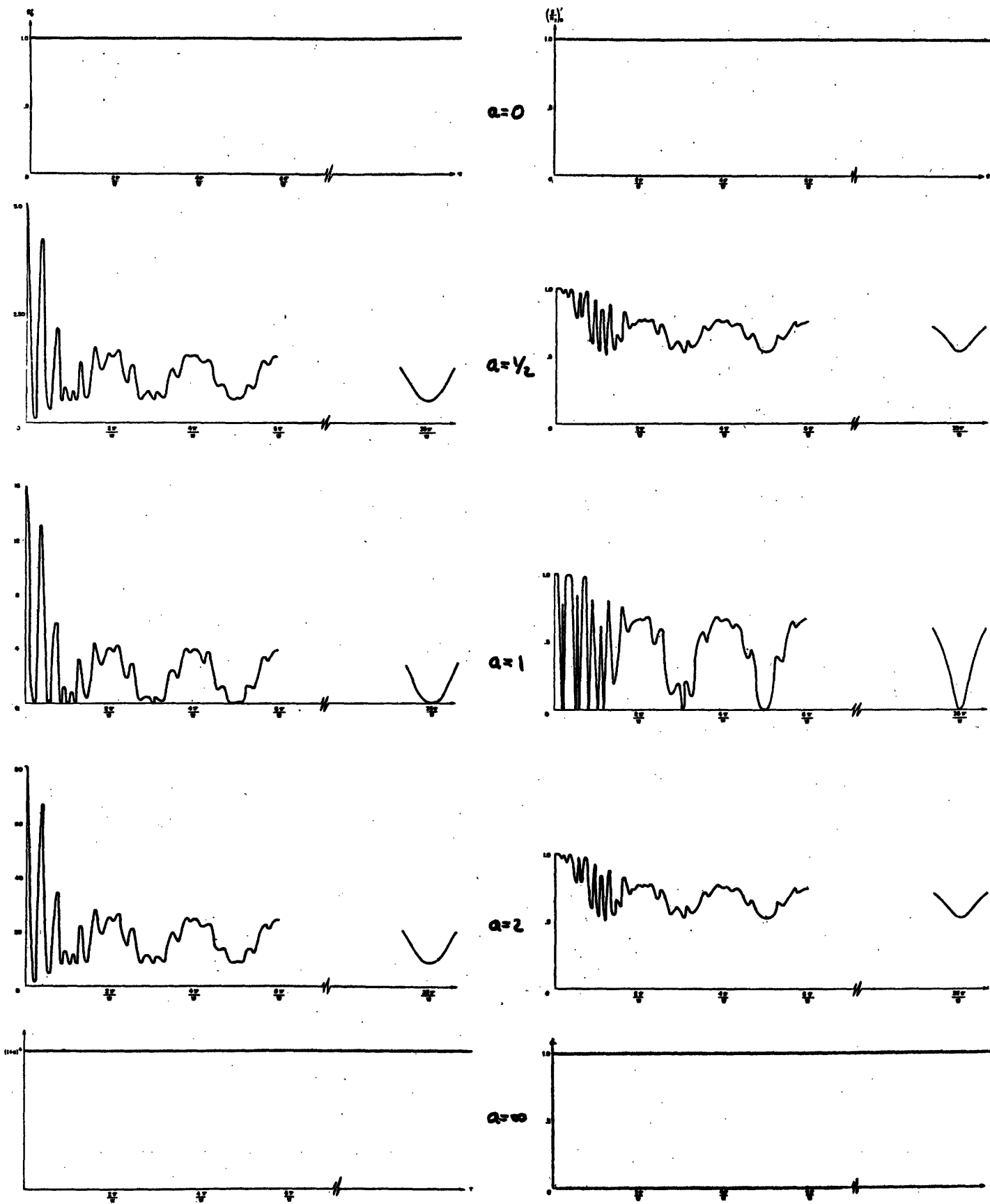


Fig. 5.4. Normalized signal output power (left curves) and output signal-to-self-noise ratio (right curves) for transmitted reference system using band-pass continuous detection.

$$\left(\frac{S}{N_s}\right)' = \frac{W_r}{4\pi W} \left(\frac{S}{N_s}\right)' =$$

$$\left\{ \begin{aligned} & 1+2a^2 \frac{\sin W\tau/2}{W\tau/2} + a^4 + \cos \Delta\tau \left[2a^2 + 2a(1+a^2) \cos \omega_0\tau \frac{\sin W\tau/2}{W\tau/2} + 2a^2 \cos 2\omega_0\tau \frac{\sin W\tau/2}{W\tau/2} \right]^2 \\ & + 2a(1+a^2) \cos \omega_0\tau \frac{\sin W\tau/2}{W\tau/2} + \sin \Delta\tau \left[2a(1+a^2) \sin \omega_0\tau \frac{\sin W\tau/2}{W\tau/2} + 2a^2 \sin 2\omega_0\tau \frac{\sin W\tau/2}{W\tau/2} \right]^2 \end{aligned} \right\}$$

$$\left\{ \begin{aligned} & 1+2a^2 + a^4 + \cos \Delta\tau \left[2a^2 + 2a(1+a^2) \cos \omega_0\tau \frac{\sin W\tau/2}{W\tau/2} + 2a^2 \cos 2\omega_0\tau \frac{\sin W\tau}{W\tau} \right] \\ & + 2a(1+a^2) \cos \omega_0\tau \frac{\sin \tau W/2}{\tau W/2} + \sin \Delta\tau \left[2a(1+a^2) \sin \omega_0\tau \frac{\sin W\tau/2}{W\tau/2} + 2a^2 \sin 2\omega_0\tau \frac{\sin W\tau}{W\tau} \right] \end{aligned} \right\}$$

(5.46)

From this signal power S'_0 and also $(S/N_s)'_0$ are plotted in Figure 5.4, arbitrarily setting $\Delta=W$ (as it might be in a practical case). In all three Figures 5.2, 5.3, and 5.4, ω_0 was chosen arbitrarily as $6W$ for convenience of presentation.

For the matched filter system and the stored-signal system employing fixed signals, the behavior of the output signal-to-noise ratio is given by the numerator S'_0 of equation 5.45.

A number of conclusions may be drawn from the curves of Figures 5.2, 5.3, and 5.4. To aid in this, the asymptotic behavior of the quotient

$(S/N_s)_o'$ is summarized in Table III for the conditions of large and small a and τ .

TYPE SYSTEM	Eq.No.	$a \ll 1$	$a \gg 1$	$\tau \ll 2\pi/\omega_o$	$\tau \gg 2\pi/W$
Stored signal, band-pass detection	(5.44)	$\frac{1}{1}$	$\frac{a^2 (\frac{\sin W\tau/2}{W\tau/2})^2}{a^2}$	$\frac{(1+a)^2}{(1+a)^2}$	$\frac{1}{1+a^2}$
Stored signal, low-pass detection	(5.45)	$\frac{1}{1}$	$\frac{a^2 (\cos \omega_o \tau \frac{\sin W\tau/2}{W\tau/2})^2}{\frac{a^2}{2} (1 + \cos 2\omega_o \tau \frac{\sin W\tau}{W\tau})}$	$\frac{(1+a)^2}{(1+a)^2}$	$\frac{1}{1 + \frac{a^2}{2}}$
Transmitted-reference, band-pass averaging	(5.46)	$\frac{1}{1}$	$\frac{a^4}{a^4}$	$\frac{(1+a)^4}{(1+a)^4}$	$\frac{1+2a^2 \cos W\tau + a^4}{(1+a^2)^2 + 2a^2 \cos W\tau}$

TABLE III

Asymptotic behavior of $(S/N_s)_o'$ for two path condition.

For large a we have the case of $h(t)$, a pure time shift, and the signal power from the stored signal system shows the behavior described previously in Sections 3.2-D and E. That is, the output signal voltage as a function of τ is $\beta(\tau)$ for low-pass detection, and the envelope of $\beta(\tau)$ for band-pass detection. Also, the self-noise denominator is constant with τ for band-pass detection (since the phase of $H(\omega)$ does not appear in equation 5.1), and for low-pass detection it drops in an oscillatory fashion to one-half its original value as τ increases from zero.

In the transmitted-reference system, the delay τ is immaterial since both signals are equally delayed.

For small a, the second path has negligible effect, and the output signal-to-noise ratio is the same as would be calculated from equations 2.60 and 2.61, applicable when only one path is present. The single path condition also exists for any value of a as $\tau \rightarrow 0$ and the two paths coalesce into one path of strength $1+a$.

For values of a which are neither much greater nor much smaller than unity, we have the following picture as τ varies: With an increase of τ from zero, there is alternate constructive and destructive interference at a rate given by ω_0 , the band center frequency. These rapid fluctuations, which are due to the interaction between signals delivered by the two paths, decrease in amplitude roughly as the autocorrelation envelope $(\sin W\tau/2) / (W\tau/2)$. For τ greater than several multiples of the reciprocal of the bandwidth in cycles, $2\pi/W$, vanishing correlation between the two signals gradually eliminates this fine structure and a convergence to the asymptotic values of Table III ensues. For the stored-signal system, this means that for large τ , the signal power is due entirely to the synchronized path, and the self-noise power is the sum of the contributions of the separate paths. For the transmitted-reference system at large τ there is an oscillation of the signal output as the difference frequency outputs produced by the two paths fall in and out of phase. The self-noise, which is a slowly modulated sine wave at the difference frequency shows somewhat the same effect.

We may now make the following statements about the relative performance of the various types of NOMAC system:

For values of τ less than the order of $2\pi/W$:

1. For all systems the output signal-to-noise ratio is critically a function of the time difference τ of signal arrival times due to paths of comparable strength. As τ is varied, the output signal-to-noise ratio fluctuates at a rate on the order of $\omega_0\tau$.

(For certain conditions this is mitigated somewhat by the small "duty cycle" of τ over which these severe reductions of output signal-to-noise ratio take place. See S'_0 of Figures 5.1, 5.2, and 5.3 for $a=1$.) The fact that these fluctuations disappear if τ is somewhat greater than the reciprocal of the bandwidth constitutes a strong argument for the use of wideband signals. As discussed in Chapter I, the use of wideband signals was motivated principally by military considerations. We see now that the practice of distributing signal energy continuously over a wide bandwidth has attractive possibilities for communication situation in which multipath is an important factor.

For path differences greater than the order of $2\pi/W$:

2. The stored-signal system responds only to signals supplied by paths very nearly in synchronism with the stored signal. If continuous detection is used, other paths not only fail to contribute to the signal output, but actually increase the self-noise.

3. The transmitted-reference system, on the other hand, has an output from every component path, and these outputs may interfere destructively so as to effect a serious reduction in output signal-to-noise ratio.

The condition of low output signal-to-noise ratio even for high input signal-to-noise ratio has been observed in operating transmitted-reference NOMAC systems, and is considered still another serious disadvantage to the

use of this type of operation. The advantages of going to wide bandwidths to reduce the violent decreases in $(S/N)_0$ shown in the figures are thus largely lost in the transmitted-reference system. In the stored-signal system, even though there may be some self-noise from out-of-synchronization paths, at least this is an added noise component and not a signal cancellation.

In an effort to predict the performance of a stored-signal type system in an actual communication circuit, preliminary data were taken in the form of a 24-hour observation of the pattern of Loran pulses received over a 470 nautical mile path. These observations showed that the output signal-to-self-noise ratio calculated from equation 5.20 would have been below -3 db roughly one percent of the time. It would have been below -15 db only for several seconds at a time, principally at times around midnight and dawn, and the total time out of 24 hours that this would have occurred was about 60 seconds.

We can make the following statements about the operation of the matched filter system when τ is greater than several multiples of $2\pi/W$.

4. The operation of the matched filter, when sampled at the fixed time representing termination of the signal delivered by the $\tau=0$ path, is to respond only to this signal.

5. Since the matched filter delivers a non-interfering output for every input path, if the modified sampling operation described at the close of Section 5.4 could be developed, one might envision making use of the entire succession of multipath signals, instead of just one as in (2) and (4) above.

This represents an important possibility for the use of the matched filter, and one which should be investigated further should a practical matched filter be developed.

CHAPTER VI

CONCLUSIONS

The type of communication system discussed in this paper is the outgrowth of recent studies of the communication process as one which is basically statistically in nature. We have seen in the introductory chapter how a certain set of basic communication requirements led to a logical system structure, which promises certain tactical advantages. The development of a basic point of view such as this in the science of radio communication represents an advance over the type of thinking which led to most of the more conventional systems. These systems evolved more as a matter of equipment expediency than from a penetrating analysis of what was really involved in the communication process.

The communication system of the present study, the NOMAC system, is an example of the more modern point of view, and it is seen that questions of equipment simplicity emerge as somewhat subordinate to a basic set of functions which the system should perform.

In studying the particular problem of communication through additive white gaussian noise, it is found that these functions are of a rather straightforward type. The most difficult operation in practice is that of signal storage, and the various types of NOMAC systems are described in terms of the manner in which the storage is effected. The stored signal type involves storing the reference waveforms as functions of time, whereas with the matched filter system, each waveform is stored as the time reversed

impulse response of some linear system. These two systems are referred to collectively as stored-reference type systems as contrasted with a third type, the transmitted-reference system in which the reference signals are not stored at all, but are transmitted to the receiver instead via an auxiliary communication link.

The transmitted-reference system has the advantage of simplicity, since storage and synchronization problems are largely eliminated. However, we have seen that this type of system has a number of important disadvantages when compared with either stored-reference type system. In the first place, the output signal-to-noise ratio (which determines the error probability) is lower for a given channel signal-to-noise ratio. If the channel interference is not merely random noise but is a deliberately chosen jamming signal, it was seen that the system is extremely vulnerable in that output signal-to-noise ratio may be severely reduced by modest jamming power. If the aim of an enemy interceptor is to recover the message, he may do so with ease since the key signal waveforms are available to him. And finally, when an examination of multipath effects was made, it was found that the transmitted-reference system offers very little improvement over conventional systems since destructive interference effects are still present.

The stored-reference system, on the other hand, provides good performance in all these respects. The effect of jamming signals other than a direct reconstruction of the reference signal can be alleviated by increasing the signals bandwidth. In order to determine the message content, the enemy must embark on a program of cryptanalysis. Predicted performance in

the presence of multipath is judged to be quite promising. By using wide enough bandwidths, the usual destructive interference can be eliminated. There remains, in the case of the stored-signal configuration, a self-noise component if continuous type operation is used. Preliminary data indicate that this may not be a serious factor in actual operation. It could be removed entirely by going to fixed operation or by employing matched filter detection.

Each of the two types of stored-reference system has its peculiar advantages. With the matched-filter type, there is the possibility of an appreciable relaxation of the time synchronization requirement (although rate synchronization may be found to cause difficulty). This may be done (at the price of a certain increase in output noise) by observing the output over an interval instead of sampling at a particular instant. The matched filter also offers the possibility of operation in the presence of multipath in such a way as to utilize the signal energy delivered by more than one path. The problem of constructing physical matched filters with the desired characteristics has proved to be of great difficulty. However, it is felt that the potentialities of this type of detection are great enough so that every effort should be made to find a solution to this problem. The notion of observing the output over an interval should also be investigated further.

The stored-signal system does not involve the difficult storage problems of the matched filter, since waveform storage is as a function of time, and not as the impulse response of a filter. The synchronization problem,

which is more acute than with matched filter operation with observation over an interval, is still of manageable proportions if the proper choice of correlation detector is made. In particular, the use of what has been termed a band-pass detector allows a greater latitude in synchronization than any other type, and has the additional advantage of great equipment simplicity.

The experimental system described in Chapter IV represents one example of a partial solution to the problem of realization of the stored-signal type system. The synchronization problem is relieved as much as possible by relying on time scale control by quartz crystals, which are probably capable of greater accuracy than any other component in common use by communication engineers. The system, which should be regarded at best as an exploratory development, operated as anticipated under laboratory conditions. Suggestions for effecting the synchronization operation in an operating communication circuit have been given. It is recommended that these suggestions be taken as the starting point for an effort at assembly of a complete operating system. Continued attention should be given to the problem of developing simpler, more reliable, and more secure sources of the stored noise-like signal. For example, the suitability of galactic signals for this type of system should be thoroughly investigated.

One question which was not pursued to any great extent in the present analysis, but which should be made a part of all future considerations of NOMAC system operation, is the cryptographic nature of this type of system.

There has been a gradual awakening to the very real necessity of evaluating military communication system design from the standpoint of vulnerability to countermeasures. Usually this takes the form of studies of the effect of the less subtle types of jamming. In the present systems, which are impervious enough to jamming so that they may be called upon to handle high-level traffic, it is imperative to take every precaution to protect the system against cryptanalysis too. It is suggested that future development of NOMAC systems be accompanied by much thought on such questions as the desired length of the periodic noise-like signal, the type of key, the key size, the frequency of key change, and also by exhaustive analyses in a search for unexpected cryptanalytic weaknesses.

REFERENCES

1. P. M. Woodward and I. L. Davies, Information theory and inverse probability in telecommunications, Proc. I.E.E., Part III, pp. 37-44, March 1952
2. N. Wiener, Generalized harmonic analysis, Acta Mathematica, v. 55, pp. 173-258, 1930
3. N. Wiener, Interpolation, extrapolation, and smoothing of stationary time series, NDRC Report, 1942; Wiley, New York, 1949
4. A. A. Michelson, Application of interference methods to spectroscopic measurements, Phil. Mag., v. 31, p. 340, April 1891
- P. E. Green, Jr., A historical note on the autocorrelation function, Proc. I. R. E., 1953. Letter submitted to the editor, publication forthcoming.
5. Y. W. Lee, T. P. Cheatham, Jr., and J. B. Wiesner, The application of correlation functions in the detection of small signals in noise, M.I.T., R.L.E. Tech. Rpt. 141, Oct. 13, 1949
6. R. M. Fano, Short-time autocorrelation functions and power spectra, J. Acoust. Soc. Am., v. 22, pp. 546-550, Sept. 1950
7. W. B. Davenport, Jr., Correlator errors due to finite observation intervals, M.I.T., R.L.E. Tech. Rpt. 191, March 8, 1951
8. R. M. Fano, Signal to noise ratio in correlation detectors, M.I.T., R.L.E. Tech. Rpt. 186, Feb. 19, 1951
9. M.I.T., R.L.E. and Project Lincoln Quarterly Progress Report, Jan. 30, 1952, Section 1.05

10. M.I.T., Project Hartwell, A report on the security of overseas transport, Final Rpt. (Secret), Sept. 21, 1950, Appendix G
11. B. L. Basore, Noise-like signals and their detection by correlation, M.I.T., R.L.E. and Lincoln Lab. Tech. Rpt. 7 (Secret), May 26, 1952
12. M.I.T., R.L.E. and Project Lincoln Quarterly Prog. Rpts. (Secret), October 30, 1951 to April 30, 1952, and Lincoln Lab. Quart. Prog. Rpts. (Secret), July 1, 1952 to present

B. J. Pankowski, Multiplexing a radio teletype system using a random carrier and correlation detection, M.I.T., R.L.E. and Lincoln Lab. Tech. Rpt. 5 (Secret), May 16, 1952
13. D. J. Gray, A new method of teletype modulation, M.I.T., Lincoln Lab. Tech. Rpt. 9, (Secret), Sept. 22, 1952

R. M. Lerner, The use of matched filters in remote triggering, M.I.T., Lincoln Lab. Quart. Prog. Rpt. (Secret), Oct. 1952, Section II-E

Andersen Labs., Inc., Research report on arbitrary linear system synthesis, A. F. contract 19(122)458, Subc. 11 (Restricted) June 29, 1953
14. G. L. Turin, Probability of error in frequency shift NOMAC systems, M.I.T., Lincoln Lab. Group 34 Internal Memo. 11 (Secret), March 27, 1953
15. S. O. Rice, Mathematical analysis of random noise, B.S.T.J., July 1944 and Jan. 1945, Section 2.8
16. J. L. Lawson and G. E. Uhlenbeck, Threshold Signals, M.I.T. Radiation Lab. Series, v. 24, McGraw-Hill, New York, 1950, pg. 176
17. W. B. Davenport, Jr., R. A. Johnson, and D. Middleton, Statistical errors in measurements on random time functions, J.A.P., v. 23, pp. 377-388, April, 1952


18. Reference 15, Section 4.3
19. Reference 15, Section 3.10
20. C. E. Shannon, Communication in the presence of noise, Proc. I.R.E., v. 37, pp. 10-21, Jan. 1949, Section 2
21. Ref. 15, Section 3.7
22. W. B. Davenport, Jr., NOMAC systems employing randomly amplitude and phase modulated carriers, M.I.T., Lincoln Lab. Group 34 Internal Memo. 10 (Secret), March 13, 1953
23. J. J. Bussgang, Crosscorrelation functions of amplitude-distorted gaussian signals, M.I.T., R.L.E. Tech. Rpt. 216, March 26, 1952
24. D. Middleton, Some general results in the theory of noise through non-linear devices, Quart. Appl. Math., v. 5, pp. 445-498, Jan. 1948
25. Model 500 Low-Flutter Magnetic Tape Recorder, Ampex Electric Corp., San Carlos, California, 1951
26. F. C. Williams and J. C. West, The positional synchronization of a rotating drum, Proc. I.E.E., v. 98, Part III, pp. 29-34, February, 1951
27. C. N. Pederson, A. A. Gerlach, and R. E. Zenner, Precise function generator, Electronics, v. 25, pp. 140-144, May 1952
28. A. J. Lephakis, An electrostatic-tube storage system, M.I.T., R.L.E. Tech. Rpt. 154, Mar. 27, 1950
29. Engineering Research Associates Staff, High-Speed Computing Devices, McGraw-Hill, New York, 1950, Section 14.2.6
30. A. C. B. Lovell and J. A. Clegg, Radio Astronomy, Wiley, New York, 1952

31. F. G. Smith, C. G. Little, and A. C. B. Lovell, Origin of the fluctuations in the intensity of radio waves from galactic sources, *Nature*, v. 165, pp. 422-424, March 18, 1950
32. L. B. Meacham, The bridge-stabilized oscillator, *Proc. I.R.E.*, v. 26, p. 1278, October 1933
33. H. C. Martel, The development of an electronic commutator, M.S. Thesis, M.I.T., 1950
34. C. E. Shannon, Communication theory of secrecy systems, *B. S. T. J.*, v. 28, pp. 656-715, Oct. 1949
35. D. Middleton, Theory of random noise. Phenomenological models. Part I, *J. A. P.*, v. 22, pp. 1143-1152, Sept. 1951
36. F. E. Terman, Radio Engineer's Handbook, McGraw-Hill, New York, 1943, Section 10
37. R. Price, Statistical theory applied to communication through multi-path disturbances, M.I.T., Lincoln Lab. Tech. Rpt. 34, In preparation.
38. Reference 37, Section II-C-2
39. A. J. Lephakis, Correlation analysis of VHF signals, M.I.T., Lincoln Lab. Tech. Rpt. 21 (Confidential), May 18, 1953

APPENDIX

SCHEMATIC DIAGRAMS OF EXPERIMENTAL STORED-SIGNAL SYSTEM

On the following pages are the schematic circuit diagrams for the various units comprising the experimental system depicted in the block diagram form in Figures 4.1 and 4.4.

The following nomenclature is used: All resistor values are in ohms with $K=10^3$ and $M=10^6$. All capacitor values less than unity are in μfd . Those greater than unity are in $\mu\mu\text{fd}$, unless otherwise specified. The diode symbol  (in which the left side is the cathode) indicates a type 1N34-A diode unless otherwise specified.

SECRET
SECURITY INFORMATION

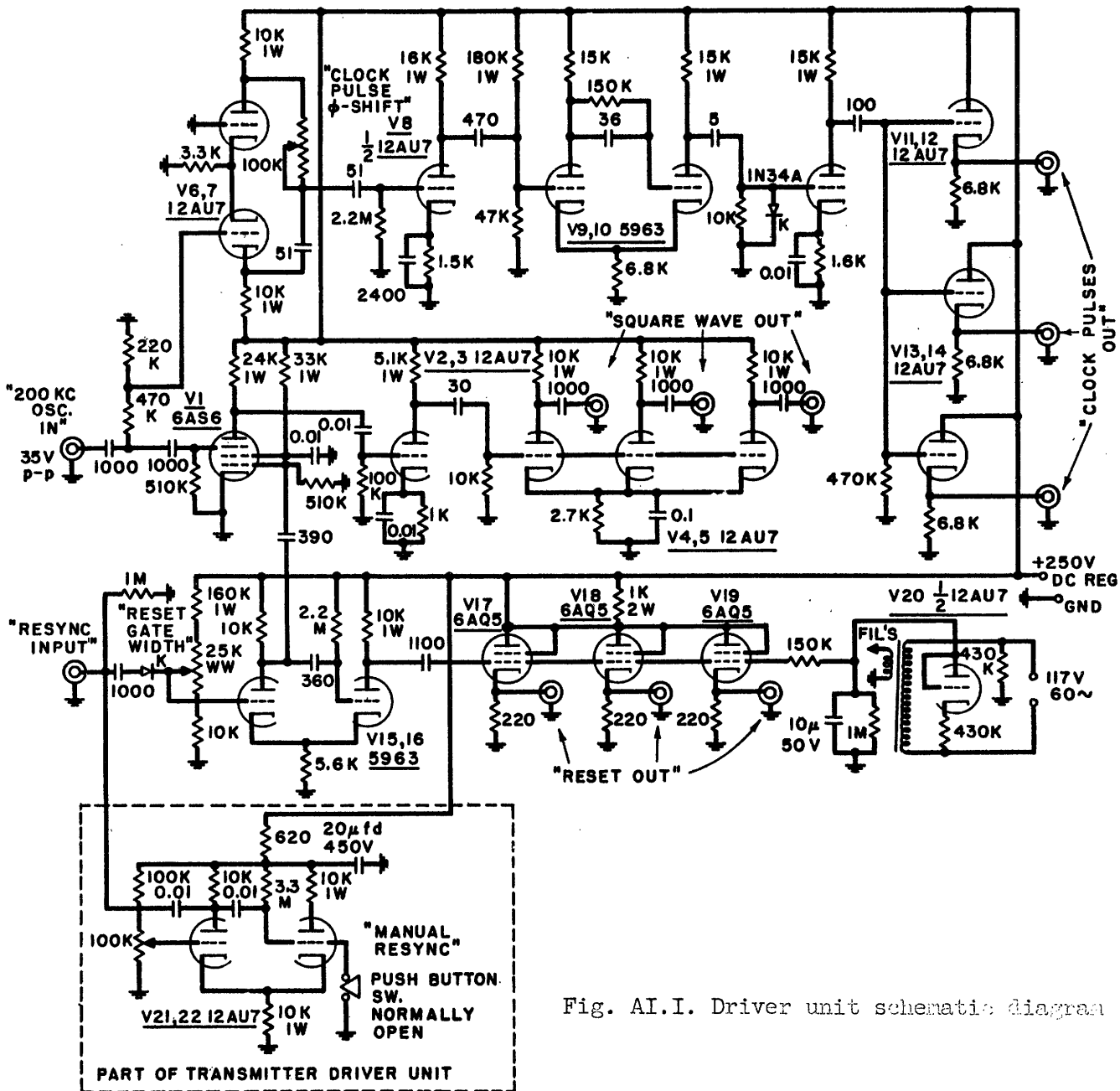
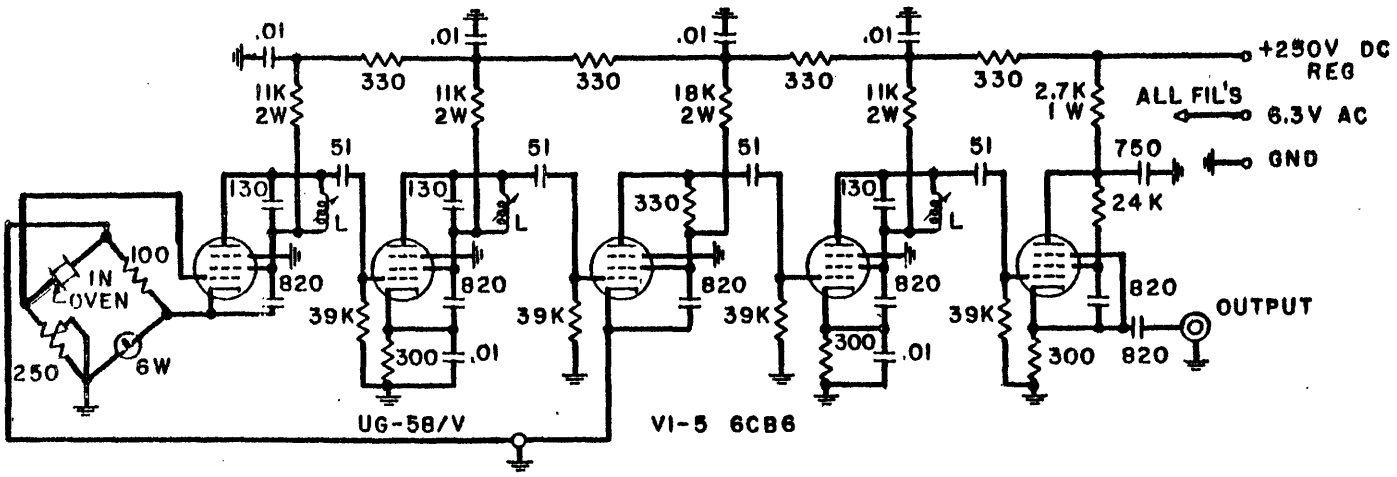


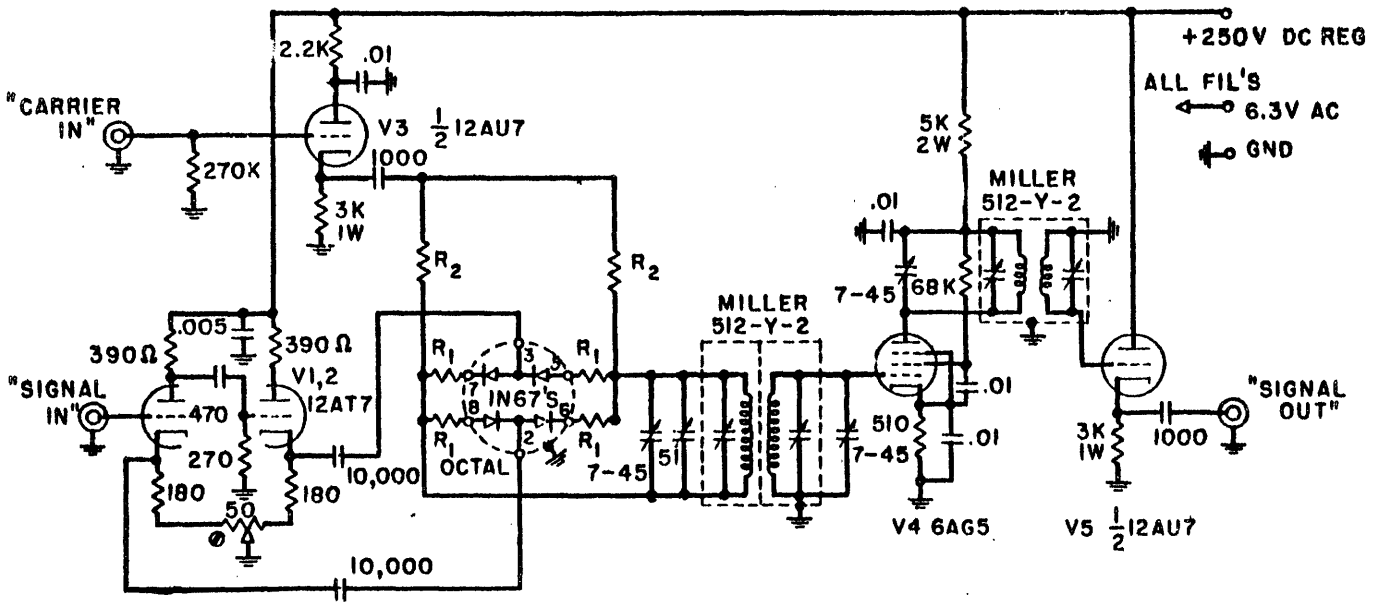
Fig. AI.I. Driver unit schematic diagram

SECRET
SECURITY INFORMATION



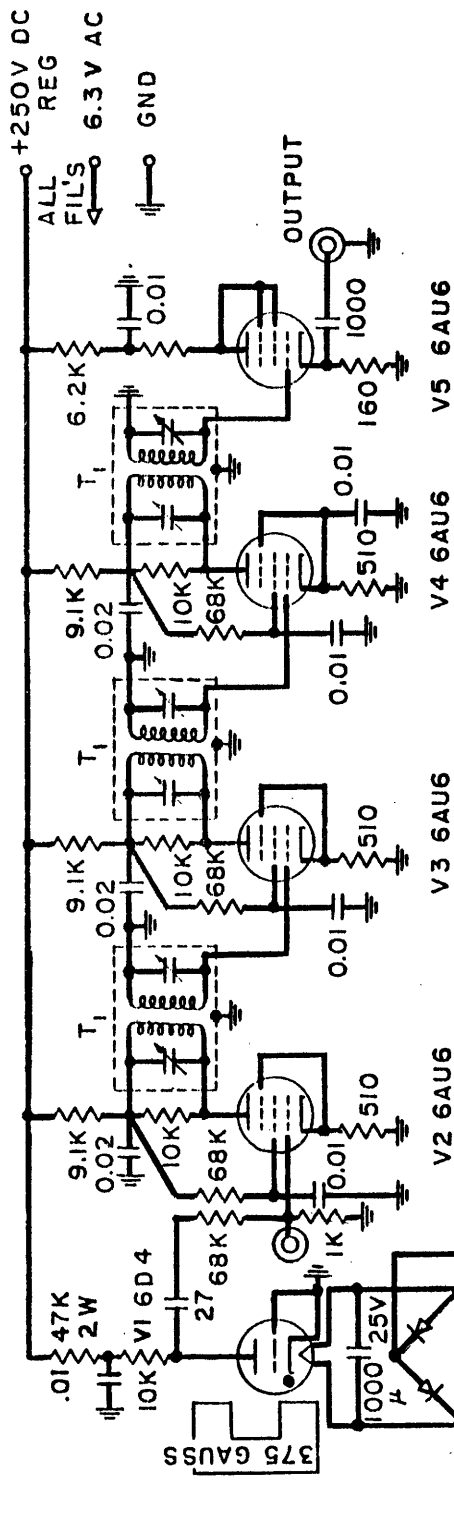
L = 30 TURNS # 36 ON CTC-LS6FORM

Fig. A1.4. 5-Mc oscillator schematic diagram.



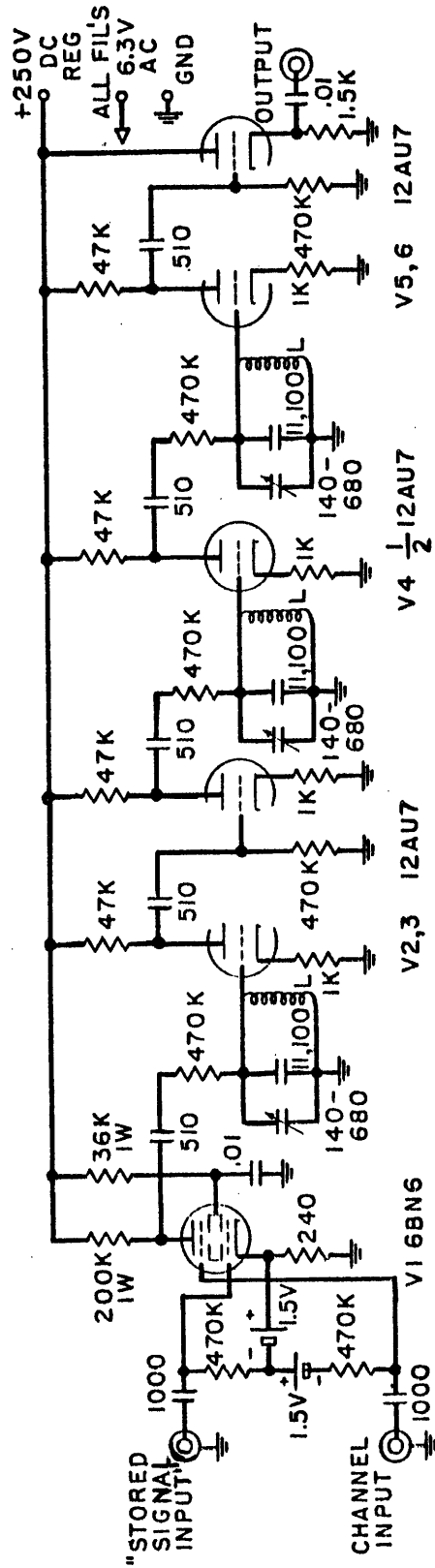
R₁ = 1K MATCHED
R₂ = 10K MATCHED

Fig. A1.5. Sideband generator schematic diagram.



T₁ = MILLER 512-Y-2

Fig. A1.6. Channel noise source schematic diagram.



L = 860 μh TOROID
MAX. Q AT 50 KC

Fig. A1.7 Correlator unit schematic diagram.

UNCLASSIFIED

Biographical Note

Paul Eliot Green, Jr. was born in Chapel Hill, North Carolina, on January 14, 1924. He received his primary education in the public schools of Chapel Hill, and attended the University of North Carolina, where he studied physics, receiving the Bachelor of Arts degree in 1944. He enjoyed a brief naval career from 1943, when he entered the Naval R.O.T.C., until 1946 when he was released to inactive service as a full Ensign. As a result of his Navy electronics training, he decided on a career in Electrical Engineering, and obtained his Master of Science degree in this specialty from North Carolina State College in 1948. The subject of his thesis research was the plotting of electric fields by automatic means. In April, 1948, he was appointed Research Assistant Professor of Agricultural Engineering at the same institution and devoted a year and a half to the investigation of photoelectric techniques for measuring color changes in tobacco. In September, 1949, he entered the graduate school at the Massachusetts Institute of Technology. Concurrently with his studies, he was employed by this institution as a Research Assistant and worked on communication problems in the Research Laboratory of Electronics under J. B. Wiesner and Y. W. Lee. In March, 1951, he joined the Communication Techniques group of M.I.T.'s Lincoln Laboratory where he has since been engaged in the study of certain classified communication problems under Dr. W.B. Davenport, Jr. Mr. Green is a member of Eta Kappa Nu and Sigma Xi, honorary societies, and Chi Phi, social fraternity. In 1948, he married Miss Dorrit Gegan of Boston. They have two children, Dorrit, age three, and Nancy, age one.